Charles University in Prague

First Medical Faculty

Biology and Pathology of the Cell

Limbal stem cell transplantation and their utilization for ocular surface reconstruction

Doctoral Thesis

Anna Lenčová, MD

Supervisor:	Prof. Martin Filipec, MD, PhD
Supervisor-specialist:	Prof. Vladimír Holáň, PhD, DSc

Prague, 2015

Prohlášení:

Prohlašuji, že jsem závěrenou práci zpracovala samostatně a že jsem ádně uvedla a citovala všechny použité prameny a literaturu. Současně prohlašuji, že práce nebyla využita k získání jiného nebo stejného titulu.

Souhlasím s trvalým uložením elektronické verze mé práce v databázi systému meziuniverzitního projektu Theses.cz za čelem soustavné kontroly podobnosti kvalifikačních prací.

15.3.2015

.....
Anna Lenčová

Identifikační záznam:
LENČOVÁ, Anna. *Transplantace limbálních kmenových buněk a jejich využití k rekonstrukci povrchu oka. [Limbal stem cell transplantation and their utilization for ocular surface reconstruction].* Praha, 2015. Počet stran 116, 4 přílohy. Disertační práce (PhD). Univerzita Karlova v Praze, 1. lékařská fakulta, Ústav experimentální medicíny, Akademie věd České Republiky v Praze. Školitel Filipec, Martin. Školitel-specialista Holáň, Vladimír.

ACKNOWLEDGMENTS

I would like to thank my supervisors Prof. Martin Filipec, MD, PhD and Prof. Vladimír Holáň, PhD, DSc, for their interest in the research, tremendous support throughout my study and experiments and their invaluable advice during this period, as well as for helping me achieve the goal of finishing this thesis.

My sincere thanks go to Kateřina Pokorná, MSc, PhD for her help and support during my experiments. I am extremely grateful to the entire team at the Professor Vladimír Holáň's laboratory at the Institute of Experimental Medicine, Academy of Sciences of the Czech Republic in Prague, especially to Alena Zajícová, PhD, DSc. In particular, I would like to thank Assoc. Prof. Jitka Čejková, MD, DSc and her team at the Institute of Experimental Medicine laboratory, Academy of Sciences of the Czech Republic in Prague.

Special thanks go to my partner Michal and to my parents for their enormous support. My gratitude also goes to František Kolečáni and Tracy Murphy for their help with correcting the English in my papers and thesis. Finally, I would like to thank my sister, Michala Lenčová, for helping me with the illustrations for this thesis and Ivan Kolín for his help with the photographic documentation.

Contents

List of Figures

List of Abbreviations

3D	three dimensional
ALDH3A1	antioxidant aldehyde dehydrogenase 3A1
AM	amniotic membrane
ATP	adenosine triphosphate
CD	cluster of differentiation
COMET	cultured oral mucosal epithelium transplantation
DNA	deoxyribonucleic acid
DTH	delayed-type hypersensitivity
E-GFP	enhanced green fluorescent protein
FBS	fetal bovine serum
FCS	fetal calf serum
GFP	green fluorescent protein
HLA	human leukocyte antigen
IFN-γ	interferon-gamma
IL	interleukin
iNOS	inducible nitric oxide synthase
K	keratin
LEC	limbal epithelial crypt
LR	living-related
LSC	limbal stem cell
LSCD	limbal stem cell deficiency
mAb	monoclonal antibodies
MDA	malondialdehyde
MHC	major histocompatibility complex
mm	millimetre
MMP9	matrix metalloproteinase 9
MSC	mesenchymal stem cell
NaOH	sodium hydroxide
NO	nitric oxide
NT	nitrotyrosine
RNA	ribonucleic acid
SC	stem cell
SP	side-population
Sry	sex determining Y protein
TAC	transient amplifying cell
TDC	terminally differentiated cell
Th1	T helper cells type 1
Th2	T helper cells type 2
VEGF	vascular endothelial growth factor

Abstract

Aims: Limbal stem cell (LSC) deficiency is one of the most challenging ocular surface diseases. The aim of this thesis was to study damaged ocular surface reconstruction. Therefore, a mouse model of limbal transplantation was established. Furthermore, LSC isolation, transfer of LSCs and bone marrow-derived mesenchymal stem cells (MSCs) on nanofiber scaffolds were studied.

Material and methods: Syngeneic, allogeneic and xenogeneic (rat) limbal grafts were transplanted orthotopically into BALB/c mice. Graft survival, immune response and the effect of monoclonal antibodies (mAb) (anti-CD4 and anti-CD8 cells) were analyzed. Mouse LSCs were separated by Percoll gradient; subsequently, they were analyzed for the presence of LSC and differentiation corneal epithelial cell markers and characteristics using real-time PCR and flow cytometry. Nanofiber scaffolds seeded with LSCs and MSCs were transferred onto the damaged ocular surface in mouse and rabbit models. Cell growth on scaffolds, post-operative inflammatory response and survival of transferred cell were analyzed.

Results: Limbal allografts were rejected promptly by the Th1-type of immune response (IL-2, IFN-γ) involving $CD4^+$ cells and nitric oxide produced by macrophages, contrary to the prevailing Th1 and Th2 immune responses (IL-4, IL-10) in xenografts. Anti-CD4 mAb significantly postponed the rejection in allografts and in xenografts. The lightest and densest fraction of the Percoll gradient were both enriched with cell populations with a high expression of SC markers and side-population phenotype. Contrary to the lightest (40%), the densest (80%) fraction contained $K12^-/p63^+$ cells with characteristics that were closer to SCs. In the mouse model, the nanofiber scaffolds with LSCs and MSCs suppressed the inflammatory reaction. In the rabbit model, the MSCs on nanofiber scaffolds reduced alkali-induced oxidative stress and significantly accelerated corneal healing.

Conclusions: Limbal grafts do not enjoy any privileged position of immunity in the eye. Anti-CD4 mAb treatment is a promising immunosuppressive approach after limbal allotransplantation. By centrifugation on Percoll gradient, two distinct populations of corneal epithelial cells with SC characteristics were separated, with the $K12^-/p63^+$ population being closer to LSCs. Nanofiber scaffolds can be useful for LSC and MSC transfer and future treatment of ocular surface injuries.

Key words: limbal stem cells, limbal stem cell deficiency, limbal transplantation, mesenchymal stem cells, nanofiber scaffolds.

Abstrakt

Cíle: Deficit limbálních kmenových buněk (LSC) patří mezi nejzávažnější onemocnění povrchu oka. Cílem dizertační práce bylo studium obnovy poškozeného povrchu oka. Proto byla zavedena limbální transplantace v experimentálním myším modelu. Byla provedena izolace LSC, přenos LSC a mesenchymálních kmenových buněk (MSC) izolovaných z kostní dřeně na nanovláknových nosičích na povrch poškozeného oka u myší a u králíků.

Materiály a metody: U myší BALB/c byla provedena syngenní, alogenní a xenogenní limbální transplantace. Po transplantaci byla sledována doba přežívání štěpů, imunitní reakce a účinky monoklonálních protilátek (mAb) (anti-CD4 a anti-CD8). Myší LSC byly rozděleny pomocí centrifugace na Percollovém gradientu a následně byla provedena analýza povrchových znaků LSC pomocí PCR a průtokové cytometrie. Na myším a králíčím modelu byly přenášeny LSC a MSC pomocí nanovláknových nosičů na poškozený povrch oka. Byl sledován *in vitro* růst buněk na nosičích, pooperační zánětlivá reakce a přežívání buněk na povrchu oka po přenosu nosičů.

Výsledky: K odhojení alogenních limbálních štěpů došlo promptně a v průběhu rejekce převažovala Th1 imunitní odpověď (IL-2, IFN-γ) mediovaná $CD4^+$ buňkami a NO produkovaným makrofágy. U xenotransplantátů převažovala Th1 i Th2 (produkce IL-2, IFN-γ, IL-4 a IL-10) imunitní odpověď. Pomocí anti-CD4 monoklonálních protilátek došlo k signifikatnímu prodloužení přežívání alogenních a xenogenních štěpů. Frakce získané po izolaci z vrchní (40% Percoll) a spodní (80% Percoll) vrstvy gradientu obsahovaly buňky s vysokou expresí znaků kmenových buněk a side-population fenotypu. Spodní frakce obsahovala buňky s expresí znaků $K12^-/p63^+$ vykazující vlastnosti blížší kmenovým buňkám na rozdíl od vrchní frakce. Společný přenos LSC a MSC výrazně inhiboval zánětlivou reakci v myším modelu. Přenos MSC na nanovláknech u králíků potlačil oxidativní stres rohovky způsobený poleptáním a podpořil proces hojení.

Závěr: U transplantace limbálních štěpů se neuplatňuje imunologická privilegovanost oka. Anti-CD4 monoklonální protilátky představují slibnou imunosupresi u alotransplantátů. Pomocí centrifugace na Percollovém gradientu lze získat dvě odlišné populace buněk vykazující vlastnosti kmenových buňek, ze kterých $K12^-/p63^+$ populace je bližší k LSC. Nanovláknové nosiče jsou vhodné pro léčbu poškozeného povrchu oka pomocí LSC a MSC v experimentálním modelu.

Klíčová slova: limbální kmenové buňky, deficit limbálních kmenových buněk, limbální transplantace, mesenchymální kmenové buňky, nanovláknové nosiče.

1 GENERAL INTRODUCTION

1.1 Introduction

The integrity of the corneal epithelium is essential for maintaining corneal transparency and ensuring visual function. The corneal epithelium is renewed by the cells, which migrate from the limbus. These cells originate from the LSCs, which are located in the basal layer of the limbus (Cotsarelis et al., 1989). The limbus is a transient zone between the corneal and conjunctival epithelium. Loss of LSC source through primary disease or secondarily, due to ocular surface damage, can cause opacity, corneal cicatrization, impairment of transparency, and can lead to blindness (Dua et al., 2000). The correct assessment of LSC deficiency (LSCD) is crucial in clinical practice because these patients are not suitable candidates for conventional corneal transplantation. In these cases, lamellar or penetrating keratoplasty would provide only a short-term replacement of corneal epithelium in the recipient. It does not resolve the primary cause of the disease the loss of LSCs. The only way to cure LSCD is through transplantation of the whole limbus (Tan et al., 1996); (Holland, 1996); (Dua and Azuara-Blanco, 1999), or through transfer of cultured LSCs (Pellegrini et al., 1997); (Rama et al., 2010). When both eyes are involved, the limbal allografts must be used for transplantation. Such procedures have a high risk of rejection during the postoperative period, therefore a high dosage of systemic immunosuppression is required for a long period. The corneal transplantation can be done simultaneously with limbal transplantation or as a subsequent procedure. To date, there are limited numbers of experimental limbal transplantation studies. Further studies are necessary to improve understanding of the limbal graft and LSC survival, as well as their capacity to renew the ocular surface after transplantation. Further studies are also warranted to find effective immunosuppressive treatment. Animal models in this area can contribute substantially to improvement of LSCD treatment and, thus, improve the poor prognosis of this disease in clinical practice.

1.2 The ocular surface anatomy

1.2.1 Cornea

The cornea is a transparent tissue, responsible for light transmission and refraction and is essential for good vision. It is composed of epithelium, Bowman's membrane, stroma, the Descemet's membrane and endothelium. Recently, a well-defined, acellular and strong layer was described in the pre-Descemet's area in the human cornea (Dua et al., 2013). The human corneal epithelium consists of 5-6 layers of non-keratinized, stratified cells. The cells differ in shape across its layers. They are column-shaped in the basal layer, cuboid wing shaped in the suprabasal layer and flat squamous shaped cells in the superficial layer (Beuerman and Pedroza, 1996). Conversely, mouse corneal epithelium is more complex and consists of 13 cell layers in the center, becoming thinner in the periphery (Henriksson et al., 2009). Mouse epithelium has a stratified array, in which the basal columnar cells become flattened as they near the surface and increased cell

layers are explained by the presence of multiple squamous layers (Smith et al., 2002); (Henriksson et al., 2009). The tight junctions in the superficial layers of human corneal epithelium are responsible for epithelium barrier function (Sugrue and Zieske, 1997); (Yi et al., 2000). The basal epithelial cells are attached to the basement membrane by hemidesmosomes. The Bowman's layer is composed of a thin acellular layer of collagen fibrils with the anterior well-defined surface and posterior surface merging with the stroma (Forrester et al., 2008). There is controversy about the presence of the Bowman's layer in mice whereby some authors believe that mice do not have a true Bowman's layer, while others believe they do (Hayashi et al., 2002); (Smith et al., 2002); (Henriksson et al., 2009). The stroma is composed predominantly of regular collagenous lamellae and forms 90% of the thickness of the human cornea, contrary to the 70% seen in mice (Li et al., 1997); (Henriksson et al., 2009). It is more compact anteriorly than posteriorly and proteoglycan composition varies in the anterior and posterior parts (Bron, 2001); (Müller et al., 2001).

Keratocytes (modified fibroblast) exist between the collagen lamellae in the stroma. Descemet's membrane is a modified basement membrane of endothelium. The corneal endothelium is composed of simple squamous interdigitated cells and is essential for regulating corneal hydration. The relative acellular matrix of the cornea is fundamental to its transparency. In particular, the regular and smooth corneal epithelium (Puangsricharern and Tseng, 1995), the regular arrangement of collagen and cellular stromal components (Fini and Stramer, 2005), the level of hydration determined by endothelial pump function (Meek et al., 2003), the presence of corneal crystallins in the stroma (Jester et al., 1999), and the corneal avascularity (Nishida, 2005) are essential elements of the transparent cornea.

1.2.2 Limbus

The human limbus is described as a transition zone, 1.5-2.0 millimeter (mm) in width, between the transparent cornea and the opaque sclera, which is highly vascularized and innervated (Davanger and Evensen, 1971). The epithelium has 10 to 12 layers and overlies the stroma, which is radially arranged into the palisades of Vogt (Dua et al., 1994). The exact definition of the limbus differs among anatomists, pathologist and ophthalmic surgeons. According to Van Burskirk, the anatomical (histological) limbus is described as a V-shape transition line between the corneal lamellae and scleral lamellae (Van Buskirk, 1989) (Figure 2).

Pathologists define the limbus as a block of tissue in which the anterior border is a line connecting the junction of the conjunctival and corneal epithelium with termination of Schwalbe's line. The posterior border is a perpendicular line from the scleral spur to the ocular surface (Figure 1, 2). In clinical practice, the limbus is characterized as a blue-grey transition zone seen on slit lamp examination (Figure 1). Limbal surgical incision goes anteriorly from the trabecular meshwork and Schlemm's canal (Figure 2 and Figure 3).

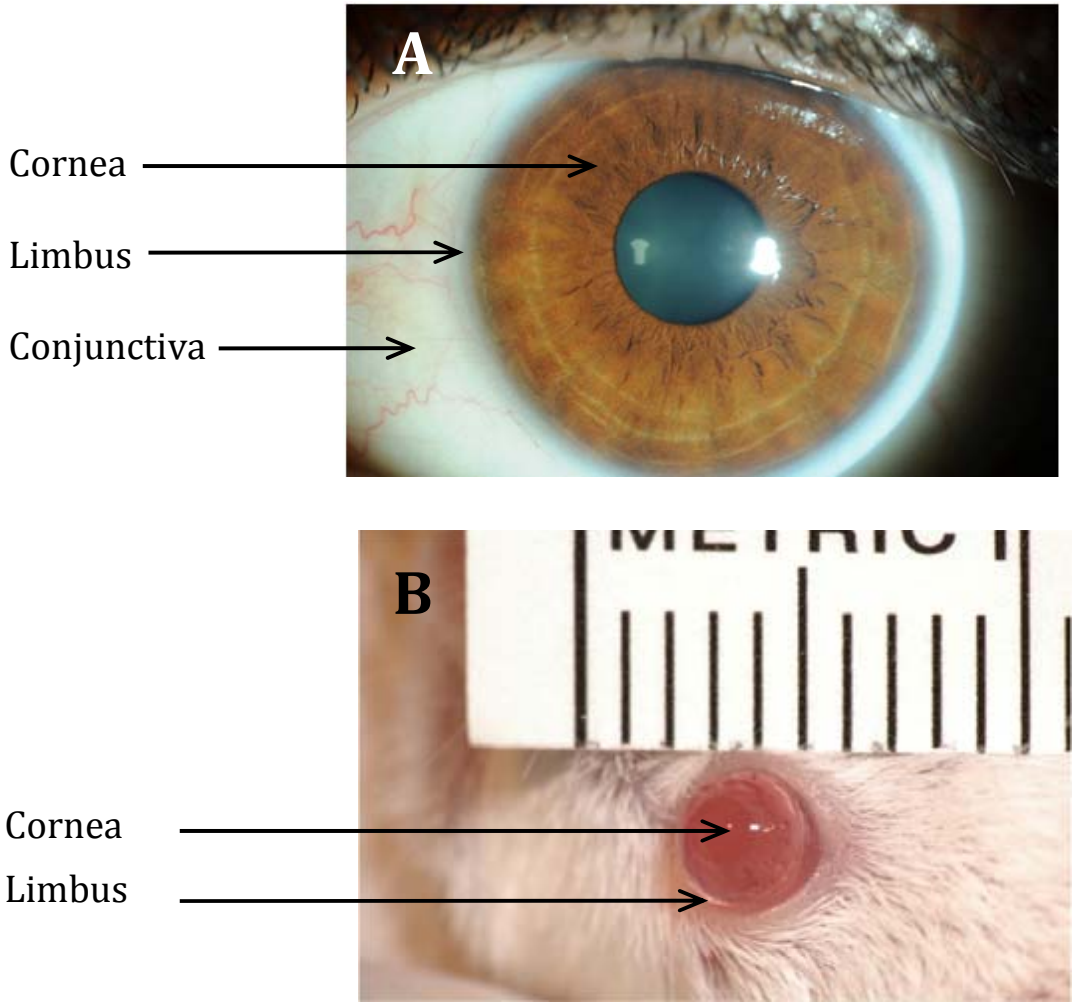

Figure 1: **Anterior segment photography: A)** Ocular surface of human eye showing the cornea, limbus and conjunctiva; **B)** Ocular surface of mice showing the cornea and limbus. (Courtesy of Ivan Kolín)

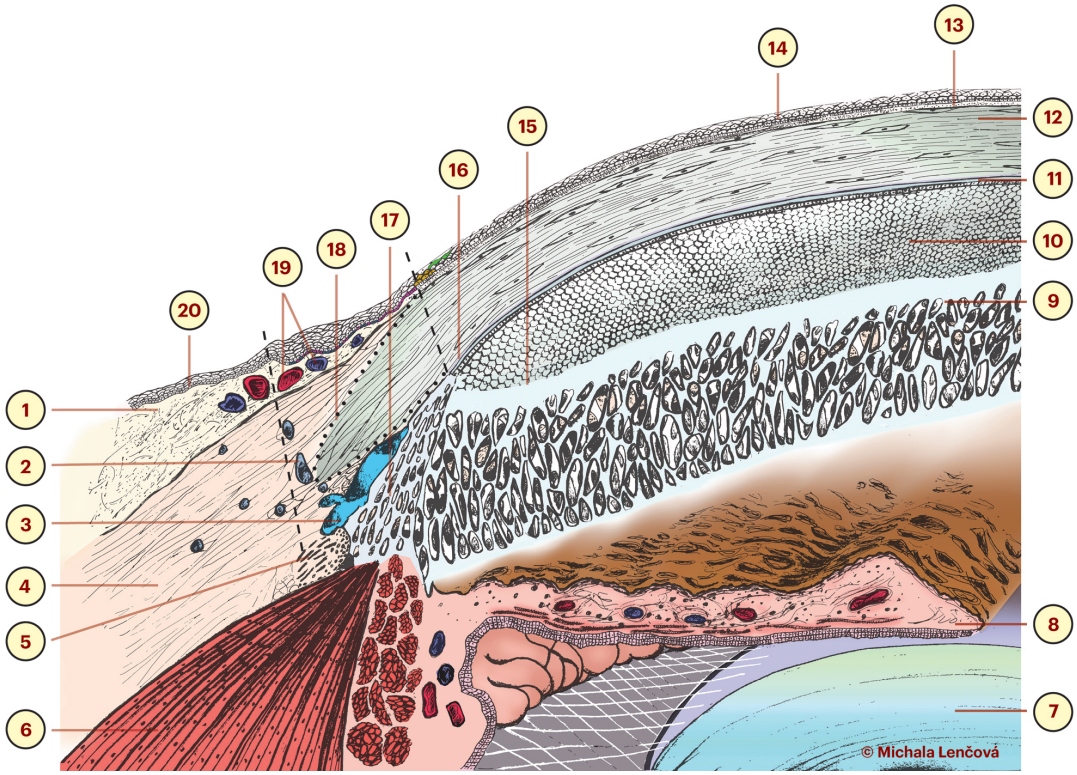

Figure 2: **Anatomy of the anterior segment of the human eye:** 1. Subepithelial connective tissue; 2. Collector channels; 3. Schlemm's canal; 4. Sclera; 5. Scleral spur; 6. Ciliary muscle; 7. Lens; 8. Iris; 9. Uveal meshwork; 10. Corneal endothelium; 11. Descemet's membrane; 12. Corneal stroma; 13. Bowman's layer; 14. Corneal epithelium; 15. Schwalbe's line; 16. Pre-Descemet's layer; 17. Trabecular meshwork; 18. Limbus; 19. Episcleral vessels; 20. Conjunctival epithelium. Dotted lines demarcate the histologist's limbus; dashes demarcate the pathologist's limbus. (Courtesy of Michala Lenčová)

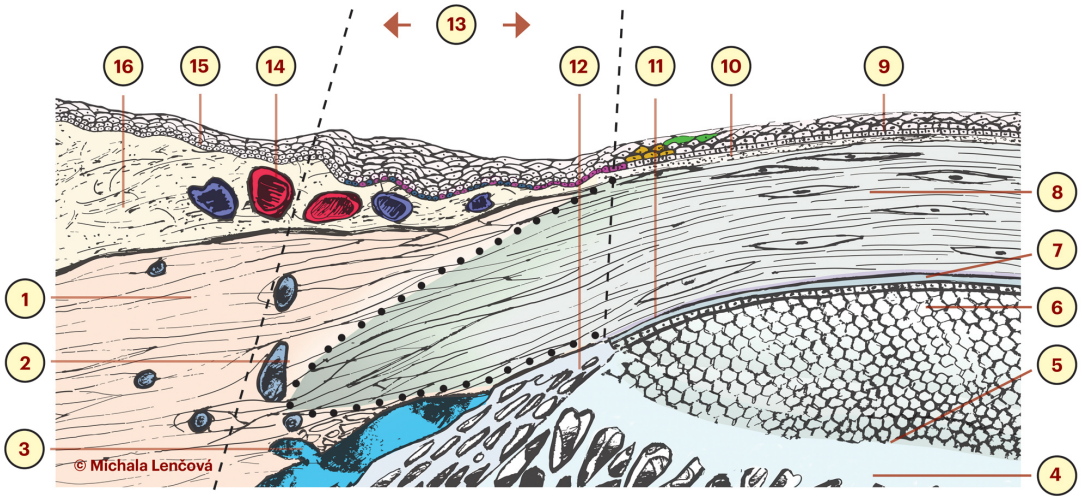

Figure 3: **Anatomy of the limbus:** 1. Sclera; 2. Collector channels; 3. Schlemm's canal; 4. Trabecular meshwork; 5. Schwalbe's line; 6. Corneal endothelium; 7. Descemet's membrane; 8. Corneal stroma; 9. Corneal epithelium; 10. Bowman's layer; 11. Pre-Descemet's layer; 12. Uveal meshwork; 13. Limbus; 14. Episcleral vessels; 15. Conjunctival epithelium; 16. Subepithelial connective tissue. (Courtesy of Michala Lenčová)

The limbal area has several physiological attributes. The limbus serves as a reservoir of LSCs, which are essential for corneal epithelium renewal and healing. In addition, the limbus has an important role in "barrier function", preventing encroachment of the conjunctival epithelium onto the cornea during homeostasis and the healing process (Thoft et al., 1979); (Tseng, 1989); (Huang and Tseng, 1991). When this function is compromised, the conjunctival epithelium, together with blood vessels and fibrous tissue, encroaches onto the cornea: this is termed as conjunctivalization, a hallmark of LSCD (Dua et al., 2009). The limbus maintains nourishment of the peripheral cornea, contains pathways of aqueous humour outflow and is the site of surgical incisions into the anterior chamber for cataract and glaucoma surgery (Van Buskirk, 1989). Several important transitions take place at the limbus; for example, the regular corneal lamellae terminate here and a more randomly structured scleral lamellae start here; the non-keratinized corneal epithelium gives way to the conjunctival epithelium; the conjunctiva has a high density of goblet cells and major histocompatibility complex (MHC) class II dendritic cells (Langerhans), which sharply declines at the limbus; the conjunctival capillaries and lymphatic capillaries terminate here; Descemet's membrane and Bowman's layer terminate here; the loose conjunctival subepithelial vascularized connective tissue (substantia propria), containing immunocompetent cell types (mast cells, plasma cells, lymphocytes) tapers off at the limbus (Forrester et al., 2008).

1.2.3 Conjunctiva

The conjunctiva is a mucous membrane consisting of stratified, squamous, non-keratinized epithelium overlying the loose connective tissue substantia propria. The conjunctival epithelium varies in structure regarding to localization and is divided into 3 regions: bulbar, forniceal and palpebral. The human bulbar conjunctiva consists of cuboidal epithelial cells in 6 to 9 layers irregularly organized compared to the cornea (Krachmer et al., 2005). The forniceal conjunctival epithelium is between the bulbar and palpebral epithelium, is more columnar in shape, and composed of just 3 cell layers overlying the thickest substantia propria (Nelson and Cameron, 2011). The palpebral epithelium is more cuboidal in nature, 2 to 3 cell layers over the superior tarsus and 4 to 5 layers over the inferior tarsus (Nelson and Cameron, 2011). In the mouse eye, the conjunctiva epithelium is much thinner and the bulbar conjunctiva consists of 2 to 4 cell layers, the tarsal conjunctiva of 2 to 4 layers and the fornix of just 1 to 2 layers (Smith et al., 2002). Goblet cells are characteristic for their conjunctival epithelium and producing mucin, which coats the ocular surface and stabilizes the tear film (Krachmer et al., 2005).

1.3 The concept of corneal epithelial maintenance and wound healing

1.3.1 Corneal epithelial maintenance

Corneal epithelium homeostasis is vital for ocular surface integrity and, thus, healthy corneal epithelium is essential for corneal transparency and vision. Human corneal epithelial cells are continually desquamated into the tear pool and replaced by cells moving centrally from the limbus and anteriorly from the basal layers of the corneal epithelium (Dua et al., 1994).

In 1971, Davenger and Evensen were the first to assume that the corneal epithelium is recovered by the cell population located in the limbal area (Davanger and Evensen, 1971). Research in the years following demonstrated further evidence of epithelial stem cells (SCs) located in the limbus and their crucial role in the renewal and repair process of the corneal ocular surface. In 1983, Thoft described the concept of corneal epithelial maintenance as the X, Y, Z hypothesis, defined as X+Y=Z, in which the epithelial cells are thought to move slowly toward the center (Thoft and Friend, 1983). The X component represents the proliferation of basal epithelial cells, the Y component the centripetal cell migration of the limbal cells, and the Z component the epithelial cell loss from the surface (Figure 4). Tissue hierarchy in corneal epithelium was proven by several studies. The corneal SCs at the limbus generate the transient amplifying cells (TACs), which proliferate, migrate into towards the cornea and become post-mitotic and terminally differentiated cells (TDC) of corneal epithelium with an ability to regenerate (Figure 3, Figure 4) (Cotsarelis et al., 1989); (Tseng, 1989); (Lehrer et al., 1998); (Schlötzer-Schrehardt and Kruse, 2005). Cell divisions have been demonstrated at the basal corneal epithelium (Haskjold et al., 1989). The vertical movement of basal cells and their daughter cells (TDC) toward the ocular surface

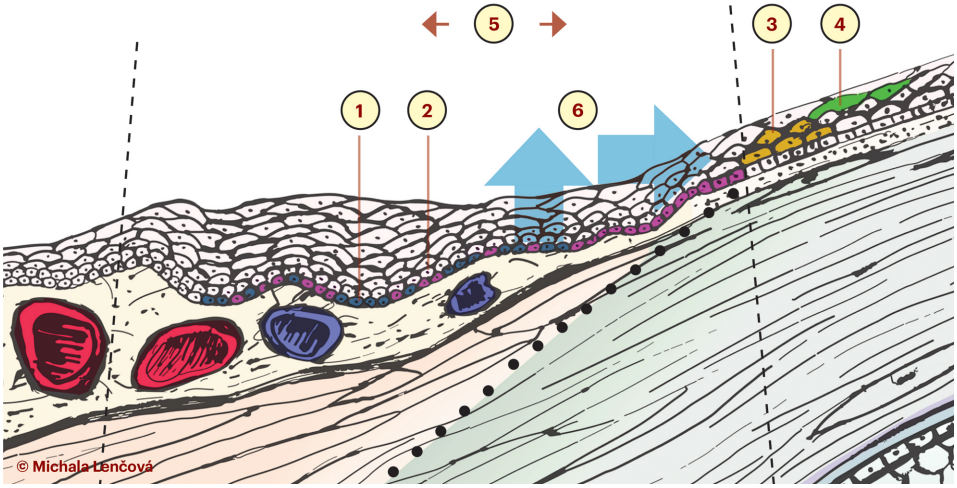

Figure 4: **The concept of corneal epithelial maintenance:** The limbal stem cells (1) at the limbus (5) generate transient amplifying cells (2), which proliferate, migrate towards the cornea (6) and become post-mitotic (3) and terminally differentiated cells (4) of corneal epithelium with no ability to self-renew. (Courtesy of Michala Lenčová)

contributes to corneal epithelial homeostasis and is stimulated by cell shedding (Beebe and Masters, 1996). The superficial corneal epithelial cells are constantly desquamated after terminal differentiation or apoptosis (Kruse, 1994); (Ren and Wilson, 1996).

1.3.2 Corneal wound healing

LSC activity is sensitive to corneal injury: cell migration starts at the limbus and moves towards a wounded cornea in a centripetal and vertical manner (Nagasaki et al., 2003); (Lempet and Mathers, 1989). Corneal and limbal epithelial healing has a characteristic clinical pattern. Following corneal epithelial injury, centripetal migration and formation of convex corneal epithelium sheets occur, these sheets undergo contact inhibition and create a characteristic geometric shape, which finally closes by contact lines "pseudo-dendrites" (Dua and Forrester, 1987). In partial limbal epithelial defect, a preferential circumferential migration of tongue-shaped sheets of limbal epithelial cells arises from either end of the remaining intact epithelium (Dua and Forrester, 1990). The circumferentially migrating "tongues" meet to restore limbal epithelial integrity and subsequently centripetal epithelium movement completes the healing process (Dua and Forrester, 1990). For epithelial maintenance and healing, it is essential that growth factors come through with the tear film (Watanabe et al., 1987), the epithelium (Rolando et al., 2001), the stromal keratocytes (West-Mays and Dwivedi, 2006) and aqueous humor (Welge-Lüssen et al., 2001).

The LSC concept of epithelial renewal was confirmed in several experimental studies. In rabbit models, partial limbal deficiency can arise from the surgical re-

moval of two thirds of the limbal zone and can result in abnormal prolonged healing, vascularization and overgrowth of conjunctival epithelium onto the cornea (Chen and Tseng, 1990); (Chen and Tseng, 1991). After total limbal removal in a rabbit model, only limited proliferative capacity of corneal epithelium remains until the corneal epithelium is wounded, following which delayed healing and corneal conjunctivalization occur (Huang and Tseng, 1991). The complete removal of limbal and corneal epithelium results in LSCD in rabbit models (Kruse et al., 1990).

1.3.3 Challenging the limbal stem cell concept

However, contrary to the accepted dogma that the cells responsible for corneal renewal reside mainly, if not exclusively, in the limbus, there are results of recent animal transplantation studies (Majo et al., 2008) and clinical observations (Dua et al., 2009); (Bi et al., 2013), which suggest that the corneal epithelium possess at least some degree of self-renewing capacity. Majo et al. described that mouse central cornea contains oligopotent SCs (Majo et al., 2008). Contrary to this hypothesis, the existing human data on epithelial differentiation and cell migration in the ocular surface do not support this theory and suggest interspecies differences in cornea anatomy (Sun et al., 2010). However, Dua et al. showed that normal central island of corneal epithelium remained in 8 patient eyes despite diagnosis of LSCD (Dua et al., 2009). The authors have given two explanations for these observations: 1) that some clinically invisible LSCs still survive and maintain the epithelium, or 2) that the basal TACs of central epithelium are independently capable of central corneal maintenance. In the recent study on human cornea maintained in organ culture, it was demonstrated that the central corneal epithelium was capable of self-regeneration following the total ablation of the limbus and thus the LSCs may not, in fact, respond immediately to an acute wound (Chang et al., 2008). The animal study in rabbits showed that after complete removal of limbus, the central epithelium survived until it was wounded (Huang and Tseng, 1991). Generally, stratified epithelial cells are renewed by SCs from their basal layers. The belief that the corneal epithelium is replenished by the centripetal movement of TACs generated from SCs at the limbus has a long proved an anomaly among stratified epithelial and has generated speculation about benefits of this mechanism (Barbaro et al., 2007). However, the further studies are needed to confirm the data about corneal self-renewal capacity.

1.4 The limbal stem cells

1.4.1 Limbal stem cell location

Histologically, the human limbal epithelium consists of more than ten cells layers and is the thickest of the three compared to one to two cell layers in the conjunctival epithelium and four to six cell layers in the corneal epithelium (Tseng, 1989). The layers are organized in papillae-like structures termed as palisades of Vogt, which are located in the sub-epithelial connective tissue (Townsend, 1991). The

LSCs reside in the basal layer of the limbus at the bottom of the Vogt palisades, which represent the well-protected environment in close contact with a specific stromal niche (Cotsarelis et al., 1989);(Li et al., 2007). In addition, the LSCs contain melanin, which has a protective role against UV light (Cotsarelis et al., 1989). Unlike the conjunctival epithelium, the limbal epithelium does not contain goblet cells (Hogan et al., 1971).

In 2005, Dua et al. identified a novel and unique anatomical structure termed as limbal epithelial crypts (LECs), which were proposed as a putative LSC niche (Dua et al., 2005). LECs extend outward from some palisades of Vogt and are found deeper in the substantia propria of the limbus providing both protection and a microenvironment of extracellular matrix with its multitude of resident cells (Dua et al., 2005); (Yeung et al., 2008). LECs occur in clusters and their size and distribution often varies (Shanmuganathan et al., 2007). LECs may be a result of normal physiological development in order to protect and maintain the SCs, the numbers probably decline with age (Yeung et al., 2009). Some epithelial cells with features of LSCs ectopically reside the peripheral cornea and adjacent conjunctiva on either side of the limbus (Kawasaki et al., 2006); (Yeung et al., 2009).

1.4.2 Limbal stem cell characteristics

Adult SCs are characterized by proliferative potential and cell phenotype. The widely accepted features of adult SCs include: 1) the ability for self-renewal and functional tissue regeneration, 2) slow cycling or long cell cycle time during homeostasis *in vivo*, 3) high proliferative potential after wounding or placement *in vitro*, 4) small size with poor differentiation and primitive cytoplasm (Cotsarelis et al., 1999); (Lavker and Sun, 2000); (Watt, 2000); (Watt and Hogan, 2000); (Blau et al., 2001).

Basal limbal cells have the characteristics of adult SCs. LSCs have a high proliferative potential *in vitro* compared to the epithelial cells in the peripheral and central cornea, a high capacity for error-free self-renewal, a long life span, slow cell cycle and the ability to retain labelled DNA precursors over a long period (Cotsarelis et al., 1989); (Pellegrini et al., 1999). Clonal analysis has shown that limbal basal cells are holoclone-forming cells in contrast to corneal epithelial cells (Pellegrini et al., 1999). LSCs undergo asymmetrical division and produce one SC to replenish the SC pool and one TAC (Daniels et al., 2001). TACs are fast-dividing progenitor cells and reside the basal epithelium of limbus and peripheral cornea. These cells give rise to post-mitotic and TDCs in the suprabasal and superficial layers (Lehrer et al., 1998); (Schlötzer-Schrehardt and Kruse, 2005) (Figure 5).

Basal limbal cells are morphologically characterized by a small size, poor differentiation, high nucleus/cytoplasm ratio, euchromatin-rich nucleus and minimally differentiated cytoplasm (Romano et al., 2003); (Chen Z. et al., 2004). In contrast, the basal central corneal epithelium is characterized by low nucleus/cytoplasm ra-

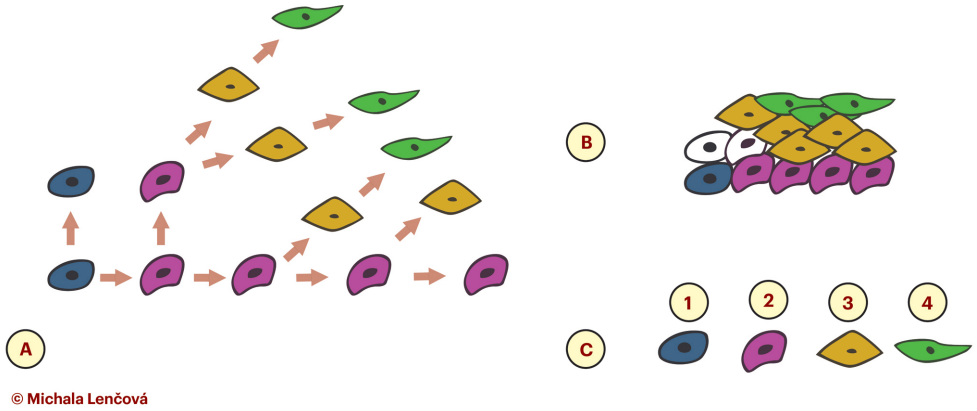

Figure 5: **Limbal stem cell concept: A)** asymmetric limbal stem cell division; **B)** Limbal and corneal epithelium stratification; **C)** Cells contributing to epithelial maintenance: 1. Limbal stem cells; 2. Transient amplifying cells; 3. Post-mitotic cells; 4. Terminally differentiated cells; (Courtesy of Michala Lenčová)

tio, heterochromatin-rich nucleus and cytoplasm with a high amount of ribosomes and tonofilaments (Chen Z. et al., 2004). The cell size correlates with cell differentiation phenotypes and proliferative capacity in human corneal epithelial cells, whereby the small cell size may represent one of the important properties of adult corneal epithelial SCs (De Paiva et al., 2006). The basal limbal cells contain a melanin pigment, which protects the cells from ultraviolet light damage (Wolosin et al., 2000).

The adult tissue-specific SCs express the side-population (SP) phenotype, which is characterized by the ability to efflux the DNA-binding vital dye Hoechst 33342 (Budak et al., 2005); (Umemoto et al., 2005). ATP-binding cassette subfamily G member 2 (ABCG2) is a transporter important for determining the limbal SP phenotype (Shaharuddin et al., 2013). The SP phenotype is a property of SCs (Shimano et al., 2003); (Zhou et al., 2001). Several animal and human studies showed that only a small fraction (from 0.2% to 0.9%) of limbal cells exhibit the SP phenotype (Watanabe et al., 2004); (Budak et al., 2005); (Umemoto et al., 2006); (Kusanagi et al., 2009); (Akinci et al., 2009).

In a mouse model, the cells with LSC markers and characteristics isolated from adult limbal tissue suppress the pro-inflammatory immune response and are themselves more resistant to apoptosis than other adult cell populations (Holan et al., 2010). These results suggest that immune-modulatory and self-protecting properties of LSCs are the general properties of SCs, which may contribute to their survival. LSCs also display an enhanced expression of genes for the anti-apoptotic proteins, a property that is imperative for the survival of transplanted tissues (Shaharuddin et al., 2013).

1.4.3 Limbal stem cell markers

The unique SC marker for LSCs has not yet been identified, therefore the LSC identification methods are indirect. A large amount of putative LSC markers were proposed. The major LSC markers include the expression of the drug resistance membrane transporter ABCG2 (De Paiva et al., 2005), the nuclear transcription factor p63α (Pellegrini et al., 2001); (Di Iorio et al., 2005), integrin α9 (Schlötzer-Schrehardt and Kruse, 2005), keratin K19 (Kasperet al., 1992), C/EBPδ and Bmi1 (Barbaro et al., 2007), the ligand-activated transmembrane receptor Notch-1 (Thomas et al., 2007) and the absence of cornea-associated differentiation markers such as the keratin K3, K12, the gap junction protein - connexin 43 and the transmembrane receptor E-cadherin (Liu et al., 1993); (Matic et al., 1997); (Chen Z. et al., 2004).

Currently, a combination of positive markers specific for undifferentiated SCs (transcription factor p63, membrane protein ABCG2, vimentin and keratin K19), and an absence of markers typical for differentiated corneal epithelium (connexin 43, keratin K3 and K12) is used for LSC determination (Schlötzer-Schrehardt and Kruse, 2005). Moreover, SC morphology can be used in combination with putative SC markers (O'Sullivan and Clynes, 2007). The finding of universal SC markers would enable LSC identification, isolation and use of SC enriched population for the treatment of LSCD.

1.4.4 Limbal stem cell niche

It is well known that the 'niche' is an essential microenvironment for SC that nurtures the cells and maintains their stemness. The LSC niche is located at the limbus within the palisades of Vogt and the LSC stemness is controlled by various intrinsic and extrinsic factors (Li et al., 2007). The limbal niche cells have been suggested to modulate LSC maintenance, proliferation and differentiation by producing specific matrix components, secreting growth factors and signaling molecules in a tightly regulated spatial and temporal pattern (Li et al., 2007). LSCs are in close contact with specific basal membrane vessels and stromal fibroblasts. Such configuration enables LSCs to maintain their high supply of nutrition and growth factors (Schlötzer-Schrehardt and Kruse, 2005). The pronounced heterogeneity of the basement membrane at the corneal-limbal transition zone provides unique microenvironments for corneal epithelial stem cells and late progenitor cells (Schlötzer-Schrehardt et al., 2007). Specific cell surface receptors and adhesions molecules appear to mediate LSC anchorage to their niche (Ordonez and Girolamo, 2012). The underlying limbal niche stroma plays a crucial role in modulating the LSC stemness, in contrast to corneal stroma, which promotes the epithelial cell differentiation (Espana et al., 2003). Reproducing the LSC niche enables it to prepare optimal *in vitro* conditions for SC culture and thus to obtain a good quality of cell cultures for *in vivo* transfer. Therefore further investigation of niche characteristics would be beneficial for LSC *ex vivo* expansion.

1.5 Limbal stem cell deficiency

1.5.1 Etiology

LSCs are essential for corneal epithelium regeneration and also act as a barrier against conjunctival overgrowth onto the cornea. After LSC source loss, corneal conjunctivalization takes place: it is accompanied by vascularization, recurrent defects, chronic inflammation, corneal cicatrization and opacity. This condition is called LSCD and can lead to loss of vision. Corneal scarring and opacity is the fifth most common cause of global blindness (Resnikoff et al., 2004). However, the incidence and prevalence of LSCD throughout the world is unknown. The incidence of LSCD in North America is estimated to be in the thousands (Schwab et al., 2000), LSCD prevalence in India is approximately 1.35 million (Vemuganti and Sangwan, 2010). Global blindness caused by LSCD could, in fact, be higher due to corneal scarring caused by trachoma, which is the sixth most common cause of global blindness (Resnikoff et al., 2004).

LSCD can be subdivided into congenital, acquired and idiopathic (Espana et al., 2002). Congenital LSCD is characterized by insufficient stromal microenvironment for LSC support and the absence of external causes. This group includes aniridia (Nishida et al., 1995); (Skeens et al., 2011), multiple endocrine deficiencies (Puangsricharern and Tseng, 1995), epithelial and stromal dystrophies (Dunaief et al., 2001), lacrimo-auriculo-dento-digital syndrome (Cortes et al., 2005), and xeroderma pigmentosa (Fernandes et al., 2004). Hereditary aniridia is characterized by non-development of the iris (Hill et al., 1991). The PAX6 (paired box 6) gene is one of the main regulatory genes involved in the development of the eye and LSCs: therefore the gene defect disrupts normal corneal epithelium formation (Collinson et al., 2004). Clinically congenital aniridia is characterized by weak corneal epithelium differentiation, corneal conjunctivalization and neovascularization (Li et al., 2008).

Acquired LSCD is more common in clinical practice than congenital LSCD. LSC and niche destruction is caused by external insults through direct damage or as a consequence of a post-injury inflammatory process. The acute and chronic inflammation of the ocular surface leads to exhaustion of the LSC population, which causes conjunctivalization and, ultimately, complete corneal opacity and blindness (Dua et al., 2010). Examples of acquired LSCD include chemical or thermal injuries (Fish and Davidson, 2010), exposure to ultraviolet and ionizing radiation (Fujishima et al., 1996), (Shortt et al., 2014), advanced ocular cicatricial pemphigoid (Shimazaki et al., 2007), multiple surgeries or cryotherapies (Puangsricharern and Tseng, 1995), long-standing contact lens wear (Chan and Holland, 2013) and extensive or chronic infection such as trachoma (Kremer et al., 2009).

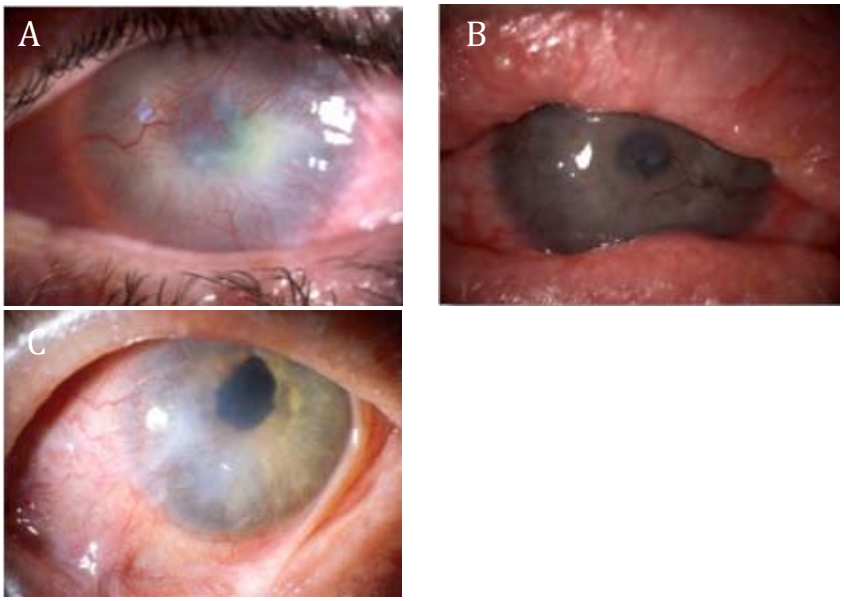

Figure 6: **Clinical picture of limbal stem cell deficiency (LSCD): A)** Total LSCD after chemical burn injury; **B)** Total LSCD in ocular cicatricial pemphigoid; **C)** Partial LSCD after chemical injury. (Courtesy of Ivan Kolín)

1.5.2 Clinical signs

LSCD symptoms include impaired vision, photophobia, and tearing, recurrent episodes of pain, blepharospasm, and red eye (Dua and Azuara-Blanco, 2000). Clinical features of LSCD include corneal conjunctivalization, neovascularization, chronic inflammation, recurrent and persistent epithelial defects, scarring, fibrovascular pannus, ulceration, keratolysis, perforation, and keratinisation (Dua, 2006)(Figure 6). The conjunctival epithelium over the cornea is irregular and thin with a dull reflex and there is stippled staining of fluorescein dye comparing to corneal epithelium (Dua et al., 1994). The alteration of limbal anatomy with loss of the palisades of Vogt can also be seen (Dua et al., 2003).

1.5.3 Diagnosis

Diagnosis of LSCD is based on a detailed history and clinical findings. In particular, the clinical triad of corneal conjunctivalization, neovascularization and chronic inflammation should be confirmed (Chen and Tseng, 1990); (Kruse et al., 1990); (Chen and Tseng, 1991). However, impression cytology can be used to confirm the diagnosis (Puangsricharern and Tseng, 1995). It is a useful tool to prove the presence of conjunctival epithelium and goblet cells on the conjunctivalized cornea and can be combined with immunohistochemistry of keratin K19, K7 and K13 (Donisi et al., 2003); (Singh et al., 2005); (Jirsova et al., 2011); (Ramirez-Miranda et al., 2011). Nevertheless, keratin detection could be helpful for identifying conjunctival epithelium when the impression cytology does not prove the presence of goblet cells on the conjunctivalized cornea. Goblet cells may not be detected in the presence of severe chronic inflammation (Tsubota et al.,

1995). *In vivo* confocal microscopy can be useful for diagnosis and monitoring of limbal structural changes in patients with LSCD and can be combined with impression cytology (De Nicola et al., 2005); (Barbaro et al., 2010); (Lagali et al., 2013). However, some authors believe that the clinical signs of LSCD are sufficient for diagnosis assessment and therefore do not use impression cytologic analysis in their studies (Rama et al., 2010); (Chan and Holland, 2013). In clinical practice, it may be more difficult to clearly distinguish the conjunctival epithelium from the corneal epithelium. The conjunctival epithelium is translucent and dull compared to the corneal epithelium but its opacity may be due to corneal scarring. In addition, stippled fluorescein staining due to abnormal conjunctival epithelium can be seen by the pooling of fluorescein dye at the junction of abnormal and remaining normal corneal epithelium (Dua, 2006). Biopsy of the fibrovascular pannus can show the multilayered epithelium, vascularization and intraepithelial lymphocytes along basal layers, which are the features of the conjunctival epithelium (Dua, 2006). In patients with a less clinically obvious LSCD diagnosis, biopsy of the fibrovascular pannus is desirable to exclude other pathologies like xeroderma pigmentosa (Gupta et al., 2011).

1.6 Treatment of limbal stem cell deficiency

Nomenclature for the various ocular surface transplantation procedures uses the anatomic source of the transplanted tissue (conjunctival, limbal and other mucosal grafts), the donor cell genetic source (autograft, living non-related and living related allograft, cadaveric allograft) and the donor cell type (tissue or *ex vivo* cultured cells) (Daya et al., 2011).

1.6.1 Prophylaxis of limbal stem cell deficiency

The incidence of LSCD can be diminished by prompt anti-inflammatory therapy, which reduces the risk of consequent LSC exhaustion and cicatricial complications in the chronic phase, both of which can lead to corneal blindness. Ocular surface injury involving the limbus does not ascertain that LSCs at the basal layers are completely destroyed at the time of insult (Liang et al., 2009). Therefore, appropriate treatment during the acute phase is essential, especially in chemical burns and Steven-Johnson syndrome. Persistent inflammation is described as a main risk factor for LSCD (Puangsricharern and Tseng, 1995). Early application of the amniotic membrane (AM) after chemical injury suppresses the inflammation and reduces the risk LSCD development (Meller et al., 2000). Several studies have showed that AM application after chemical burns promotes epithelial healing, reduces corneal haziness and prevents cicatricial complications such as symblepharon formation (Meller et al., 2000); (Kobayashi et al., 2003); (Prabhasawat et al., 2007). The beneficial effect of AM was also demonstrated in the acute phase of Stevens-Johnson syndrome and toxic epidermal necrolysis in other studies (Di Pascuale et al., 2005); (Kobayashi et al., 2003). As another effective treatment, modality nanofibers may be used for SC transfer and, with this in mind, we decided to investigate in greater detail.

1.6.2 Limbal tissue transplantation

LSCD therapy is based on LSC recovery. However, the treatment is complex and the outcome depends, not only on the LSC replacement, but also on timing the LSC surgery to take place during a quiescent stage; the reconstruction of ocular surface abnormalities; and treatment of underlying dry eye, glaucoma and systemic disease (Dua et al., 2010). Uncontrolled ocular inflammation and eyelid deformations have been associated with reduced graft survival (Tsai and Tseng, 1995); (DeSousa et al., 2009). LSCD patients are not suitable for conventional corneal transplantation, which offers only temporary corneal epithelium recovery in recipients and does not substitute LSC function (Dua et al., 2010). Therefore, transplantation of an LSC source is the only treatment. Current treatment of LSCD is via tissue transplantation of the limbus or via transfer of *ex vivo* cultured LSCs to an LSC deficient recipient eye. The management of LSCD depends on its extent, which is classified as unilateral or bilateral, partial or total.

In partial LSCD or in the unaffected eye in unilateral LSCD, LSCs are still present and these cells can therefore be used for tissue transplantation or LSC culture. The use of autologous tissue has the advantage of not causing immune rejection in the recipient and thus has a higher rate of survival and does not require systemic immunosuppression. In 1989, Kenyon and Tseng described how the corneal surface can be restored via direct transfer of a healthy limbal autograft. Since then, there has been much evidence of successful autologous limbal transplantation for unilateral LSCD (see review (Sangwan et al., 2014)). Autologous and living-related (LR) grafts have the advantage of being very "fresh", or relatively young. They are superior to cadaveric tissue with regard to LSC content but their availability is limited (Dua et al., 2010). However, there is a risk of iatrogenic donor-site LSCD after harvesting the limbal graft. Therefore, it is necessary to exclude clinically subtle signs of LSCD in the donor eye and graft length should not exceed 30° (Tan et al., 1996); (Miri et al., 2011). After autologous and living-relative limbal transplantation, it is necessary to observe the re-epithelization process during the postoperative period because limbal areas that are not fully covered are at risk of conjunctival epithelium overgrowth onto the cornea.

Treatment of total bilateral LSCD, in which a new source of LSCs must be provided vie allografts from LR, cadavers or *ex vivo* cultured epithelial cells is more challenging (Dua, 2006). The cadaveric grafts have the advantage of serving the whole limbus, which can cover the entire recipient bed. The disadvantage is immune non-histocompatibility with a high risk of rejection and the need for systemic immunosuppression (Holland, 1996); (Dua and Azuara-Blanco, 1999). Technically, the LR grafts are harvested in the same manner as the limbal autografts (Rao et al., 1999); (Miri et al., 2011). The cadaveric graft can be obtained from the whole eye bulbus (Tsubota et al., 1995); (Dua and Azuara-Blanco, 1999) or from the sclero-corneal ring (Holland, 1996). Several techniques involving cadaveric limbal harvesting and limbal transplantation have been described. The cadaveric donor graft can have a ring shape (Tsubota et al., 1999) or two semi-

circular segments (Holland, 1996). The grafts can be also prepared from two cadaveric donors in which one donor limbal ring is cut in one place and the gap is filled with a small limbal segment from the second donor. The posterior placement of these grafts facilitates subsequent corneal transplantation (Dua et al., 2010). Limbal transplantation can be combined with AM and penetrating keratoplasty (Dua et al., 2008); (Barreiro et al., 2014). Human leukocyte antigen (HLA) tissue matching enables the most suitable LR graft to be selected for the recipient, however, the disadvantages of this procedure are the cost and delay of tissue availability (Javadi and Baradaran-Rafii, 2009). Despite HLA matching, complete immune-histocompatibility match cannot always be obtained and systemic immunosuppression is still required after transplantation (Tsubota et al., 1995); (Dua et al., 2000).

1.6.2.1 Limbal graft rejection and survival

Limbal allograft rejection has typical clinical signs. Acute rejection is characterized by limbal edema, hyperemia and an epithelial rejection line over the cornea (Baradaran-Rafii et al., 2013). Chronic rejection is described as a low-grade inflammation with no visible signs of rejection and perilimbal engorgement with vessel stagnation may be present (Baradaran-Rafii et al., 2013). Therefore, regular follow-ups, early recognition of rejection and appropriate topical and systemic medication is necessary in the postoperative period.

The strong immune response in limbal allotransplantation differs from corneal transplantation, in which immune privilege is defined. The limbal donor graft is highly antigenic and contains Langerhans cells and HLA-DR antigens, which enable greater host recognition of the graft. Additionally, the recipient limbal area possesses blood vessels, lymphatics and Langerhans cells, enabling acute allosensitization and swift rejection (Pels et al., 1984); (Williams and Coster, 1989); (Niederkorn, 1995); (Daya et al., 2000). However, rejection has been described even after transplantation of cultured allogeneic limbal cells (Qi et al., 2013). On a cellular level, the MHC class II^+, cluster of differentiation ($CD4^+$), $CD8^+$ cells are detected during graft rejection (Miyazaki et al., 1999); (Chen W. et al., 2004); (Qi et al., 2013). The major and minor histocompatibility antigens are both related to corneal epithelial rejection and appear to be mediated primarily by a delayed-type hypersensitivity (DTH) response, similar to penetrating corneal grafts, rather than by a cytotoxic T lymphocyte (Yao et al., 1995); (Miyazaki et al., 1999); (Maruyama et al., 2003). To avoid rejection, long-term local and systemic immunosuppression is necessary after allogeneic limbal tissue or cultured limbal cell transplantation. Different protocols are currently available. Postoperative therapy includes the application of oral prednisolone, cyclosporine (Tsubota et al., 1999), azathioprine (Williams et al., 1995), tacrolimus (Dua and Azuara-Blanco, 2000); (Sloper et al., 2001), mycophenolate mofetil (Reinhard et al., 2004) or steroid sparing combined therapy of mycophenolate mofetil and tacrolimus (Holland et al., 2012). Therapy duration is not uniform among ophthalmologists. Some surgeons prefer to use life-long immunosuppression, while others for a period

of at least 2 years. Despite potent immunosuppressive therapy, severe allograft rejection may occur (Thoft and Sugar, 1993); (Holland, 1996); (Daya et al., 2000); (Cauchi et al., 2008).

There are a limited number of animal studies focusing on immunosuppression after limbal allograft transplantation. In rabbit models, rejection episodes can be reduced by topical corticosteroids or by systemic and topical cyclosporine A. Contrary to these results, human AM showed no beneficial effect to graft survival (Dios et al., 2005). In a rat model of enhanced green fluorescent protein (E-GFP) labelled limbal transplantation, significantly prolonged survival of allografts was observed in a group treated by clodronate liposome applied subconjunctivally to the untreated allografts. Minor infiltration of macrophages and lymphocytes ($CD4^+$ and $CD8^+$ cells) was shown in the treated group (Keijser et al., 2006). However, the survival of donor cells derived from limbal grafts after transplantation remains unclear. Animal studies show that the donor cells did not survive on the ocular surface despite the use of systemic immunosuppression (Mills et al., 2002). The long-term results after limbal transplantation show that the ocular surface is not regenerated by the donor graft cells despite good clinical results (Henderson et al., 2001); (Daya et al., 2005). There is a need for further research into effective and safe immunosuppression on donor graft survival. Testing of the monoclonal antibodies aimed against the immune cells as an immunosuppressive treatment may be a worthwhile approach.

1.6.2.2 Experimental models of limbal transplantation

The availability of inbred, transgenic and gene-targeted strains of rodent has provided important information on the mechanisms of corneal graft rejection (Williams and Coster, 2007). The mouse model enables a large amount of genetically targeted and inbred strains with a well-defined immune system to be used. However, the disadvantage is the small size of the eye, which makes limbal transplantation very challenging from a surgical point of view. The rat model provides a variety of inbred strains, and limbal transplantation is technically easier because of the larger eyeball. Anatomically, the rabbit model is closer to the human eye, but entirely inbred strains are not available and the immune system is not as well defined as it is in the murine model and the choice of antibodies is limited.

Early animal studies focused on limbal syngrafts and proved more beneficial effects of limbal syngrafts in restoring the ocular surface compared to conjunctival syngrafts (Tsai et al., 1990). Further rabbit studies described how the intensive stromal inflammation impedes the capability of limbal syngrafts to attain normal corneal epithelial recovery and leads to poorer prognosis (Tsai and Tseng, 1995). Taken together, not only the graft origin, but the corneal stromal environment upon which the graft is placed has an important influence upon the graft (Moore et al., 2002). For epithelial cell migration study in the murine model, the green fluorescent protein (GFP) labelled paracentral corneal and limbal autografts were

used in which the paracentral grafts demonstrated significant increase in proliferative potential on third day postoperatively than the limbal grafts (Moore et al., 2002). GFP expressing transgenic mouse, in conjunction with *in vivo* microscopy, enables the movement of epithelial cells in the normal cornea to be observed (Nagasaki et al., 2003). E-GFP-labelled isografts and allografts were used for assessment of graft survival in a rat limbal model (Keijser et al., 2006). Further studies are needed to understand limbal graft behavior after transplantation.

1.6.3 Stem cell-based therapy

The transfer of *ex vivo* cultured LSCs is currently a very favorable method for LSCD therapy. The concept of *ex vivo* cultured SCs has derived from the use of cultured human epithelial cells as autologous grafts in burns patients (Phillips and Gilchrest, 1992); (Croasdale et al., 1999). In 1997, for the first time, Pellegrini et al. reported that autologous cultured human corneal epithelial cells restored the damaged corneal surface in the long term (Pellegrini et al., 1997). Limbal epithelial cells can be harvested by biopsy from the contralateral healthy eye in unilateral LSCD. In bilateral disease, the donor cells can be obtained from the healthy limbal region of living relatives or from cadaveric corneoscleral rim. Subsequently, the cells are cultured in the laboratory until a sufficient amount of cells is obtained, which can be transferred onto the ocular surface (Schwab, 1999); (Koizumi et al., 2001); (Rama et al., 2010).

Compared to autologous and living-related tissue limbal transplantation, *ex vivo* LSC culture has the advantage of minimizing the risk of ocular surface decompensation in the healthy eye by taking only minimal limbal biopsy (2 mm x 2 mm), which can be also repeated following unsuccessful cultured limbal epithelial cell transplantation (Basu et al., 2012a). Furthermore, *ex vivo* cultured cells do not obtain the Langerhans antigen-presenting cells and blood vessels, therefore there is a reduced risk of acute and chronic rejection but the risk is not fully diminished (Schwab et al., 2000); (Shortt et al., 2007); (Qi et al., 2013).

1.6.3.1 Limbal stem cell isolation and culture methods

Since *in vitro* culture of LSC was first demonstrated by Sun and Green (1977), many epithelial cell culture strategies have been introduced (Sun and Green, 1977). Two main strategies of LSC proliferation are currently being used: the explant culture technique and the single cell suspension technique. In the explant culture technique, a small limbal explant is taken by biopsy and placed either on the human AM on the basement membrane side or on plastic culture plates with 3T3 feeder or on human AM with 3T3 feeder as a co-culture (Grueterich et al., 2003); (Sangwan et al., 2003); (Joseph et al., 2004). The AM and 3T3 feeders inhibit the differentiation of corneal epithelial cells *ex vivo* and allow the LSC to expand (Pellegrini et al., 1999); (Grueterich et al., 2002). In single cell suspension technique, the limbal epithelial cells of the explant are enzymatically separated

from the stroma by dispase. This is followed by trypsin digestion of epithelial clusters until single cell suspension is obtained. The limbal epithelial cells are placed either on human AM or on other substrates like plastic plates with 3T3 feeder, fibrin or modified surfaces (Rama et al., 2001); (Koizumi et al., 2007); (Notara et al., 2007). The cell suspension culture technique was significantly superior to the explant culture technique in terms of SC content, however, the explant technique is easy to perform and has no risk of enzymatic damage to donor cells (Koizumi et al., 2002).

The composition of the culture medium is very important, not only for epithelial cell propagation, but also for retaining the SC phenotype and for cell modulation. In 1975, in their pioneering work, Reinwald and Green described the culturing method of human epidermal keratocytes by using a mouse 3T3 feeder layers later applied to LSC culturing (Rheinwald and Green, 1975). Cell culturing enables a sufficient amount of cells needed for transplantation to be obtained. Current protocols for the *ex vivo* culture of LSC use different allogeneic and animal materials (human AM, mouse 3T3, fetal bovine serum (FBS)), which have potential risks of infection, tumorigenesis, precipitating immunologic rejection and acquisition of prion disease (Schwab et al., 2006). Therefore, there is a need to use a safer xeno-free culture system. To eliminate the risk, autologous human serum can be used as an alternative to FBS and the first reports with a completely xeno-free culture technique have recently been made available (Nakamura et al., 2006); (Mariappan et al., 2010); (Sangwan et al., 2011); (Basu et al., 2012b).

1.6.3.2 Transfer of cultured limbal stem cells

For SC-based therapy, the use of a suitable carrier for growth and transfer of cultured cells onto the ocular surface is crucial. To date, various substrates have been tested and used for culture and transplantation. The most commonly used carrier for LSC is human AM (Tsai et al., 2000). The human AM stroma serves as a pool of various growth factors, anti-inflammatory, anti-angiogenic proteins and inhibitors of proteases (Güell et al., 2006). However, due to human AM variability, risk of infection and crease formation, it is not an ideal substrate and other scaffolds have been proposed for SC therapy (Levis and Daniels, 2009). Fibrin-based scaffolds (Rama et al., 2001); (Talbot et al., 2006), contact lens-based scaffolds (Di Girolamo et al., 2009) or synthetic polymers (Sharma et al., 2011) and various types of nanofiber scaffolds (Dubský et al., 2012) have been used as an alternative scaffold for cell culture and transfer collagen scaffolds (Schwab et al., 2006); (Dravida et al., 2008).

Clinically, successful transplantation is considered to be the improvement of LSCD clinical findings and visual acuity. The long-term success rate of autologous cultured epithelial cell transplantation for LSCD was shown in several animal and clinical studies (Schwab, 1999); (Koizumi et al., 2001); (Shimazaki et al., 2007); (Rama et al., 2010); (Sangwan et al., 2011). Repeated surgery even increased the clinical outcome of the cell transplantation (Basu et al., 2012a). A recent study by

co-authors Shortt et al. showed the beneficial effect of *ex vivo* cultured allogeneic corneal epithelial cells for a period of 12 months in patients with LSCD, however clinical deterioration was observed after this period (Shortt et al., 2014). However, allogeneic *ex vivo* cultured limbal epithelial cells from cadavers have lower proliferative rate *in vitro* compared to cells from fresh limbal tissue from living donors (Vemuganti et al., 2004) and a lower corneal epithelisation rate *in vivo* compared to living relative donors (Prabhasawat et al., 2012). Despite good postoperative result after transplantation of cultured cells, there is controversy surrounding the origin of cells regenerating the surface over the long term. The clinical study of *ex vivo* cultured allografts showed that restored ocular surface is not regenerated by donor-derived cells beyond 9 months (Daya et al., 2005). These findings question the need for long-term use of systemic immunosuppression. Contrary to these results, clinical studies of limbal tissue allotransplantation proved the presence of donor-derived cells on the ocular surface after 3 years (Reinhard et al., 2004); (Djalilian et al., 2005).

Recent publications show promising results for SC-based treatment in ocular surface disorders. However, it is necessary to find an optimal scaffold for the SCs. Therefore, one of the objectives of our investigation was to test a new tool for SC transfer and analyze the effect of the co-transfer of LSCs and MSCs.

1.6.3.3 Alternative sources for cell-based therapy

In bilateral LSCD, there is no autologous limbal tissue available for ocular surface reconstruction. Therefore, the LSC source needs to be substituted by allogeneic limbal grafts either from living donors (family- or non-family related) or from cadavers. These procedures require long-term systemic immunosuppression to prevent rejection, which has a risk of side effects in patients (Sloper et al., 2001); (Liang et al., 2009). Therefore, the search for alternative non-limbal autologous cells is a promising therapeutic approach for ocular surface reconstruction in regenerative medicine with the advantage of not needing systemic immunosuppression. Epithelial and non-epithelial cells have been proposed as an alternative SCs source for LSCD.

To date, several sources of alternative epithelial cells for ocular surface reconstruction have been reported in animal and human studies. *Ex vivo* cultured oral mucosal epithelium transplantation (COMET) has been well documented. Initially, the potential of COMET was proven in animal models of LSCD (Nakamura et al., 2003); (Nakamura and Kinoshita, 2003), subsequent clinical studies have given promising long-term results in ocular surface restoration of LSCD (Nishida et al., 2004); (Shimazaki et al., 2007); (Nakamura et al., 2011); (Priya et al., 2011). Oral mucosal cells are easily available, however these cells possess more angiogenic potential than cultured corneal epithelial cells (Kanayama et al., 2007). Therefore, a varying degree of peripheral corneal neovascularization occurs following corneal transplantation (Inatomi et al., 2006). Another alternative epithelial source for treatment of LSCD is the *ex vivo* cultured conjunctival epithelium, which was

used in a rabbit model (Tanioka et al., 2006); (Ono et al., 2007); (Ang et al., 2010) and clinical studies demonstrated favorable results (Sangwan et al., 2003); (Di Girolamo et al., 2009); (Ricardo et al., 2013). Cultured epidermal epithelial cells were successfully used for corneal reconstruction in a goat model with total LSCD (Yang et al., 2008).

Several non-epithelial alternative SCs have been studied *in vitro* and *in vivo* in experimental models of damaged ocular surface. MSCs represent one of the potential sources of autologous non-epithelial SCs with promising results for ocular surface reconstruction (see review by (Li and Zhao, 2014)). MSCs have a heterogeneous population of non-hematopoietic cells with multi-lineage potential (Pittenger et al., 1999). These cells were described as spindle shaped cells derived from bone marrow that adhere to plastic and form fibrocyte-like colonies (Friedenstein et al., 1970). They can be isolated from bone marrow or other adult tissue including adipose tissue, umbilical cord blood, heart tissue, oral tissue, etc. and have the capacity for extensive proliferation *in vitro* (Zannettino et al., 2008); (Hoogduijn et al., 2007); (Zhang et al., 2009). The studies showed that bone-derived MSCs suppress T lymphocyte proliferation *in vitro* (Di Nicola et al., 2002); (Le Blanc et al., 2003), the differentiation of cytotoxic $CD8^+$ T lymphocytes (Angoulvant et al., 2004) and nitric oxide (NO) production (Sato et al., 2007). The immune-modulatory properties of MSCs have been demonstrated *in vivo* in animal models (Bartholomew et al., 2002); (Casiraghi et al., 2008). MSCs derived from bone marrow and adipose tissue have been proposed in experimental studies of corneal chemical injury (Ma et al., 2006); (Oh et al., 2008); (Ho et al., 2011). The transplantation of bone marrow-derived MSCs after corneal chemical burn showed anti-inflammatory and anti-angiogenic activity in rat models (Ma et al., 2006); (Oh et al., 2008). Bone marrow-derived MSC transplanted onto damaged rabbit cornea differentiated into corneal epithelial-like cells (Gu et al., 2009). The differentiation of engrafted MSC contributed to the corneal wound healing process and reconstruction of the ocular surface after chemical injury (Ye et al., 2006); (Jiang et al., 2010). However, there is a need for further studies to elucidate the mechanism of MSC effectiveness and find a suitable scaffold for transfer onto the ocular surface.

Another potential source of non-epithelial SCs includes cultured hair follicle-derived SCs, which were used to treat LSCD in mice and rabbit experimental models (Blazejewska et al., 2009); (Meyer-Blazejewska et al., 2011). The cultured dental pulp SCs and umbilical cord SCs were successfully transplanted for ocular surface reconstruction in the rabbit LSCD model (Gomes et al., 2010); (Reza et al., 2011). Induced epithelial progenitor cells from mouse embryonic SCs regenerated the damaged ocular surface in mice (Homma et al., 2004). Human embryonic SCs have shown the ability to differentiate into corneal-like cells *in vitro* (Ahmad et al., 2007). Recently, corneal epithelial cells were generated from induced pluripotent SCs derived from human dermal fibroblasts and corneal limbal epithelium (Hayashi et al., 2012).

2 AIM

The aim of this thesis was to study the reconstruction of damaged ocular surface by transfer of LSCs in the mouse experimental model. Due to LSC deficiency, ocular surface reconstruction is one of the most challenging issues in current ophthalmology. The loss of LSC source through ocular surface damage leading to blindness can be resolved by LSC transplantation. The clinical course and cellular mechanisms of limbal graft rejection have to be recognized in order to develop a successful strategy to manage immune reaction in limbal allo- and xeno-transplantation. This thesis summarizes the results of limbal tissue transplantation, characterization of immune response and immunosuppressive therapy in the mouse model. In addition, the LSC isolation method, *ex vivo* culture of LSCs and MSCs on nanofiber scaffolds and their *in vivo* transfer were studied and applied for ocular reconstruction in the mouse and rabbit experimental model.

1. Firstly, we introduced an experimental model of orthotopic limbal transplantation into our laboratory to evaluate limbal allograft and xenograft survival. We decided to characterize the immune response to limbal graft, analyze donor-derived cell survival and assess the effect of systemic immunosuppression in the form of monoclonal antibodies.

2. Then we investigated an optimal LSC isolation method from limbal explant, which can be used for further SC-based experiments including LSC culture and transfer for ocular surface reconstruction in the experimental mouse model.

3. We intended to test a new nanofiber scaffold for SC transfer and analyze the effect of co-transfer of LSCs and MSCs onto the damaged ocular surface in the mouse model. We investigated whether the selected nanofiber scaffolds are useful and suitable for SC culturing and transfer onto the ocular surface in the mouse model. We used our established limbal allotransplantation model to analyze the anti-inflammatory effect of the transferred cultured cells.

4. There is a need for further studies to elucidate the mechanism of MSC effect in chemical burns in the acute phase and to find a suitable scaffold for transfer before clinical application. The results from our previous experiments in the mouse model led us to investigate the effect of MSCs transferred on nanofiber scaffolds in further detail. We decided to study whether rabbit bone marrow-derived MSCs on nanofiber scaffolds effectively decrease alkali-induced oxidative stress in the rabbit cornea after chemical injury and whether this can contribute to the healing process.

The results of our experiments have already been published and the publications with detailed descriptions of the methods used, results and discussion are attached in their original published form in the appendix at the end of this thesis.

3 MATERIALS AND METHODS

Detailed descriptions of the methods used are mentioned in the publications in the appendix.

3.1 Animals

3.1.1 Mouse experimental model

Mice of both sexes of the inbred strains BALB/c and C57BL/6 (B6) at the age of 7-10 weeks and rats of the inbred strain Lewis at the age of 7-8 weeks were used for the experiments. The mice were from the breeding unit of the Institute of Molecular Genetics, Prague; rats were purchased from the Institute of Physiology, Academy of Sciences, Prague. The local Animal Ethics Committee approved all of the experiments (xenogeneic model of limbal transplantation). The mice were anesthetized before the operation by intramuscular injection with a mixture of xylasine (Rometar, Spofa, Prague, Czech Republic) and ketamine (Calypsol, Gedeon Richter Ltd, Budapest, Hungary) (Publication 1).

3.1.2 Rabbit experimental model

Adult female New Zealand white rabbits (2.5-3.0 kg) were used in our experiments. The investigation was conducted according to the ARVO Statement on the Use of Animals in Ophthalmic and Vision Research. Rabbits were anesthetized by an intramuscular injection of Rometar (Xylazinum hydrochloricum, Spofa, Prague, CR, 2%, 0.2 ml/1 kg body weight) and Narkamon (Ketaminum hydrochloricum, Spofa, 5%, 1 ml/1 kg body weight) (Publication 4).

3.2 Surgical techniques, clinical evaluation and immunosuppression

3.2.1 Technique of limbal transplantation in murine model

The surgical method of limbal transplantation was a slight modification of the transplantation method described by Maruyama et al. (Maruyama et al., 2003). In brief, donor limbal lenticule was circularly cut out from conjunctiva without scleral tissue and around the cornea and was embedded into balanced salt solution. The rest of the corneal endothelium was removed from the lenticule. The width of the limbal graft was approximately 1.0 mm. The corneal epithelium of the recipient ocular surface was debrided by a sharp needle (G23) and the limbus was cut out with Vannas scissors (Duckworth & Kent, Baldock, England). The donor limbal graft was placed orthotopically and was secured with 5 interrupted sutures with 11.0 Ethilon (Ethicon, Johnson & Johnson, Livingston, UK) (Figure 7). The ophthalmic ointment compound containing bacitracin and neomycin (Ophthalmo-Framykoin, Zentiva, Prague, Czech Republic) was applied onto the ocular surface and the eyelids were closed for 72 hours by tarsorraphy using 7.0 Resolon suture (Resorba, Nuernberg, Germany). Mice with complications such as cataracts, hemorrhage etc. were excluded from the experiments. Only the

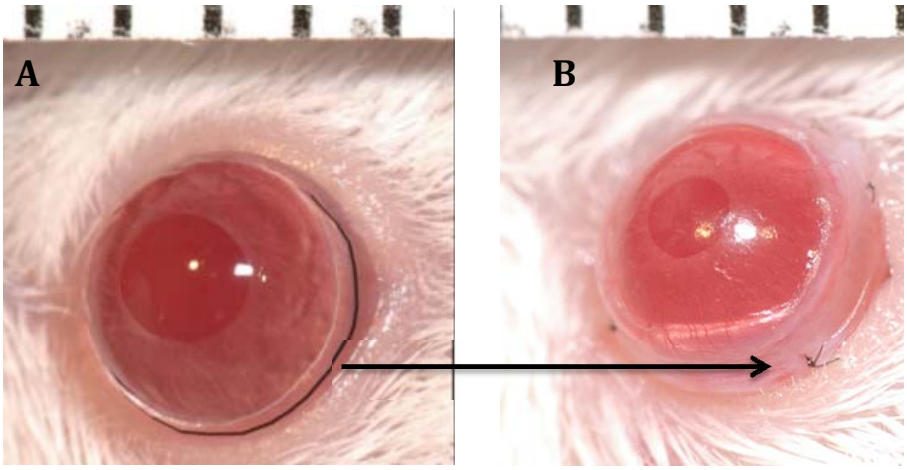

Figure 7: **Limbal transplantation technique: A)** The BALB/c mice recipient's eye before limbal transplantation, the donor limbus was circularly cut out; **B)** the recipient's limbus and corneal epithelium were surgically removed prior to surgery. The donor limbus was placed orthotopically and sutured with 5 interrupted stitches. (Courtesy of Ivan Kolín)

right eye was operated on. In all experiments BALB/c mice were used as the recipients and BALB/c mice (syngeneic grafts), B6 mice (allografts) or Lewis rat (xenografts) as the graft donors (Figure 8). To detect survival of allogeneic cells, limbal grafts from B6 male mice were grafted into BALB/c female recipients and the presence of cells expressing Sry (sex determining Y protein) (male specific) antigen was detected by real-time PCR.

3.2.2 Clinical evaluation of graft survival

Postoperatively the ocular surface was observed daily using the operating microscope. The corneal re-epithelization was followed by fluorescein staining. The cornea was scored for opacity and neovascularization and the limbal graft was evaluated for edema. A scoring scale ranging from 0 to 4 for corneal opacity was used to evaluate rejection (Maruyama et al., 2003). Corneal opacity was graded: 0) clear cornea, 1) lenticular or regional corneal epithelial edema, opacity or clearly visible iris vessels, 2) diffuse epithelial edema, opacity or both, obscuring iris vessels, 3) diffuse epithelial edema, opacity or both, iris vessels not visible, 4) anterior chamber not visible due to epithelial edema, corneal opacity, or both (Figure 9). If the opacity score reached 2 or more, the graft was considered as rejected. The following scoring system was used to evaluate limbal edema: 0) no edema, 1) focal slight limbal edema, 2) diffuse mild limbal edema, 3) moderate diffuse limbal edema, 4) severe diffuse limbal edema. The corneal neovascularization was graded as follows: 0) no vessels 1) incipient vessels reaching only the periphery of the cornea, 2) one-quarter of the cornea vascularized, 3) half of the cornea vascularized, 4) the entire cornea vascularized.

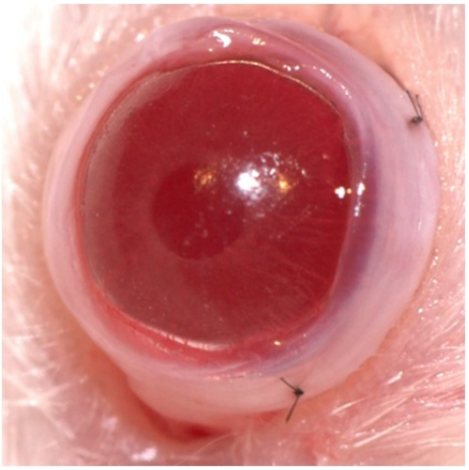

Figure 8: **Limbal graft transplantation in the mouse model:** The xenogeneic limbal graft soon after limbal orthotopical transplantation in BALB/c mice. (Courtesy of Ivan Kolín)

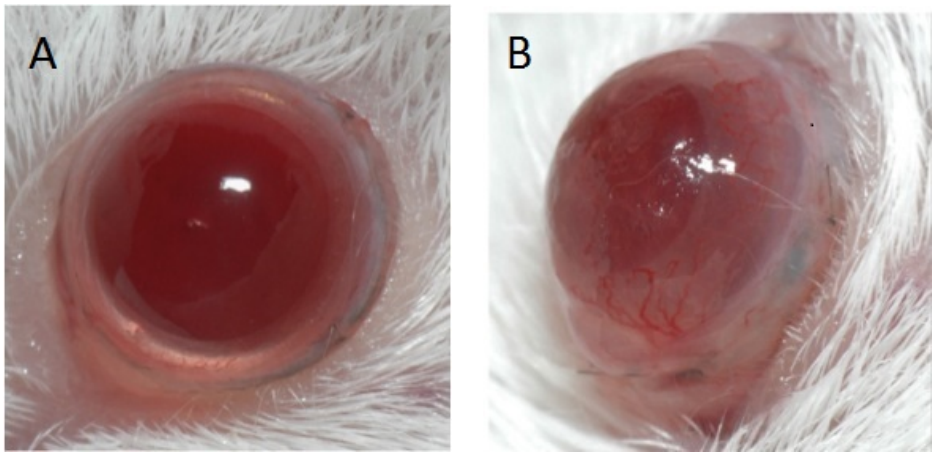

Figure 9: **Scoring of limbal graft rejection: A)** corneal opacity grade 0 (no rejection); **B)** corneal opacity grade 2 was considered as rejection of the limbal graft (Courtesy of Ivan Kolín)

3.2.3 Antibody treatment

Monoclonal antibodies (mAb) anti-CD4 (clone GK1.5) (Dialynas al., 1983) and anti-CD8 (clone TIB 150) (Gottlieb et al., 1980) were prepared in the form of ascites in nu/nu mice and were injected intraperitoneally at a dose of 200 μg of mAb per mouse per day. The treatment started on the day of grafting and continued every other day until rejection. Fluorescence-activated cell sorting analysis performed 1 week after the beginning of the treatment revealed that the numbers of targeted cell populations were reduced in both the spleen and lymph nodes to less than 1.5% of the level in control untreated animals and this selective lymphopenia was sustained for the duration of the treatment (data not shown). The control group was treated with physiological solution.

3.2.4 Transfer of nanofiber scaffolds

Three dimensional (3D) nanofiber scaffolds were prepared by an electrospinning technology from a polyamide 6/12, which was chosen according to best properties and biocompatibility for LSC and MSC growth and the stability of nanofiber scaffolds in aqueous solutions. In the mouse model, a 4-mm diameter nanofiber circle (with and without LSCs and MSCs) was used to cover the damaged limbal and corneal region. The nanofiber scaffolds were transferred with the cell side facing down to ocular surface (Figure 10). The scaffold was secured by 4 interrupted sutures using 11.0 Ethilon (Ethicon, Johnson & Johnson, Livingston, England). The eyelids were closed by tarsorrhaphy by 1 suture (Resorba 7.0, Resolon) for 3 days. The scaffolds were transferred in two models. The one model was characterized by removal of corneal epithelium and limbus in BALB/c mice. The transferred LSCs from BALB/c mice were labelled with PKH26 dye and the fate of cell survival was analyzed on the cryosections postoperatively. In the second model, a strong immune response was induced by allogeneic limbal transplantation (CB7BL/6 donor, BALB/c recipient). The co-transfer of LSCs and MSCs was performed after this procedure. A control group with empty nanofiber scaffolds and a group with no treatment were also studied. Real-time PCR was used to assess the postoperative inflammatory response in all groups.

In the rabbit alkali model, nanofiber scaffolds from polymer poly (L-lactid acid) were used. These nanofiber scaffolds were prepared by the original needleless electrospinning procedure as described previously (Publication 3; (Holan et al., 2011). Nanofiber scaffolds were cut into squares (approximately 1.5 x 1.5 cm) and fixed into $CellCrownTM^{24}$ inserts (Scaffdex, Tampere, Finland). The inserts with nanofiber scaffolds were sterilized and transferred into 24-well tissue culture plates (Corning, Schipol-Rijk, Netherlands). One hundred thousand cells in a volume of 700 μl of culture medium with 10% FCS were transferred into each well. The cells were cultured on nanofiber scaffolds for 24 hours (Publication 4). A 10-mm diameter nanofiber circle seeded with rabbit bone marrow-derived MSCs and without MSCs was applied onto the corneal surface. The scaffolds were sutured to the conjunctiva with four interrupted sutures and the eyelids were closed for 2 days using the same technique as the mouse model (Figure 11) (Publication 4).

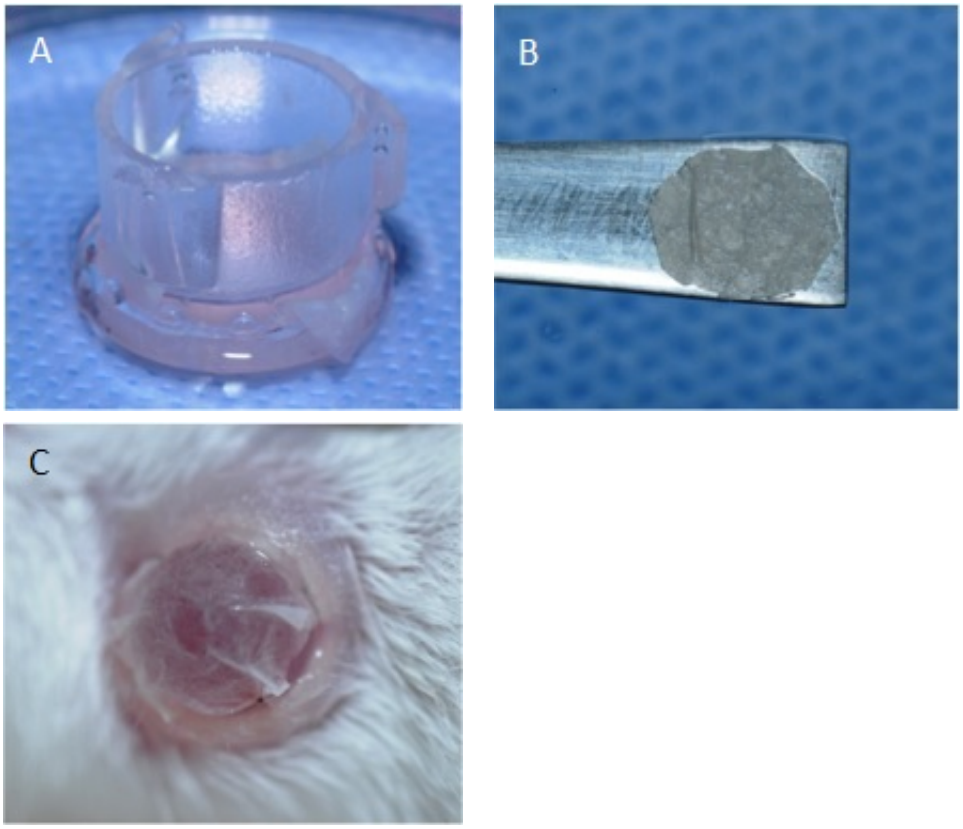

Figure 10: **The nanofiber scaffold transfer in the mouse model: A)** The cells were cultured on PA6/12 nanofiber scaffolds; **B)** The scaffold was transferred onto the damaged ocular surface; **C)** The scaffold was secured by 4 interrupted sutures with the cell side facing down. (Courtesy of Ivan Kolín)

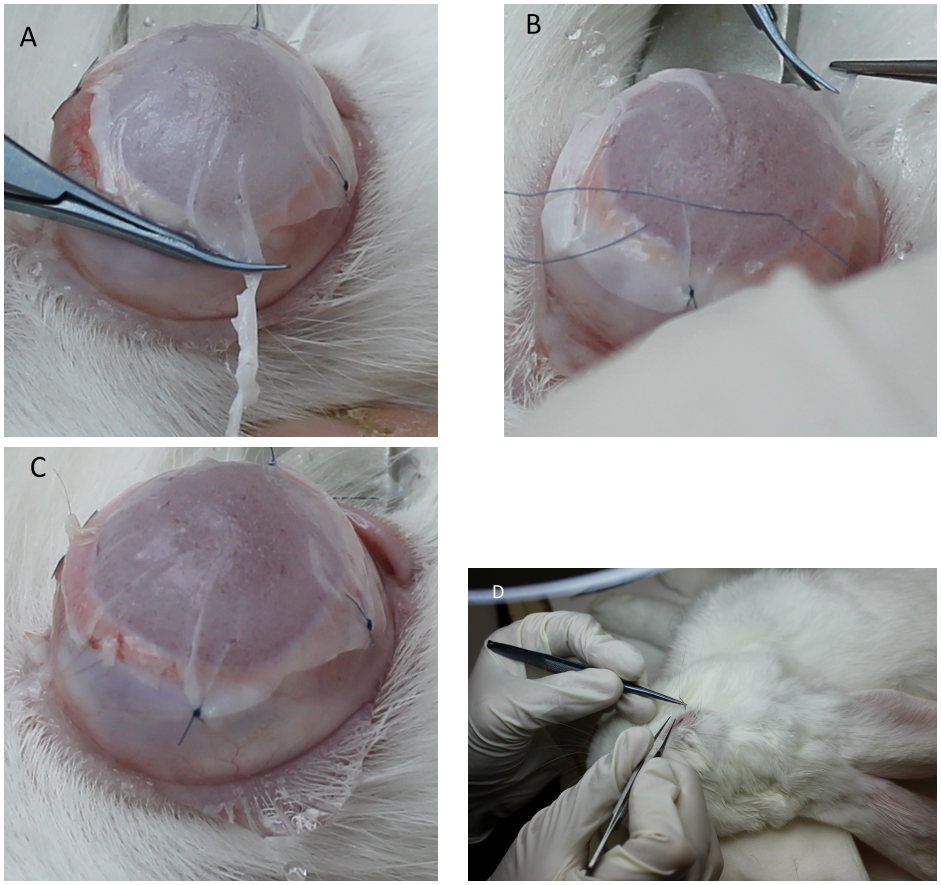

Figure 11: **The nanofiber scaffold transfer in a rabbit model with alkali injury: A)** The cells were transferred onto the scaffold, which was prepared with polymer poly using an electrospinning needleless procedure; **B)** A 10 mm nanofiber circle was cut out and used for covering the corneal and limbal area immediately after the injury; **C)** The scaffold was secured by 4 interrupted sutures with the cell side facing down. D) The eyelids were closed by tarsorrhaphy for 48 hours. (Courtesy of Čestmír Čejka)

3.2.5 Alkali injury in the rabbit model

The right corneas of anesthetized rabbits were injured by applying 0.15 N NaOH (sodium hydroxide) onto the corneal surface for 1 minute, then the eyes were rinsed with tap water. The rabbits were divided into four groups. In each experimental group six corneas were investigated. In the first group of rabbits, the injured corneas were left without any treatment. In the second group, the injured cornea were treated with MSCs and the eyelids were sutured for two days. In the third group, nanofiber scaffolds seeded with MSCs (in the fourth group nanofibers alone) were transferred onto the corneas immediately after the injury and the eyelids were sutured (Publication 4).

3.3 Cellular and molecular methods

3.3.1 Limbal stem cell isolation

Limbal tissue was obtained by scissor dissection of the eyes of mice (guided by an operating microscope). Limbal tissues from 10 to 12 BALB/c mice were pooled and cut into small pieces in RPMI 1640 medium (Sigma-Aldrich, St. Louis, MO). The tissue was centrifuged (8 minutes at 250 g), and the pellet was subjected to digestion with trypsin from porcine pancreas (Sigma-Aldrich, St. Louis, MO). The procedure consisted of 10 trypsinization cycles (300 μL of 0.5% trypsin solution per 10 limbuses, 10 minutes incubation in 37°C). The supernatants (tissue-free solution) from each trypsinization step were harvested into an excess (30 mL) of RPMI 1640 medium with 10% fetal calf serum (FCS; Sigma-Aldrich, St. Louis, MO) on ice and the trypsinization procedure was repeated on the residual pellet. After the last trypsinization step, the harvested cell suspension was filtrated through a nylon mesh and centrifuged for 8 minutes at 250 g. The pellet was resuspended in 1.2 mL of RPMI 1640 medium, and the number of cells was determined by hemocytometry (Publication 2).

3.3.2 Mesenchymal stem cell isolation

Mouse MSCs were isolated from the bone marrow of BALB/c mice. The bone marrow from the femurs and tibias was flushed out, homogenized, filtered through a nylon mash, and cultured in RPMI 1640 medium in tissue culture plates. Rabbit MSCs were isolated from the bone marrow of adult New Zealand white rabbits and were cultured and characterized as described for mouse MSCs (Svobodova et al., 2012) (Publication 3 and 4).

3.3.3 Percoll gradient centrifugation

To prepare a stock solution, nine parts Percoll was mixed with one part 10x concentrated phosphate buffered saline (PBS). From the stock solution, a 40%, 50%, 60%, 70%, or 80% Percoll solution was prepared by dilution in 1x PBS. A Percoll gradient was prepared in a 10-mL test tube by overlaying of 1.0 mL of each Percoll dilution 80% through 40%. Finally, 1.0 mL of suspension of trypsin-dissociated limbal cells was gently overlaid on the top of the Percoll gradient.

The gradient was centrifuged for 10 minutes at 300 g at 4°C. After centrifugation, the separated layers of cells on individual Percoll concentrations could be directly visualized and individual cell layers (as well as the cell pellet) were harvested into RPMI 1640 medium with 5% of FCS and washed three times by centrifugation (8 minutes at 250 g). After the last washing, the cells were re-suspended in 500 μL of RPMI 1640 medium containing 10% of FCS, 10 mM HEPES buffer, antibiotics (100 U/mL of penicillin, 100 μg/mL of streptomycin) and 5×10^{-5} M 2-mercaptoethanol (hereinafter called complete RPMI 1640 medium). The number of cells in each fraction was then determined. Subsequently, cells from five individual fractions were characterized for the presence of limbal SC markers and differentiation markers of corneal epithelial cells by Real-time PCR. The SP phenotype was determined by flow cytometry and the growth properties were analyzed *in vitro* (Publication 2).

3.3.4 Cell culture

After cell isolation, the mouse LSCs were seeded into 12-well tissue culture plates (Nunc, Roskilde, Netherlands) and, after one week, expanded in $25 - cm^2$ tissue culture flasks (Corning, Schipol-Rijk, Netherlands). Cells growing *in vitro* for 2-3 weeks were used for growth on nanofiber scaffolds (Publication 3).

The mouse MSCs were cultured at a concentration of 4×10^6 cells/ml in complete RPMI 1640 medium in $25 - cm^2$ tissue culture flasks (Corning, Schipol-Rijk, Netherlands). On the following day, the non-adherent cells were washed out and the adherent cells were cultured. After one day, the non-adherent cells were washed out and adherent cells were cultured for at least 3 weeks. After 3 weeks of culturing, the cells were characterized phenotypically by flow cytometry (over 90% of the growing cells were MHC class II$^-$ molecules, CD86$^-$ and CD11b$^-$, but CD105$^+$) and by their ability to differentiate into adipocytes (Publication 3).

The rabbit MSCs were cultured at a concentration of 4×10^6 cells/ml in 6 ml of culture medium in $25 - cm^2$ tissue culture flasks (Nunc, Roskilde, Denmark). After a 24-h incubation period, the non-adherent cells were removed by washing and the remaining adherent cells were cultured with a regular exchange of the culture medium and passaging of the cells. After approximately 3 weeks of being cultured (2-3 passages), the cells were harvested by gentle scraping and used for transplantation onto the ocular surface (Publication 4).

3.3.5 RNA isolation and reverse transcription from limbal grafts

Total RNA was extracted from the samples of limbal grafts using TRI Reagent (Molecular Research Center, Cincinnati, OH) in accordance with the manufacturer's instructions. The grafts were cut out by Vannas scissors, embedded in TRI Reagent and homogenized. Two μg of total RNA were treated using deoxyribonuclease I (Sigma, St. Louis, MO) and used for subsequent reverse transcription. The first-strand cDNA was synthesized using random hexamers (Promega, Madi-

son, WI) in a total reaction volume of 25 μl using M-MLV Reverse Transcriptase (Promega) (Publication 1).

3.3.6 DNA isolation for detection of limbal graft cell survival

Cells from B6 mouse were detected according to the presence of the Sry gene (Masaki et al., 1995) by analyzing DNA from limbal grafts of male origin. Genomic DNA was extracted from B6 male limbal grafts in BALB/c female recipients using NucleoSpin Tissue XS extraction kit (Macherey-Nagel, Dueren, Germany) in accordance with the manufacturer's instructions (Publication 1).

3.3.7 Quantitative real-time polymerase chain reaction in mouse model of limbal transplantation

Quantitative Real-time RT-PCR (polymerase chain reaction) was performed on the iCycler (BioRad, Hercules, CA) and the data were analyzed on the iCycler Detection system (Version 3.1). Levels of mRNA for various cytokines (IL-2, IL-4, IL-10, IFN-γ) and the expression of gene for inducible nitric oxide synthase (iNOS) were detected. The specificity of the amplified products was checked by the melting analyses. iQ SYBR Green Supermix (BioRad) was used for all experiments. Experiments were conducted in triplicates and the relative quantification model was applied to calculate the expression of target genes in comparison to GADPH, which was used as the housekeeping gene. The list of primers is described in Table 1 (Publication 1). The PCR parameters for 25 μl reactions included denaturation at 95°C for 3 min, then 40 cycles at 95°C or 10 seconds, annealing at 60°C for 20 seconds and elongation at 72°C for 20 seconds. Data were collected at each cycle after the elongation step at 80°C for 5 seconds (Publication 1).

3.4 Statistical analysis

The statistical significance of differences in graft survival between experimental and control groups was calculated using the Mann-Whitney U test; differences in gene expression were calculated using the Students t-test. A p-value less than 0.05 was considered statistically significant (Publication 1).

4 RESULTS

4.1 Limbal tissue transplantation in a mouse model

Allografts, syngrafts and xenografts were grafted orthotopically in BALB/c mice. Graft rejection was assessed on the basis of clinical evaluation (corneal opacity score grade ≥ 2) and donor cell survival detection by RT-PCR postoperatively. The clinical observation of allografts and xenografts showed that limbal rejection was accompanied by limbal edema, limbal graft neovascularization, corneal neovascularization and opacity (Publication 1, Figure 1). The postoperative limbal edema was strongly developed in the xenogeneic model compared to the allogeneic and syngeneic model (Publication 1, Figure 2A). Postoperative corneal neovascularization was present in all quadrants in xenografts, less in allografts, unlike in the syngeneic model where only minimal peripheral neovascularization was present (Publication 1, Figure 2B). While syngeneic limbal grafts survived permanently ($>$ 28 days, n=10), the limbal allografts were rejected in 9.0 ± 1.8 days (n=14) and limbal xenografts in 6.5 ± 1.1 days (n=10) (Publication 1, Figure 2C)(Figure 12).

The survival of donor limbal graft cells and the donor-derived cells on recipient cornea were detected by Real-time PCR using primers for MHC class I molecules in xenogeneic model and for Sry in allogeneic male-to-female transplantation. The clinical manifestation of graft rejection onset correlated with the kinetics of donor cell survival in the graft and on the recipient cornea in the allograft and xenograft model. Xenogeneic cells were detected on day 8 but not on day 12 after transplantation and allogeneic cells were detected up to day 14 after grafting in the limbal graft and on the corneal surface (Publication 1, Figure 3). When syngeneic grafts from male donors were grafted into female recipients, the male cells were still detected in the graft on day 28 after grafting.

The intragraft expression of cytokine response (IL-2, IL-4, IL-10, IFN-γ) and iNOS were detected by real-time PCR during the onset of graft rejection. Distinct patterns of intragraft gene expression of Th1 cytokines (IL-2 and INF-γ) and Th2 cytokines (IL-4 and IL-10) were detected during rejection of limbal allografts and xenografts. A significant expression of genes for Th1 cytokines IL-2 and IFN-γ was found in allografts, but the expression of genes for Th2 cytokines IL-4 and IL-10 did not exceed the levels in syngeneic grafts. Rejection of limbal xenografts was accompanied by the high expression of genes for both Th1 (IL-2 and IFN-γ) and Th2 (IL-4, IL-10) cytokines (Publication 1, Figure 4). Significant iNOS gene expression was detected during rejection in both allografts and xenografts (Publication 1, Figure 4). The rejection reaction was prevented by systemic immunosuppression in the form of anti-CD4 mAb, and allograft survival was significantly prolonged (22.8 ± 4.2 days, n=8). The survival of limbal xenografts was postponed by anti-CD4 mAb (9.5 ± 1.8 days, n=6), but all grafts were rejected within 12 days (Publication 1, Figure 5) (Figure 13). The administration of anti-CD8 mAb did not prolong the allo- and xenograft survival significantly.

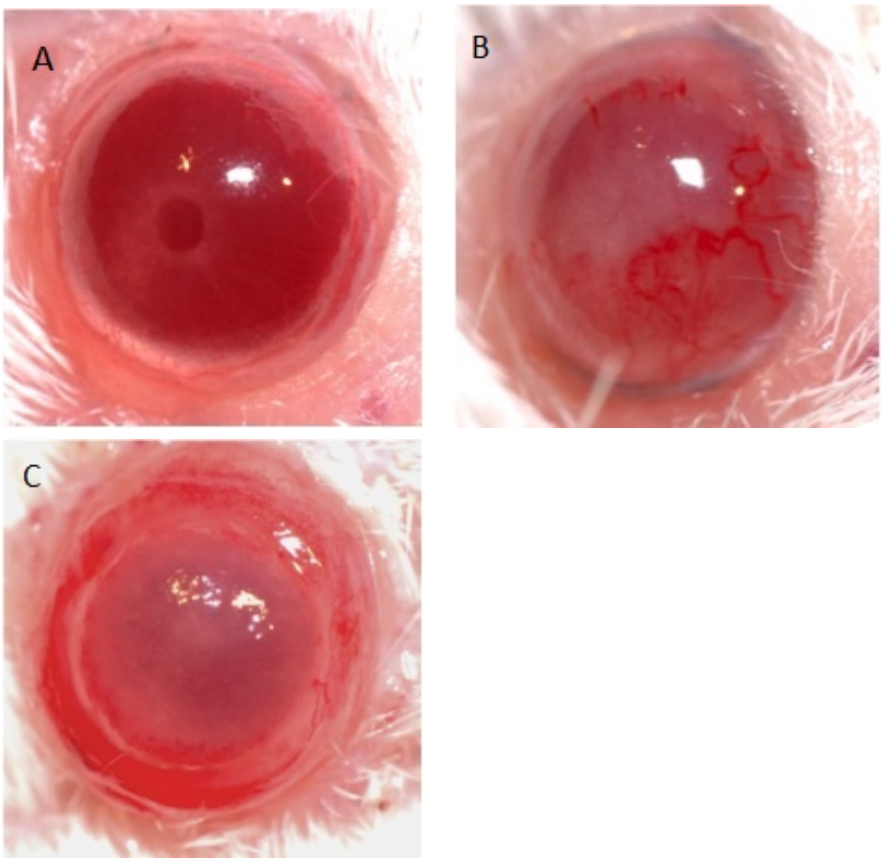

Figure 12: **Limbal graft transplantation in the mouse model: A)** The syngeneic limbal graft on the 21st day after limbal transplantation. **B)** The allogeneic limbal graft during the onset of rejection on the 12th day after limbal transplantation. **C)** The xenogeneic limbal graft during the onset of rejection on the 5th day after limbal transplantation. (Courtesy of Ivan Kolín)

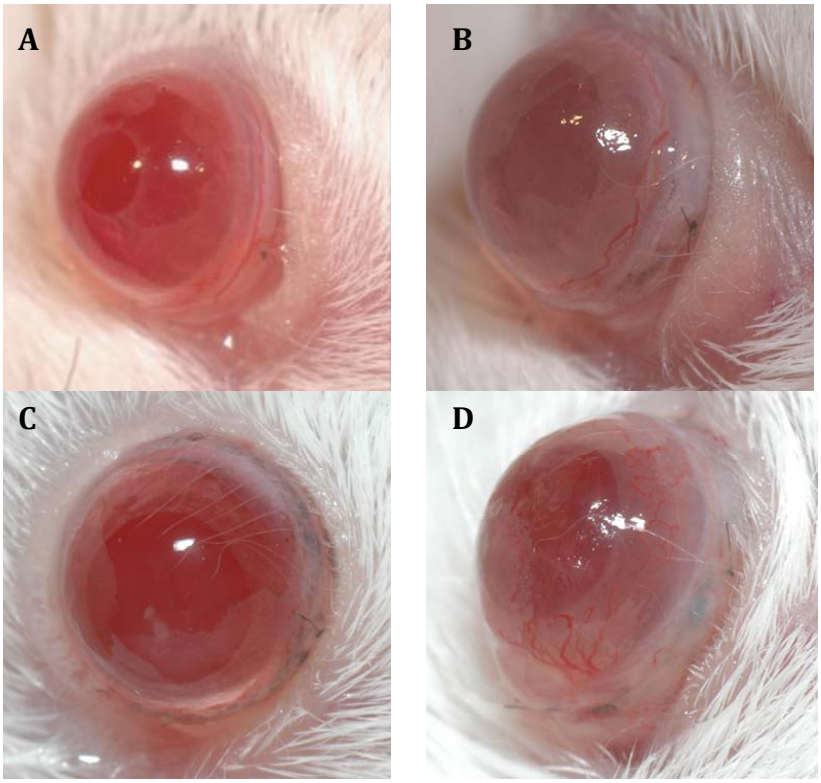

Figure 13: **Limbal grafts in the mouse model treated with systemic immunosuppression: A)** The syngeneic limbal graft on the 18th day after limbal transplantation; **B)** Limbal allograft rejection on the 8th day after transplantation in the control group; **C)** The allogeneic limbal graft on the 21st day after transplantation in the anti-CD4 mAb treated group; D) Allogeneic limbal graft rejection on the 11th day after transplantation in the anti-CD8 mAb treated group. (Courtesy of Ivan Kolín)

4.2 Isolation and characterization of mouse limbal stem cells

We described that Percoll density gradient centrifugation is a convenient method of harvesting cells with SC characteristics from limbal tissue. These cells can subsequently be used for *in vitro* tissue culturing. In our experiments, the mouse limbal epithelial cells were separated and analyzed for expression of SC markers and characteristics.

In practice, a single cell heterogenous population was obtained after trypsin-dissociation of limbal tissue (Publication 2, Figure 1). Next, the cell suspension was separated by the Percoll gradient (Publication 2, Table 1). The Percoll gradient centrifugation was used to separate the isolated cells into 5 individual fractions (40%, 50%, 60%, 70% and 80% Percoll gradient). Each fraction was characterized through Real-time PCR for both the presence of limbal SC markers (ABCG2, Lgr5, p63) and a differentiation marker of corneal epithelial cells (K12) (Publication 2, Figure 2).

SCs express the SP phenotype based on the ability to efflux the DNA-binding dye Hoechst 33342. The SP phenotype is associated with ABCG2 expression. The SP phenotype was determined by flow cytometry (Publication 2, Figure 3). Cells retained in the lightest fraction (40% Percoll) and in the densest fraction (80% Percoll) of the gradient were both enriched for populations with a high expression of the SC markers ABCG2 and Lgr5 and also expressed the SP phenotype (Publication 2, Figure 2 and 3). However, the lightest fraction (representing approximately 12% of total limbal cells) contained cells with the strongest spontaneous proliferative capacity and expressed the corneal epithelial differentiation marker K12 (Publication 2, Figures 2D and 5A). In contrast, the densest fraction (<7% of original cells) was K12 negative and contained small, non-spontaneously proliferating cells, which instead were positive for p63 (Publication 2, Figures 2D, 4C and 5A). Unexpectedly, cells from this fraction had the highest proliferative activity when cultured on a 3T3 feeder cell monolayer (Publication 2, Figure 5B).

4.3 Limbal and mesenchymal stem cell transfer on nanofiber scaffolds for treatment of ocular surface damage in a mouse model

The LSCs and MSCs were successfully cultured and transferred onto the mouse ocular surface. Nanofiber 3D scaffolds were prepared by electrospinning from polyamide 6/12 (PA6/12). The copolymer PA6/12 was selected on the basis of the nanofibers stability in aqueous solutions and its biocompatibility for LSC and MSC growth (Publication 3).

We found that the metabolic and proliferative activities of LSC and MSC on plastic culture plates or on PA6/12 nanofiber scaffolds were comparable (Publication 3, Figure 1A, 1B). The growth of LSCs and MSCs seeded on a plastic surface and on PA6/12 nanofiber scaffolds was similar: gradually increasing dur-

ing a 48-hour incubation (Publication 3, Figure 2). The morphology of growing LSCs was analyzed based on the cell shape and organization of actin cytoskeleton. A comparable morphology of LSCs growing on PA6/12 and on the poly-L-lysin coated glass surface was found (Publication 3, Figure 3).

The LSC transfer and co-transfer of LSC and MSC onto scaffolds PA6/12 were performed on the damaged ocular surface of BALB/c mice. The damaged ocular surface was induced by corneal epithelium and limbus removal in BALB/c mice. The LSC from BALB/c mice were labeled with PKH26 dye, cultured on nanofiber scaffolds and transferred onto damaged ocular surface. The PKH26-labeled LSCs migrated to the corneal surface from the nanofiber scaffold and were detected on cryosections on day 7 and 14 postoperatively (Publication 3, Figure 4).

The immunosuppressive properties of MSCs were demonstrated *in vitro* by their ability to inhibit T-cell proliferation and IFN-γ production (Publication 3, Figure 5). To demonstrate the suppression of a local inflammatory reaction by the co-transfer of LSCs and MSCs *in vivo*, two experimental models were used. In the first model, the damaged ocular surface was induced by corneal epithelium and limbus removal in BALB/c mice. The second model combined the mechanical trauma and allogeneic (C57BL/6) orthotopic limbal transplantation in BALB/c mice. Both models were used in order to study the immunosuppressive effect of LSC and MSC. The co-transfer of LSC and MSC on the scaffolds was performed immediately after the ocular surface damage. The control group was treated with empty nanofiber scaffolds. The group with non-damaged eye was also analyzed. The postoperative inflammatory response after scaffolds transfer was assessed by Real-time PCR. The mechanical trauma induced a moderate inflammatory associated with IFN-γ and iNOS production. This response was inhibited by the co-transport of LSCs and MSCs. In the model of limbal allotransplantation, the LSC and MSC co-transport on nanofibrous scaffolds significantly inhibited the local strong inflammatory reaction characterized by expression of IL-2, IFN-γ and iNOS genes determined by real-time PCR (Publication 3, Figure 6). The inflammatory reaction was slightly suppressed in the control group with cell-free nanofiber scaffolds and not affected in the group with no treatment (Publication 3, Figure 6).

4.4 Mesenchymal stem cell transfer on nanofiber scaffolds for treatment of chemical corneal injury in a rabbit model

In our study, we demonstrated the suppression of oxidative alkali-induced injury by transfer of MSCs on nanofiber scaffolds in the experimental rabbit model. The model of alkali injury was induced by the alkali (0.15 N NaOH) applied on the cornea of the right eye and then rinsed with tap water. In the first group of rabbits the injured corneas remained untreated. In the second group, the MCSs were applied on the injured ocular surface after the injury and the eyelids were sutured for two days. In the third group, nanofiber scaffolds seeded with MSCs (in

the fourth group nanofibers alone) were transferred onto the corneas immediately after the injury and the eyelids were sutured. The rabbit corneas were examined immunohistochemically, morphologically and for the central corneal thickness.

The injured untreated corneas showed decreased expression of the antioxidant aldehyde dehydrogenase 3A1 (ALDH3A1) in the corneal epithelium, particularly in superficial parts, where apoptic death (detected by active caspase 3) was high. ALDH3A1 is an enzyme protecting the cornea from oxidative stress caused by chemical injury. High expressions of matrix metalloproteinase 9 (MMP9) and markers of lipid peroxidation and oxidative stress (malondialdehyde (MDA) and nitrotyrosine (NT)) were found in this untreated group. In contrast, the injured rabbit corneas treated with MSCs on nanofiber scaffolds showed a high expression of ALDH3A1 in the epithelium, which was similar to the control untreated corneas. A low expression of MMP9 and active caspase 3, absent expression of MDA and NT were detected in this group, similarly as in the control corneas (Publication 4, Figure 1 5). Immunohistochemical staining also confirmed significantly lower expression of IL-8 and IL-1β in the group treated with MSC compared to the group without treatment (Publication 4, Figure 6 and 7). The corneas were harvested on day 10 after an alkali injury in order to detect the gene expression of pro-inflammatory cytokines. The gene expression of IL-1β, IL-2 and IFN-γ determined by real-time PCR was significantly reduced in the group treated with MSC compared to the group without treatment (Publication 4, Figure 12). The expression of genes for the pro-inflammatory cytokines corresponded with their immunohistochemical expression.

At the end of the experiment (on day 15), the injured untreated corneas were vascularized (with high vascular endothelial growth factor (VEGF) expression) and numerous inflammatory cells (macrophages/monocytes) were present in the corneal stroma. The stromal inflammatory infiltration was also significantly suppressed in corneas treated with MSCs on nanofiber scaffolds (Publication 4, Figure 9). Clinically, a significant suppression of corneal neovascularization was detected in corneas treated with MSCs on nanofiber scaffolds compared to the untreated corneas with extensive neovascularization on day 15 and corresponded with neovascularization quantification by VEGF gene expression with real-time PCR (Publication 4, Figure 10). 10 days after chemical injury, corneal thickening was noticed in both groups. The corneal thickening and opacity after alkali injury have regained their normal characteristics only in the group treated with MSCs on nanofiber scaffolds (Publication 4, Figure 8). The results from injured corneas treated with nanofiber scaffolds alone and with MSCs without scaffolds showed similar results to the untreated injured corneas.

5 DISCUSSION

5.1 Limbal tissue transplantation in a mouse model

LSCD is a blinding eye condition and its treatment is very challenging. The only way to treat severe LSCD and restore the patient's vision is via limbal tissue or cultured LSC transplantation. Successful ocular surface transplantation restores ocular surface stability, reduces symptoms and improves the patient's vision. For bilateral ocular surface disease, the limbal allograft must be used and the immune-associated rejection remains the main risk factor responsible for the low success rate. Several studies have shown beneficial effects of limbal transplantation in patients with LSCD (Dua and Azuara-Blanco, 1999); (Daya et al., 2000); (Cauchi et al., 2008). However, the major problem with limbal allotransplantation is the high risk of immune rejection and the necessity for systemic immunosuppression (Tsubota et al., 1999); (Daya et al., 2000). Conversely, the corneal allografts often survive with only topical prophylactic immunosuppressive treatment. This stark contrast between incidence of rejection in corneal and limbal allografts may be, in part, due to a stronger vascular supply, and a higher density of antigen presenting cells, such as Langerhans cells, in the limbal region (Gillette et al., 1982); (Niederkorn, 1995). Additionally, the corneal epithelium is a highly immunogenic ocular tissue and the epithelial rejection takes the main place after limbal transplantation (Treseler et al., 1985); (Qi et al., 2013). Therefore, the clinical course and cellular mechanisms of limbal graft rejection have to be recognized in order to develop a successful strategy to manage immune reaction in limbal transplantation.

Our experimental limbal transplantation confirmed high incidence of rapid rejection similar to that observed in other experimental studies (Mills et al., 2002); (Maruyama et al., 2003). Allogeneic donor cells were not detectable in the recipient 2 weeks after transplantation indicating potent and rapid immune rejection (Mills et al., 2002). To elucidate the immunological mechanism responsible for low survival rate of limbal grafts, we studied the murine model of limbal allotransplantation and developed a novel method of xenotransplantation. The clinical features of limbal rejection in patients after allogeneic limbal tissue transplantation include limbal congestion, edema, vessel dilatation and significant corneal opacity (Shi et al., 2008); (Baradaran-Rafii et al., 2013). Similarly to these observations, the rejection of limbal allografts and xenografts in our experiments was characterized by graft and corneal neovascularization, limbal graft edema and significant corneal opacity with more profound reactions in xenogeneic models.

There is much controversy about the fate of donor limbal graft and donor-derived cells on the ocular recipient's surface after limbal transplantation. Some studies showed that donor cells did not survive despite good clinical results (Williams et al., 1995); (Henderson et al., 2001)) while others confirmed long-term donor cell survival (Reinhard et al., 2004); (Djalilian et al., 2005); (Egarth et al., 2005). Several methods are described for the detection of donor cell survival onto ocular surface after transplantation (Yin et al., 2013). In our allograft male-to-female

model, the presence of corneal opacity (grade ≥ 2) coincided with the complete disappearance of allogeneic donor cells from both the limbus and corneal epithelium at 7-12 days after transplantation. To elucidate the limbal graft failure due to a technical issue, male donor limbal grafts were transplanted into female BALB/c recipients in a syngeneic model. Detection of donor male cells 4 weeks after surgery in the male-to-female model indicated that the prompt drop in allogeneic limbal cells is not due to surgical failure. No clinical signs of rejection of H-Y incompatible limbal grafts were observed in our study: similar to the results in H-Y incompatible corneal grafts in BALB/c mice (Hasková et al., 1997). In contrast, limbal grafts, incompatible in another relatively weak antigen enhanced green fluorescent protein, were rejected by the rat recipients (Keijser et al., 2006). These differences may reflect interspecies differences or suggest that BALB/c female mice are non-responder to the male-specific antigen. All limbal xenografts were rejected within 8 days of transplantation and no xenogeneic cells were detected by the real-time PCR beyond this period in the donors. These data suggest that limbal allografts and xenografts are promptly rejected and do not enjoy the immune privilege of the anterior part of the eye. The clarification of donor cell survival after the LSC transfer is essential for deciding immunosuppressive therapy duration in clinical practice.

Rejection of limbal allografts was associated with a strong Th1 cytokine response characterized by the expression of genes for IL-2 and IFN-γ in the rejected limbal grafts. Expression of the gene for IL-4 was not detected in rejected limbal allografts and also expression of the gene for IL-10, another Th2 cytokine, did not exceed the baseline levels in syngeneic limbal grafts. On the contrary, a strong expression of genes for Th2 cytokines IL-4 and IL-10, in addition to Th1 cytokines, was detected in rejected limbal xenografts. This pattern of cytokine expression during limbal graft rejection resembles cytokine profiles after corneal allo- and xenotransplantation, but the role of the Th2 cytokines in the rejection of xenografts is unclear (Pindjáková et al., 2005). Macrophages and their product nitric oxide have been shown to play a more important role in graft rejection. Mills et al. observed a significant infiltration of limbal allografts in rats by macrophages and we found a strong expression of the gene for iNOS in both rejected limbal allografts and xenografts (Mills et al., 2002). It has already been shown in various allo- and xenotransplantation models, including corneal transplantation, that the inhibition of iNOS activity may prolong graft survival (Krulová et al., 2002); (Strestíková et al., 2003)). The production of NO by graft infiltrating macrophages depends on the availability of IFN-γ, which was also detected during rejection of both limbal allo- and xenografts and is a key factor in delayed-type hypersensitivity (DTH) reaction. This suggests that strategies directed to inhibit IFN-γ (Th1 response), NO production and the DTH reaction should be beneficial in the promotion of limbal graft survival. Indeed, Maruyama et al. have shown that the Th2-biased immune system and the suppression of the DTH reaction may support the survival of limbal allografts in mice (Maruyama et al., 2003).

The success rate of limbal tissue allotransplantation differs among published

studies from as low as 33.3% with inappropriate immunosuppression to as high as 77.2% with adequate immunosuppressive therapy (Miri et al., 2010); (Holland et al., 2012); (Tan et al., 2012). In clinical practice, various protocols of systemic treatment are being used after limbal allotransplantation. There is evidence of the systemic use of steroids, cyclosporin (Tsubota et al., 1999), tacrolimus (Dua and Azuara-Blanco, 2000) and mycophenolate mofetil (Reinhard et al., 2004). It is widely recommended to use systemic immunosuppression for a period of at least 2 years postoperatively. The systemic therapy is associated with a serious side effects such as higher susceptibility to infectious and cancerous diseases. Therefore, a new approach would be welcomed for postponing the rejection in limbal allografting. In our study, we showed that targeting of $CD4^+$ cells by systemic application of mAb results in a suppression of the rejection reaction and in a significant prolongation of limbal allograft and xenograft survival. The effect of anti-CD4 therapy may be due to the elimination of $CD4^+$ T cells, which mediate the DTH reaction and are an important source of IFN-γ for iNOS expression (Krulová et al., 2002). In addition, the anti-CD4 antibody can inactivate $CD4^+$ macrophages, which play a role in both the afferent phase of transplantation reaction as antigen-presenting cells and in the effector phase as cytotoxic macrophages (Keijser et al., 2006); (Strestíková et al., 2003); (Slegers et al., 2004). It has been shown that a subpopulation of macrophages expresses CD4 molecules, and these $CD4^+$ macrophages have been shown to be involved in graft rejection (Wallgren et al., 1995). Nevertheless, anti-CD4 mono-therapy did not ensure a permanent limbal allograft survival. The rejections observed in the anti-CD4 treated recipients may be due to the activity of other $CD4^+$ cell-independent mechanisms (such as $CD8^+$ cell-activated macrophages, cytotoxic T cells, etc.). The results also showed that anti-CD8 treatment was not effective in the prevention of limbal allograft rejection, similar to the case of corneal transplantation (He et al., 1991); (Vítová et al., 2004). For the first time, our study demonstrates intragraft cytokine response in orthotopic limbal allo- and xenograft recipients and indicates the key role of Th1 response and $CD4^+$ cells in limbal graft rejection. Therefore, the strategies targeting $CD4^+$ cells as the main mediators of Th1 response and activators of macrophages for NO production were suggested to prevent limbal graft rejection. This suggestion was confirmed by the effectiveness of anti-CD4 treatment in the suppression of graft rejection in allogeneic limbal transplantation in the mouse model.

5.2 Isolation and characterization of mouse limbal stem cells

LSC-based therapy for LSCD has great potential. However, LSCs comprise just a minor fraction of the whole limbal tissue and there is a need to find an optimal isolation method. Indeed, the limbus has a very heterogeneous cell population with LSCs residing in the basal layer. At this epithelial level, there are several other cell types in the vicinity such as the immediate progeny, i.e. early TAC, melanocytes, Langerhans cells and corneal epithelial basal cells (Li et al., 2007). The transplantation of LSCs contributes to long-term homeostasis and the lack of

SCs in the graft may be the cause of the failure (O'Callaghan and Daniels, 2011). Therefore, the ability to isolate a cell population with a high number of LSCs is essential for successful transplantation.

Our experiments have shown that cells sharing morphologic, phenotypical, and functional characteristics of LSCs can be found in the mouse limbus. LSCs are characterized by small size, a low replication rate, expression of certain markers such as a transporter ABCG2, p63, integrin 9, or K19, and expression of the SP phenotype, which have been described in human, rat and rabbit models (Chen Z. et al., 2004); (Schlötzer-Schrehardt and Kruse, 2005); (Umemoto et al., 2005); (De Paiva et al., 2006); (Park et al., 2006)). We found two distinct, separable populations of corneal epithelial cells with SC characteristics (expression of ABCG2 and Lgr5, and SP phenotype) obtained from the mouse limbus by Percoll gradient centrifugation. The presence of SCs (less than 7% of original cells) was found in the densest fraction (80% Percoll gradient) containing small, non-spontaneously proliferating cells, positive for p63, and negative for K12. These cells occurred in a quiescent state and did not proliferate within the first 3 days in tissue culture, as has been described for SP cells in rabbits (Park et al., 2006). However, this cell population acquired a high proliferative activity when cultured on a 3T3 feeder cell monolayer. Thus, the quiescent cells from the densest fraction may require a specific niche to facilitate proliferation. The densest fraction also expressed the SP phenotype (>30% in comparison to 2%-5% in the whole limbus). All these characteristics mimicked the LSCs described in the human and rabbits more closely (Chen Z. et al., 2004); (Schlötzer-Schrehardt and Kruse, 2005); (De Paiva et al., 2006); (Park et al., 2006); (Umemoto et al., 2006).

A second cell fraction showing some characteristics of LSCs (positive expression of ABCG2 and Lgr5) was detected in the lightest cell population (40% Percoll gradient) and represented approximately 12% of the total limbal cell population and over 20% of the cells expressed in the SP phenotype. However, the light cell population was positive for the corneal differentiation marker K12. This population had the highest spontaneous proliferative capacity compared to unseparated limbal cells. Their proliferation response did not increase when they were cultured on a feeder cell monolayer.

The SP phenotype is a property of SCs (Shimano et al., 2003); (Zhou et al., 2001) and is associated with ABCG2 expression, however not all cells expressing ABCG2 exhibit the SP phenotype (Kim et al., 2002). The SP phenotype was reported in the conjunctival and limbal epithelium in humans and rabbits but not in the corneal epithelium (Watanabe et al., 2004); (Umemoto et al., 2005). Both populations contained cells expressing the SP phenotype based on the efflux of Hoechst 33342 dye. The number of SP cells in the unseparated mouse limbus was 3.8% of the total limbal cells, substantially higher than the number of slow cycling corneal epithelial cells found at the mouse limbus or the number of SP cells in human, rabbit, and rat limbal epithelia (De Paiva et al., 2005), (Umemoto et al., 2005); (Pajoohesh-Ganji et al., 2006); (Park et al., 2006). However, it corresponds to the number of SP cells found in the rat cornea (Umemoto et

al., 2006). The studies of Umemoto and coworkers in humans (Watanabe et al., 2004), rabbits (Umemoto et al., 2006) and rats (Umemoto et al., 2005) showed that although the number of cells exhibiting the SP phenotype was less than 2% in the limbus, immunochemistry revealed that a larger proportion (approximately 10%) of limbal basal epithelial cells expressed ABCG2 transporter (Umemoto et al., 2005). Similarly, (Budak et al., 2005) suggested the existence of a significantly higher number of ABCG2$^+$ cells than SP cells. This discrepancy was explained by the differences in the transport activity of ABCG2. (Umemoto et al., 2005) also showed that in the rat, unlike the human and rabbit, the central cornea contains cells with the SP phenotype but that these cells expressed significantly lower levels of putative SC markers than the SP cells in the limbus (Umemoto et al., 2005). In addition, SP cells found in the rat cornea had a different profile on forward scatter analyses than SP cells in the limbus.

Our study showed that mouse limbal cells with the SP phenotype from the light cell fraction of the Percoll gradient (40%) had distinctive light-scattering properties from SP cells from the dense cell fraction (80%). It appears that the light cell fraction positive for K12 resembles the SP cells described by Umemoto et al. (Umemoto et al., 2005) in the rat central cornea rather than the basal LSCs. The interspecies differences exist in the distribution and properties of corneal epithelial cells with LSC characteristics and the mouse may represent a unique species that is different to human, rabbit, or rat.

5.3 Limbal and mesenchymal stem cell transfer on nanofiber scaffolds for treatment of ocular surface damage in a mouse model

Recent publications have shown promising results of SC-based treatment for ocular surface disorders. However, there is a need to find an optimal scaffold for the SC transfer. Nowadays, there is growing evidence of *in vitro* experiments using various electrospun nanofibers of various polymers to enable cell adhesion, proliferation and differentiation (Das et al., 2009); (Bhattarai et al., 2005); (Schindler et al., 2005). However, there is a limited evidence of *in vivo* use of nanofiber scaffolds in models of ocular surface disease. Therefore, we investigated whether these nanofiber polyamide scaffolds are useful and suitable for the SC culture and transfer onto the ocular surface in the mouse model. For the LSC isolation we used the Percoll method described in our previous experiments (Publication 2). To analyze the anti-inflammatory effect of the transferred cultured cells, our already established limbal allotransplantation model was used to induce a strong immune response (Publication 1).

The human AM is currently the most widely used carrier of LSCs (Tsai et al., 2000). However, due to human AM variability, the risk of infection transmission and crease formation it is not an ideal substrate and other scaffolds have been proposed for SC therapy (Levis and Daniels, 2009). Alternative scaffolds for cell culture and transfer have been used and include collagen scaffolds (Schwab et al.,

2006); (Dravida et al., 2008), fibrin-based scaffolds (Rama et al., 2001); (Talbot et al., 2006), contact lens-based scaffolds (Di Girolamo et al., 2009) and synthetic polymers (Sharma et al., 2011). The synthetic (polyamide) scaffolds have advantage of biocompatibility, easy accessibility, no risk of infection transmission and good manipulation.

Previous experimental studies have shown that embryonic SCs can be grown and differentiated on nanofiber scaffolds (Nur-E-Kamal et al., 2006); (Smith et al., 2009). Our results with nanofiber scaffolds demonstrated that the scaffolds prepared by electrospinning technology from polyamide PA6/12 can be used for the culture and transfer of LSCs and MSCs. The 3D structure of nanofiber materials has a large surface area, which can mimic the extracellular matrix and is therefore supports cell growth and function. Up to day 14 after transfer, it was important for us to detect the labelled LSCs on the ocular surface. These results support the fact that nanofiber scaffolds PA6/12 are suitable for SC transfer and that 3 days of coverage is sufficient for LSC migration onto the damaged ocular surface. In our pilot experiments, we found that the nanofiber scaffolds from PA6/12 are stable with no cytotoxicity and surgical manipulation was simple. And the experimental study showed that these scaffolds are suitable for various cell types to be cultured (Dubský et al., 2012).

In our experiments, we found that the scaffolds without cells reduced the inflammatory reaction as well, but less so compared to the scaffolds with LSC and MSC. In view of these results, these scaffolds may serve as therapeutic bandage scaffolds for promoting epithelial healing. The advantage of this compared to human AM is easy accessibility, mechanical stability and no risk of infection transmission. However these scaffolds are not transparent and need to be removed. The 3D reconstruction of LSC niche in which the SCs are associated with adjacent epithelial and stromal cells has been demonstrated (Dziasko et al.,2014). Therefore the 3D structure of nanofiber scaffolds can mimic the extracellular structure of limbal niche. A transfer of scaffold with LSC in the limbal region may serve as a long-term source of LSCs and allow cell migration. However, further studies are needed to show that the scaffolds are able to allow the cells to maintain their SC properties and to serve as a niche.

We used the co-transfer of LSCs and MCSs on nanofiber scaffolds for ocular surface reconstruction in our experiments because these cells may act synergistically and may be both beneficial for ocular surface healing in clinical practice. The LSCs were used from the aspect that they serve as a source of SCs on damaged ocular surface and our experiments proved the migration of LSCs on ocular surface. MSCs were used as they have anti-inflammatory properties, which are proven in previous experimental studies (Ma et al., 2006); (Oh et al., 2008). Inflammation is one of the highest risk factors for the failure of SC based therapy for ocular surface reconstruction and the suppression of inflammation is crucial (Shortt et al., 2010). In our experiments, the co-transfer had immunosuppressive properties, significantly inhibited the local inflammatory reaction and supported healing of the damaged ocular surface.

Two main mechanisms are generally used for transferring cultured LSCs onto a damaged ocular surface. Primarily, the LSCs act as a source of SCs. Secondarily, the transferred LSCs may have a stimulatory effect on residual LSCs, even on an ocular surface with (a clinical diagnosis of) LSCD. This is supported by the fact that the long-term survival of transferred cells was not detected despite good clinical results (Rama et al., 2010). Additionally, the LSCs alone have immunemodulatory properties, which may be beneficial for suppressing inflammation and postponing the rejection (Holan et al., 2010). The co-transfer with MSCs may have another additional benefit, namely that MSCs have the potential to differentiate into different cell types, including the corneal epithelial cells (Pittenger et al., 1999); (Neuss et al., 2008); (Gu et al., 2009). However, there is controversy in current literature surrounding *in vivo* MSCs' ability to trans-differentiation into corneal epithelial cells (Reinshagen et al., 2011).

Used together, our results showed that the nanofiber scaffolds from PA6/12 polyamide are suitable for the growth and transfer of adult tissue specific SCs in the treatment of ocular surface disease in the mouse model. In the future, the nanofiber scaffolds may have a great potential to serve as a scaffold for a wider spectrum of adult SCs and could be used for treatment of various SC deficiencies in humans. However, further studies are needed to test SC survival and the preservation of SCs' properties after transfer onto the ocular surface.

5.4 Mesenchymal stem cell transfer on nanofiber scaffolds for the treatment of chemical corneal injury in a rabbit model

Chemical corneal injuries are one of the most common causes of LSCD. Alkali injuries cause extensive damage to the ocular surface, which can lead to loss of vision. After the injury, acute inflammation, corneal neovascularization, recurrent epithelial erosions and corneal ulcers are present. In the acute phase after injury, there is a need for a prompt anti-inflammatory therapy to reduce the risk of subsequent LSCD development. Appropriate anti-inflammatory treatment reduces the risk of LSCs exhaustion, which is believed to be the more common cause of LSCD than the primary LSC damage caused by the chemical injury. However, current therapy is not always efficient enough and it is necessary to look for alternative treatment options. The discovery of new effective treatment strategies may diminish the incidence of LSCD after chemical corneal injury, thus reducing the risk of vision loss and improving guarded prognosis. Currently, there is growing evidence that MSCs have great potential in regenerative medicine in terms of their anti-inflammatory and immune-modulatory properties (Uccelli et al., 2008); (Nauta and Fibbe, 2007); (Zhao et al., 2010). Based on our previous experience with SC transfer on nanofiber scaffolds (Publication 3), we studied the effect of MSCs after ocular surface injury in a rabbit model. The rabbit eye model is closer to the human eye and may have more similar applications in clinical practice.

Previous studies focused on healing after alkali injury in rats demonstrated the anti-inflammatory and anti-angiogenic effect of MSCs transferred onto human AM (Ma et al., 2006), applied topically (Oh et al., 2008) and injected subconjunctivally (Yao et al., 2012). Similar to these results, we found that MSCs transferred onto nanofiber scaffolds contributed to the healing process in the cornea after alkali injury. To elucidate the mechanisms of the healing process, we showed the positive effect of MSCs on nanofiber scaffolds on alkali-induce oxidative stress in the cornea for the first time. We found a higher antioxidant expression and lower expression of oxidative stress markers in the cornea after MSC therapy. On a cellular basis, the reduced stromal inflammatory infiltration by macrophages was found in the MSCs treated group during post-operative period. The expression of genes for pro-inflammatory cytokines (IL-1β, IL-6 and IFN-γ) was significantly reduced in the group treated with MSCs on nanofiber scaffolds compared to the group without treatment. The nanofiber scaffolds are suitable for SC growth and transfer and are easily transferred onto the ocular surface.

In view of the current knowledge, both mechanisms of MSCs (suppression of inflammation and differentiation into corneal-like epithelium) may participate in the healing process of ocular surface damage after alkali injury. The MSCs are able to differentiate *in vivo* into corneal epithelium-like cells after transfer onto damaged ocular surface (Gu et al., 2009). There are studies that demonstrate the therapeutic effects of MSCs for treating LSCD due to differentiation (Jiang et al., 2010); (Ye et al., 2006). However, the study of Reinshagen et al. did not prove the clinical improvement of LSCD in rabbits after the MSCs were injected under human AM secured on the corneal surface (Reinshagen et al., 2011). They described that the possible causes of therapy failure may be due to cell spread under conjunctiva or the washing out effect of tear film after transfer. Human AM has the disadvantage of inducing epithelial repair accompanied by dense vascularization (Kim and Tseng, 1995); (Reinshagen et al., 2011).

For corneal transparency and to maintain good vision, it is essential to maintain the avascularity and uniform ultrastructure of collagen fibrils. Both attributes can be damaged after alkali injury. We found that corneal neovascularization was significantly suppressed after MSC transfer in alkali-injured corneas. This anti-angiogenic therapeutic effect may be given by a concurrent anti-inflammatory effect. But the exact mechanism is not known. Corneal swelling is a sign of corneal damage after alkali injury and can be measured by an ultrasound pachymeter (O'Donnell et al., 2006); (Cejka et al., 2010). We found that the MSCs transferred on nanofiber scaffolds normalized the corneal hydration after 10 days. Thus the corneal ultrasound pachymetry is a good tool for monitoring corneal restoration and thus following the healing process.

In conclusion, the use of autologous MSCs cells have the advantage of not inducing immune rejection. The MSCs are easy to isolate, therefore there is a high potential for clinical application. In addition, the rabbit eye model is closer to the human eye and, therefore, the results of our experiments may have more clinical applications.

6 CONCLUSIONS

The aim of this thesis was the reconstruction of the damaged ocular surface by LSC transfer in the experimental mouse and rabbit model. To achieve ocular surface recovery in LSCD, it is necessary to understand the cellular mechanism of LSC transplantation, immune response and graft survival. Based on the promising results of recent publications, there is a need to focus, not only on tissue transfer, but also on SC-based treatment for ocular surface disorders in more depth. The main conclusions of this study are as follows:

1. Allogeneic limbal grafts do not enjoy any immune privileged position of the eye and are rejected promptly by the Th1-type of immune response involving $CD4^+$ cells and NO produced by macrophages. Anti-CD4 treatment thus represents a promising immunosuppressive approach after limbal allotransplantation. Th1 and Th2 immune responses were detected in the xenogeneic model during the rejection. Depletion of $CD4^+$ cells significantly prolonged the limbal survival in the allograft and in the xenograft model. Limbal graft transplantation is a useful model for testing various immunosuppressive approaches. This surgical technique was successfully used for further experiments with nanofiber scaffolds and enabled a better understanding of the immune mechanism of SC transfer.

2. By centrifugation in Percoll gradient of epithelial LSCs, two distinct populations of corneal epithelial cells with LSC characteristics were separated in the 40% and 80% Percoll fraction of the gradient. The densest fraction (less than 7% of original cells) contained small, non-spontaneously proliferating cells, $K12^-/p63^+$, with a high *ex vivo* proliferative activity culturing on a 3T3 feeder cell monolayer. The $K12^-/p63^+$ population is closer to the primitive LSCs. Therefore this technique can be used for SC isolation from limbal explant and subsequently for SC based therapy of ocular surface disorders. This method was used for our further experiments with LSC transfer and is still used as a standard method for LSC isolation in mouse model.

3. The nanofiber scaffolds from a polyamide 6/12 can be useful for growth and transfer of LSCs and bone marrow-derived MSCs, and can be utilized for future treatment of ocular surface injuries and LSCD. The co-transfer of LSCs and MSCs suppressed the inflammatory reaction and therefore improved corneal healing in the mouse model.

4. Bone marrow-derived MSCs on nanofiber scaffolds reduced the alkali-induced oxidative stress in the cornea after alkali injury and significantly accelerated corneal healing in the experimental rabbit model. The transferred MCSs protected against the peroxynitrite production, suppressed the cell apoptosis, matrix metalloproteinase levels and pro-inflammatory cytokine production. Reduced inflammation resulted in decreased corneal neovascularization after alkali injury.

The understanding of cellular and molecular mechanism of limbal tissue transplantation and finding of new treatment strategies may improve long-term limbal graft survival, clinical outcome and thus may be beneficial for patients with LSCD diagnosis. Additional to that, the better understanding of mechanism of SC-based therapy may give us more knowledge for future treatment options for patients with this severe diagnosis, especially in cases of bilateral LSCD. Therefore, this field of experimental ophthalmology has a great potential for patients with LSCD, who have a very poor prognosis. Further studies are necessary to determine the long-term effect of LSC transfer, the fate of donor cells on ocular surface in term of SCs properties and the long-term cell survival after the transfer of *ex vivo* cultured LSCs and MSCs on the ocular surface.

7 REFERENCES

Ahmad S, Stewart R, Yung S, Kolli S, Armstrong L, Stojkovic M, Figueiredo F, Lako M. Differentiation of human embryonic stem cells into corneal epithelial-like cells by in vitro replication of the corneal epithelial stem cell niche. Stem Cells. 2007 May;25(5):1145-55.

Akinci MA, Turner H, Taveras M, Wolosin JM. Differential gene expression in the pig limbal side population: implications for stem cell cycling, replication, and survival. Invest Ophthalmol Vis Sci. 2009 Dec;50(12):5630-8.

Ang LP, Tanioka H, Kawasaki S, Ang LP, Yamasaki K, Do TP, Thein ZM, Koizumi N, Nakamura T, Yokoi N, Komuro A, Inatomi T, Nakatsukasa M, Kinoshita S. Cultivated human conjunctival epithelial transplantation for total limbal stem cell deficiency. Invest Ophthalmol Vis Sci. 2010 Feb;51(2):758-64.

Angoulvant D, Clerc A, Benchalal S, Galambrun C, Farre A, Bertrand Y, Eljaafari A. Human mesenchymal stem cells suppress induction of cytotoxic response to alloantigens. Biorheology. 2004;41(3-4):469-76.

Baradaran-Rafii A, Eslani M, Djalillian AR. Complications of keratolimbal allograft surgery. Cornea. 2013 May;32(5):561-6.

Barbaro V, Ferrari S, Fasolo A, Pedrotti E, Marchini G, Sbabo A, Nettis N, Ponzin D, Di Iorio E. Evaluation of ocular surface disorders: a new diagnostic tool based on impression cytology and confocal laser scanning microscopy. Br J Ophthalmol. 2010 Jul;94(7):926-32.

Barbaro V, Testa A, Di Iorio E, Mavilio F, Pellegrini G, De Luca M. C/EBPdelta regulates cell cycle and self-renewal of human limbal stem cells. J Cell Biol. 2007 Jun 18;177(6):1037-49.

Barrandon Y. Crossing boundaries: stem cells, holoclones, and the fundamentals of squamous epithelial renewal. Cornea. 2007 Oct;26(9 Suppl 1):S10-2.

Barreiro TP, Santos MS, Vieira AC, de Nadai Barros J, Hazarbassanov RM, Gomes JA. Comparative study of conjunctival limbal transplantation not associated with the use of amniotic membrane transplantation for treatment of total limbal deficiency secondary to chemical injury. Cornea. 2014 Jul;33(7):716-20.

Bartholomew A, Sturgeon C, Siatskas M, Ferrer K, McIntosh K, Patil S, Hardy W, Devine S, Ucker D, Deans R, Moseley A, Hoffman R. Mesenchymal stem cells suppress lymphocyte proliferation in vitro and prolong skin graft survival in vivo. Exp Hematol. 2002 Jan;30(1):42-8.

Basu S, Ali H, Sangwan VS. Clinical outcomes of repeat autologous cultivated limbal epithelial transplantation for ocular surface burns. Am J Ophthalmol. 2012 Apr;153(4):643-50. (a)

Basu S, Fernandez MM, Das S, Gaddipati S, Vemuganti GK, Sangwan VS. Clinical outcomes of xeno-free allogeneic cultivated limbal epithelial transplantation for bilateral limbal stem cell deficiency. Br J Ophthalmol. 2012 Dec;96(12):1504-9. (b)

Beebe DC, Masters BR. Cell lineage and the differentiation of corneal epithelial cells. Invest Ophthalmol Vis Sci. 1996;37:1815-25.

Beuerman RW, Pedroza L. Ultrastructure of the human cornea. Microsc Res Tech. 1996 Mar 1;33(4):320-35.

Bhattarai N, Edmondson D, Veiseh O, Matsen FA, Zhang M. Electrospun chitosan-based nanofibers and their cellular compatibility. Biomaterials. 2005 Nov;26(31):6176-84.

Bi YL, Bock F, Zhou Q, Cursiefen C. Central corneal epithelium self-healing after ring-shaped glycerin-cryopreserved lamellar keratoplasty in Terrien marginal degeneration. Int J Ophthalmol. 2013 Apr 18;6(2):251-2.

Blau HM, Brazelton TR, Weimann JM. The evolving concept of a stem cell: Entity or function? Cell 2001;105:829-41.

Blazejewska EA, Schltzer-Schrehardt U, Zenkel M, Bachmann B, Chankiewitz E, Jacobi C, Kruse FE. Corneal limbal microenvironment can induce transdifferentiation of hair follicle stem cells into corneal epithelial-like cells. Stem Cells. 2009 Mar;27(3):642-52.

Bron AJ. The architecture of the corneal stroma. Br J Ophthalmol. 2001 Apr;85(4):379-81.

Budak MT, Alpdogan OS, Zhou M, Lavker RM, Akinci MA, Wolosin JM. Ocular surface epithelia contain ABCG2-dependent side population cells exhibiting features associated with stem cells. J Cell Sci. 2005 Apr 15;118(Pt 8):1715-24.

Casiraghi F, Azzollini N, Cassis P, Imberti B, Morigi M, Cugini D, Cavinato RA, Todeschini M, Solini S, Sonzogni A, Perico N, Remuzzi G, Noris M. Pretransplant infusion of mesenchymal stem cells prolongs the survival of a semiallogeneic heart transplant through the generation of regulatory T cells. J Immunol. 2008 Sep 15;181(6):3933-46.

Cauchi PA, Ang GS, Azuara-Blanco A, Burr JM. A systematic literature review of surgical interventions for limbal stem cell deficiency in humans. Am J Ophthalmol. 2008 Aug;146(2):251-259.

Cejka C, Plátenník J, Sirc J, Ardan T, Michálek J, Brůnová B, Cejková J. Changes of corneal optical properties after UVB irradiation investigated spectrophotometrically. Physiol Res. 2010;59(4):591-7.

Chan CC, Holland EJ. Severe limbal stem cell deficiency from contact lens wear: patient clinical features. Am J Ophthalmol. 2013 Mar;155(3):544-49.

Chang CY, Green CR, McGhee CN, Sherwin T. Acute wound healing in the human central corneal epithelium appears to be independent of limbal stem cell influence. Invest Ophthalmol Vis Sci. 2008 Dec;49(12):5279-86.

Chen JJ, Tseng SC. Corneal epithelial wound healing in partial limbal deficiency. Invest Ophthalmol Vis Sci. 1990 Jul;31(7):1301-14.

Chen JJ, Tseng SC. Abnormal corneal epithelial wound healing in partial-thickness removal of limbal epithelium. Invest Ophthalmol Vis Sci. 1991 Jul;32(8):2219-33.

Chen W, Cao L, Hara K, Yoshitomi T. Effect of immunosuppression on survival of allograft limbal stem cells. Jpn J Ophthalmol. 2004 Sep-Oct;48(5):440-7.

Chen Z, de Paiva CS, Luo L, Kretzer FL, Pflugfelder SC, Li DQ. Characterization of putative stem cell phenotype in human limbal epithelia. Stem Cells. 2004;22(3):355-66.

Collinson JM, Chanas SA, Hill RE, West JD. Corneal development, limbal stem cell function, and corneal epithelial cell migration in the Pax6(+/-) mouse. Invest Ophthalmol Vis Sci. 2004 Apr;45(4):1101-8.

Cortes M, Lambiase A, Sacchetti M, Aronni S, Bonini S. Limbal stem cell deficiency associated with LADD syndrome. Arch Ophthalmol. 2005 May;123(5):691-4.

Cotsarelis G, Cheng SZ, Dong G, Sun TT, Lavker RM. Existence of slow-cycling limbal epithelial basal cells that can be preferentially stimulated to proliferate: implications on epithelial stem cells. Cell. 1989 Apr 21;57(2):201-9.

Cotsarelis G, Kaur P, Dhouailly D, Hengge U, Bickenbach J. Epithelial stem cells in the skin: definition, markers, localization and functions. Exp Dermatol. 1999 Feb;8(1):80-8.

Croasdale CR, Schwartz GS, Malling JV, Holland EJ. Keratolimbal allograft: recommendations for tissue procurement and preparation by eye banks, and standard surgical technique. Cornea. 1999 Jan;18(1):52-8.

Daniels JT, Dart JK, Tuft SJ, Khaw PT. Corneal stem cells in review. Wound Repair Regen. 2001 Nov-Dec;9(6):483-94.

Das H, Abdulhameed N, Joseph M, Sakthivel R, Mao HQ, Pompili VJ. Ex vivo nanofiber expansion and genetic modification of human cord blood-derived progenitor/stem cells enhances vasculogenesis. Cell Transplant. 2009;18(3):305-18.

Davanger M, Evensen A. Role of the pericorneal papillary structure in renewal of corneal epithelium. Nature. 1971 Feb 19;229(5286):560-1.

Daya SM, Bell RW, Habib NE, Powell-Richards A, Dua HS. Clinical and pathologic findings in human keratolimbal allograft rejection. Cornea. 2000 Jul;19(4):443-50.

Daya SM, Chan CC, Holland EJ; Members of The Cornea Society Ocular Surface Procedures Nomenclature Committee. Cornea Society nomenclature for ocular surface rehabilitative procedures. Cornea. 2011 Oct;30(10):1115-9.

Daya SM, Watson A, Sharpe JR, Giledi O, Rowe A, Martin R, James SE. Outcomes and DNA analysis of ex vivo expanded stem cell allograft for ocular surface reconstruction. Ophthalmology. 2005 Mar;112(3):470-7.

De Nicola R, Labbé A, Amar N, Dupas B, Baudouin C. In vivo confocal microscopy and ocular surface diseases: anatomical-clinical correlations. J Fr Ophtalmol. 2005 Sep;28(7):691-8.

De Paiva CS, Chen Z, Corrales RM, Pflugfelder SC, Li DQ. ABCG2 transporter identifies a population of clonogenic human limbal epithelial cells. Stem Cells. 2005;23(1):63-73.

De Paiva CS, Pflugfelder SC, Li DQ. Cell size correlates with phenotype and proliferative capacity in human corneal epithelial cells. Stem Cells. 2006 Feb;24(2):368-75.

DeSousa JL, Daya S, Malhotra R. Adnexal surgery in patients undergoing ocular surface stem cell transplantation. Ophthalmology. 2009 Feb;116(2):235-42.

Di Girolamo N, Bosch M, Zamora K, Coroneo MT, Wakefield D, Watson SL. A contact lens-based technique for expansion and transplantation of autologous epithelial progenitors for ocular surface reconstruction. Transplantation. 2009 May 27;87(10):1571-8.

Di Iorio E, Barbaro V, Ruzza A, Ponzin D, Pellegrini G, De Luca M. Isoforms of DeltaNp63 and the migration of ocular limbal cells in human corneal regeneration. Proc Natl Acad Sci U S A. 2005 Jul 5;102(27):9523-8.

Di Nicola M, Carlo-Stella C, Magni M, Milanesi M, Longoni PD, Matteucci P, Grisanti S, Gianni AM. Human bone marrow stromal cells suppress T-lymphocyte proliferation induced by cellular or nonspecific mitogenic stimuli. Blood. 2002 May 15;99(10):3838-43.

Di Pascuale MA, Espana EM, Liu DT, Kawakita T, Li W, Gao YY, Baradaran-Rafii A, Elizondo A, Raju VK, Tseng SC. Correlation of corneal complications with eyelid cicatricial pathologies in patients with Stevens-Johnson syndrome and toxic epidermal necrolysis syndrome. Ophthalmology. 2005 May;112(5):904-12.

Dialynas DP, Wilde DB, Marrack P, Pierres A, Wall KA, Havran W, Otten G, Loken MR, Pierres M, Kappler J, et al. Characterization of the murine antigenic determinant, designated L3T4a, recognized by monoclonal antibody GK1.5: expression of L3T4a by functional T cell clones appears to correlate primarily with class II MHC antigen-reactivity. Immunol Rev. 1983;74:29-56.

Dziasko MA, Armer HE, Levis HJ, Shortt AJ, Tuft S, Daniels JT. Localisation of epithelial cells capable of holoclone formation in vitro and direct interaction with stromal cells in the native human limbal crypt. PLoS One. 2014 Apr 8;9(4):e94283.

Dios E, Herreras JM, Mayo A, Blanco G. Efficacy of systemic cyclosporine A and amniotic membrane on rabbit conjunctival limbal allograft rejection. Cornea. 2005 Mar;24(2):182-8.

Djalilian AR, Mahesh SP, Koch CA, Nussenblatt RB, Shen D, Zhuang Z, Holland EJ, Chan CC. Survival of donor epithelial cells after limbal stem cell transplantation. Invest Ophthalmol Vis Sci. 2005 Mar;46(3):803-7.

Djouad F, Plence P, Bony C, Tropel P, Apparailly F, Sany J, Nol D, Jorgensen C. Immunosuppressive effect of mesenchymal stem cells favors tumor growth in allogeneic animals. Blood. 2003 Nov 15;102(10):3837-44.

Donisi PM, Rama P, Fasolo A, Ponzin D. Analysis of limbal stem cell deficiency by corneal impression cytology. Cornea. 2003 Aug;22(6):533-8.

Dravida S, Gaddipati S, Griffith M, Merrett K, Lakshmi Madhira S, Sangwan VS, Vemuganti GK. A biomimetic scaffold for culturing limbal stem cells: a promising alternative for clinical transplantation. J Tissue Eng Regen Med. 2008 Jul;2(5):263-71.

Dua HS, Azuara-Blanco A. Allo-limbal transplantation in patients with limbal stem cell deficiency. Br J Ophthalmol. 1999 Apr;83(4):414-9.

Dua HS, Azuara-Blanco A. Limbal stem cells of the corneal epithelium. Surv Ophthalmol. 2000 Mar-Apr;44(5):415-25.

Dua HS, Faraj LA, Said DG, Gray T, Lowe J. Human corneal anatomy redefined: a novel pre-Descemet's layer (Dua's layer). Ophthalmology. 2013 Sep;120(9):1778-85.

Dua HS, Forrester JV. Clinical patterns of corneal epithelial wound healing. Am J Ophthalmol. 1987 Nov 15;104(5):481-9.

Dua HS, Forrester JV. The corneoscleral limbus in human corneal epithelial wound healing. Am J Ophthalmol. 1990 Dec 15;110(6):646-56.

Dua HS, Gomes JA, Singh A. Corneal epithelial wound healing. Br J Ophthalmol. 1994 May;78(5):401-8.

Dua HS, Joseph A, Shanmuganathan VA, Jones RE. Stem cell differentiation and the effects of deficiency. Eye (Lond). 2003 Nov;17(8):877-85.

Dua HS, Miri A, Alomar T, Yeung AM, Said DG. The role of limbal stem cells in corneal epithelial maintenance: testing the dogma. Ophthalmology. 2009 May;116(5):856-63.

Dua HS, Miri A, Said DG. Contemporary limbal stem cell transplantation - a review. Clin Experiment Ophthalmol 2010 Mar;38(2):104-17.

Dua HS, Rahman I, Jayaswal R, Said DG. Combined limbal and corneal grafts: should we or should we not? Clin Experiment Ophthalmol. 2008 Aug;36(6):497-8.

Dua HS, Saini JS, Azuara-Blanco A, Gupta P. Limbal stem cell deficiency: concept, aetiology, clinical presentation, diagnosis and management. Indian J Ophthalmol. 2000 Jun;48(2):83-92.

Dua HS, Shanmuganathan VA, Powell-Richards AO, Tighe PJ, Joseph A. Limbal epithelial crypts: a novel anatomical structure and a putative limbal stem cell niche. Br J Ophthalmol. 2005 May;89(5):529-32.

Dua HS, Transplantation of limbal stem cells. In: Rienhard T, Larkin F (Eds). Cornea and External Eye Disease. Berlin: Springer, 2006. pp. 3564. ISBN 0323023150.

Dubský M, Kubinová S, Sirc J, Voska L, Zajíček R, Zajícová A, Lesný P, Jirkovská A, Michálek J, Munzarová M, Holáň V, Syková E. Nanofibers prepared by needleless electrospinning technology as scaffolds for wound healing. J Mater Sci Mater Med. 2012 Apr;23(4):931-41.

Dunaief JL, Ng EW, Goldberg MF. Corneal dystrophies of epithelial genesis: the possible therapeutic use of limbal stem cell transplantation. Arch Ophthalmol. 2001 Jan;119(1):120-2.

Egarth M, Hellkvist J, Claesson M, Hanson C, Stenevi U. Longterm survival of transplanted human corneal epithelial cells and corneal stem cells. Acta Ophthalmol Scand. 2005 Oct;83(5):456-61.

Espana EM, Grueterich M, Romano AC, Touhami A, Tseng SC. Idiopathic limbal stem cell deficiency. Ophthalmology. 2002 Nov;109(11):2004-10.

Espana EM, Kawakita T, Romano A, Di Pascuale M, Smiddy R, Liu CY, Tseng SC. Stromal niche controls the plasticity of limbal and corneal epithelial differentiation in a rabbit model of recombined tissue. Invest Ophthalmol Vis Sci. 2003 Dec;44(12):5130-5.

Fernandes M, Sangwan VS, Vemuganti GK. Limbal stem cell deficiency and xeroderma pigmentosum: a case report. Eye (Lond). 2004 Jul;18(7):741-3.

Fini ME, Stramer BM. How the cornea heals: cornea-specific repair mechanisms affecting surgical outcomes. Cornea. 2005 Nov;24(8 Suppl):S2-S11.

Fish R, Davidson RS. Management of ocular thermal and chemical injuries, including amniotic membrane therapy. Curr Opin Ophthalmol. 2010 Jul;21(4):317-21.

Forrester JV, Dick AD, McMenamin PG, Roberts F. Anatomy of the eye and orbit. In: Forrester JV, Dick AD, McMenamin PG, Roberts F. The Eye - basic science in practice. Philadelphia: Elsevier Health Sciences, 2008. pp. 16-26. ISBN 9780702028410.

Friedenstein AJ, Chailakhjan RK, Lalykina KS. The development of fibroblast colonies in monolayer cultures of guinea-pig bone marrow and spleen cells. Cell Tissue Kinet. 1970 Oct;3(4):393-403.

Fujishima H, Shimazaki J, Tsubota K. Temporary corneal stem cell dysfunction after radiation therapy. Br J Ophthalmol. 1996 Oct;80(10):911-4.

Gillette TE, Chandler JW, Greiner JV. Langerhans cells of the ocular surface. Ophthalmology. 1982 Jun;89(6):700-11.

Gomes JA, Geraldes Monteiro B, Melo GB, Smith RL, Cavenaghi Pereira da Silva M, Lizier NF, Kerkis A, Cerruti H, Kerkis I. Corneal reconstruction with tissue-engineered cell sheets composed of human immature dental pulp stem cells. Invest Ophthalmol Vis Sci. 2010 Mar;51(3):1408-14.

Gottlieb PD, Marshak-Rothstein A, Auditore-Hargreaves K, Berkoben DB, August DA, Rosche RM, Benedetto JD. Construction and properties of new Lyt-congenic strains and anti-Lyt-2.2 and anti-Lyt-3.1 monoclonal antibodies. Immunogenetics. 1980;10(6):545-55.

Grueterich M, Espana E, Tseng SC. Connexin 43 expression and proliferation of human limbal epithelium on intact and denuded amniotic membrane. Invest Ophthalmol Vis Sci. 2002 Jan;43(1):63-71.

Grueterich M, Espana EM, Tseng SC. Ex vivo expansion of limbal epithelial stem cells: amniotic membrane serving as a stem cell niche. Surv Ophthalmol. 2003 Nov-Dec;48(6):631-46.

Gu S, Xing C, Han J, Tso MO, Hong J. Differentiation of rabbit bone marrow mesenchymal stem cells into corneal epithelial cells in vivo and ex vivo. Mol Vis. 2009;15:99-107.

Güell JL, Torrabadella M, Calatayud M, Gris O, Manero F, Gaytanua J. Limbal stem cell culture. In: Rienhard T, Larkin F (Eds). Cornea and External Eye Disease. Berlin: Springer, 2006; 57-64. ISBN 0323023150.

Gupta N, Sachdev R, Tandon R. Ocular surface squamous neoplasia in xeroderma pigmentosum: clinical spectrum and outcome. Graefes Arch Clin Exp Ophthalmol. 2011 Aug;249(8):1217-21.

Haskjold E, Refsum SB, Bjerknes R. Circadian variation in the mitotic rate of the rat corneal epithelium: cell divisions and migration are analyzed by a mathematical model. Virchows Arch B Cell Pathol. 1989;58(2):123-127.

Hasková Z, Filipec M, Holáň V. [The significance of gender incompatibility in donors and recipients and the role of minor histocompatibility antigens in corneal transplantation]. [Article in Czech] Cesk Slov Oftalmol. 1997 May;53(2):128-35.

Hayashi R, Ishikawa Y, Ito M, Kageyama T, Takashiba K, Fujioka T, Tsujikawa M, Miyoshi H, Yamato M, Nakamura Y, Nishida K. Generation of corneal epithelial cells from induced pluripotent stem cells derived from human dermal fibroblast and corneal limbal epithelium. PLoS One. 2012;7(9):e45435.

Hayashi S, Osawa T, Tohyama K. Comparative observations on corneas, with special reference to Bowman's layer and Descemet's membrane in mammals and amphibians. J Morphol. 2002 Dec;254(3):247-58.

He YG, Ross J, Niederkorn JY. Promotion of murine orthotopic corneal allograft survival by systemic administration of anti-CD4 monoclonal antibody. Invest Ophthalmol Vis Sci. 1991 Sep;32(10):2723-8.

Henderson TR, Coster DJ, Williams KA. The long term outcome of limbal allografts: the search for surviving cells. Br J Ophthalmol. 2001 May;85(5):604-9.

Henriksson JT, McDermott AM, Bergmanson JP. Dimensions and morphology of the cornea in three strains of mice. Invest Ophthalmol Vis Sci. 2009 Aug;50(8):3648-54.

Hill RE, Favor J, Hogan BL, Ton CC, Saunders GF, Hanson IM, Prosser J, Jordan T, Hastie ND, van Heyningen V. Mouse small eye results from mutations in a paired-like homeobox-containing gene. Nature. 1991 Dec 19-26;354(6354):522-5.

Ho JH, Ma WH, Tseng TC, Chen YF, Chen MH, Lee OK. Isolation and characterization of multi-potent stem cells from human orbital fat tissues. Tissu Eng Part A. 2011 Jan; 17(1-2):255-66.

Hogan MJ, Alvarado JA, and Weddell JE. The Limbus. In: Hogan MJ, Alvarado JA, and Weddell JE. Histology of the human eye. Philadelphia: WB Saunders. 1971. pp. 112-182, ISBN 0721647200.

Holan V, Pokorna K, Prochazkova J, Krulova M, Zajicova A. Immunoregulatory properties of mouse limbal stem cells. J Immunol. 2010 Feb 15;184(4):2124-9.

Holan V, Chudickova M, Trosan P, Svobodova E, Krulova M, Kubinova S, Sykova E, Sirc J, Michalek J, Juklickova M, Munzarova M, Zajicova A. Cyclosporine A-loaded and stem cell-seeded electrospun nanofibers for cell-based therapy and local immunosuppression. J Control Release. 2011 Dec 20;156(3):406-12.

Holland EJ. Epithelial transplantation for the management of severe ocular surface disease. Trans Am Ophthalmol Soc 1996; 94:677-743.

Holland EJ, Mogilishetty G, Skeens HM, Hair DB, Neff KD, Biber JM, Chan CC. Systemic immunosuppression in ocular surface stem cell transplantation: results of a 10-year experience. Cornea. 2012 Jun;31(6):655-61.

Homma R, Yoshikawa H, Takeno M, Kurokawa MS, Masuda C, Takada E, Tsubota K, Ueno S, Suzuki N. Induction of epithelial progenitors in vitro from mouse embryonic stem cells and application for reconstruction of damaged cornea in mice. Invest Ophthalmol Vis Sci. 2004 Dec;45(12):4320-6.

Hoogduijn MJ, Crop MJ, Peeters AM, Van Osch GJ, Balk AH, Ijzermans JN, Weimar W, Baan CC. Human heart, spleen, and perirenal fat-derived mesenchymal stem cells have immunomodulatory capacities. Stem Cells Dev. 2007 Aug;16(4):597-604.

Huang AJ, Tseng SC. Corneal epithelial wound healing in the absence of limbal epithelium. Invest Ophthalmol Vis Sci 1991 Jan;32(1):96-105.

Inatomi T, Nakamura T, Kojyo M, Koizumi N, Sotozono C, Kinoshita S. Ocular surface reconstruction with combination of cultivated autologous

oral mucosal epithelial transplantation and penetrating keratoplasty. Am J Ophthalmol. 2006 Nov;142(5):757-64.

Javadi MA, Baradaran-Rafii A. Living-related conjunctival-limbal allograft for chronic or delayed-onset mustard gas keratopathy. Cornea. 2009 Jan;28(1):51-7.

Jester JV, Moller-Pedersen T, Huang J, Sax CM, Kays WT, Cavangh HD, Petroll WM, Piatigorsky J. The cellular basis of corneal transparency: evidence for 'corneal crystallins'. J Cell Sci. 1999 Mar;112 (Pt 5):613-22.

Jiang TS, Cai L, Ji WY, Hui YN, Wang YS, Hu D, Zhu J. Reconstruction of the corneal epithelium with induced marrow mesenchymal stem cells in rats. Mol Vis. 2010 Jul 14;16:1304-16.

Jirsova K, Dudakova L, Kalasova S, Vesela V, Merjava S. The OV-TL 12/30 clone of anti-cytokeratin 7 antibody as a new marker of corneal conjunctivalization in patients with limbal stem cell deficiency. Invest Ophthalmol Vis Sci. 2011 Jul 29;52(8):5892-8.

Joseph A, Powell-Richards AO, Shanmuganathan VA, Dua HS. Epithelial cell characteristics of cultured human limbal explants. Br J Ophthalmol. 2004 Mar;88(3):393-8.

Kanayama S, Nishida K, Yamato M, Hayashi R, Sugiyama H, Soma T, Maeda N, Okano T, Tano Y. Analysis of angiogenesis induced by cultured corneal and oral mucosal epithelial cell sheets in vitro. Exp Eye Res. 2007 Dec;85(6):772-81.

Kasper M, Stosiek P, Lane B. Cytokeratin and vimentin heterogeneity in human cornea. Acta Histochem. 1992;93(2):371-81.

Kawasaki S, Tanioka H, Yamasaki K, Yokoi N, Komuro A, Kinoshita S. Clusters of corneal epithelial cells reside ectopically in human conjunctival epithelium. Invest Ophthalmol Vis Sci. 2006 Apr;47(4):1359-67.

Keijser S, de Keizer RJ, Prins FA, Tanke HJ, van Rooijen N, Vrensen GF, Jager MJ. A new model for limbal transplantation using E-GFP for follow-up of transplant survival. Exp Eye Res. 2006 Nov;83(5):1188-95.

Kenyon KR, Tseng SC. Limbal autograft transplantation for ocular surface disorders. Ophthalmology. 1989 May;96(5):709-22.

Kim JC, Tseng SC. Transplantation of preserved human amniotic membrane for surface reconstruction in severely damaged rabbit corneas. Cornea. 1995 Sep;14(5):473-84.

Kim M, Turnquist H, Jackson J, Sgagias M, Yan Y, Gong M, Dean M, Sharp JG, Cowan K. The multidrug resistance transporter ABCG2 (breast cancer resistance protein 1) effluxes Hoechst 33342 and is overexpressed in hematopoietic stem cells. Clin Cancer Res. 2002 Jan;8(1):22-8.

Kobayashi A, Shirao Y, Yoshita T, Yagami K, Segawa Y, Kawasaki K, Shozu M, Tseng SC. Temporary amniotic membrane patching for acute chemical burns. Eye (Lond). 2003 Mar;17(2):149-58.

Koizumi N, Cooper LJ, Fullwood NJ, Nakamura T, Inoki K, Tsuzuki M, Kinoshita S. An evaluation of cultivated corneal limbal epithelial cells, using cell-suspension culture. Invest Ophthalmol Vis Sci. 2002 Jul;43(7):2114-21.

Koizumi N, Inatomi T, Suzuki T, Sotozono C, Kinoshita S. Cultivated corneal epithelial stem cell transplantation in ocular surface disorders. Ophthalmology. 2001 Sep;108(9):1569-74.

Koizumi N, Rigby H, Fullwood NJ, Kawasaki S, Tanioka H, Koizumi K, Kociok N, Joussen AM, Kinoshita S. Comparison of intact and denuded amniotic membrane as a substrate for cell-suspension culture of human limbal epithelial cells. Graefes Arch Clin Exp Ophthalmol. 2007 Jan;245(1):123-34.

Krachmer JH, Mannis MJ, Holland EJ (Eds). Cornea, 2nd ed. VOl 1. Philadelphia: Elsevier Mosby; 2005:37-43. ISBN 0323032150.

Kremer I, Ehrenberg M, Weinberger D. Fresh-tissue corneolimbal covering graft for large corneal perforation following childhood trachoma. Ophthalmic Surg Lasers Imaging. 2009 May-Jun;40(3):245-50.

Krulová M, Zajícová A, Fric J, Holáň V. Alloantigen-induced, T-cell-dependent production of nitric oxide by macrophages infiltrating skin allografts in mice. Transpl Int. 2002 Mar;15(2-3):108-16.

Kruse FE, Chen JJ, Tsai RJ, Tseng SC. Conjunctival transdifferentiation is due to the incomplete removal of limbal basal epithelium. Invest Ophthalmol Vis Sci. 1990 Sep;31(9):1903-13.

Kruse FE. Stem cells and corneal epithelial regeneration. Eye 1994; 8:170-83.

Kusanagi R, Umemoto T, Yamato M, Matsuzaki Y, Nishida K, Kobayashi Y, Fukai F, Okano T. Nectin-3 expression is elevated in limbal epithelial side population cells with strongly expressed stem cell markers. Biochem Biophys Res Commun. 2009 Nov 13;389(2):274-8.

Lagali N, Edén U, Utheim TP, Chen X, Riise R, Dellby A, Fagerholm P. In vivo morphology of the limbal palisades of vogt correlates with progressive stem cell deficiency in aniridia-related keratopathy. Invest Ophthalmol Vis Sci. 2013 Aug 7;54(8):5333-42.

Lavker RM, Sun TT. Epidermal stem cells: Properties, markers, and location. Proc Natl Acad Sci U S A. 2000 Dec 5;97(25):13473-5.

Le Blanc K, Tammik L, Sundberg B, Haynesworth SE, Ringdn O. Mesenchymal stem cells inhibit and stimulate mixed lymphocyte cultures and mitogenic responses independently of the major histocompatibility complex. Scand J Immunol. 2003 Jan;57(1):11-20.

Lehrer MS, Sun TT, Lavker RM. Strategies of epithelial repair: modulation of stem cell and transit amplifying cell proliferation. J Cell Sci. 1998 Oct; 111 (Pt 19):2867-75.

Lemp MA, Mathers WD. Corneal epithelial cell movement in humans. Eye (Lond). 1989;3 (Pt 4):438-45.

Levis H, Daniels JT. New technologies in limbal epithelial stem cell transplantation. Curr Opin Biotechnol. 2009 Oct;20(5):593-7.

Li HF, Petroll WM, Pedersen TM, Maurer JK, Cavanagh HD, Jester JV. Epithelial and corneal thickness measurements by in vivo confocal microscopy through focusing (CMTF). Curr Eye Res. 1997 Mar;16(3):214-21.

Li W, Chen YT, Hayashida Y, Blanco G, Kheirkah A, He H, Chen SY, Liu CY, Tseng SC. Down-regulation of Pax6 is associated with abnormal differentiation of corneal epithelial cells in severe ocular surface diseases. J Pathol. 2008 Jan;214(1):114-22.

Li W, Hayashida Y, Chen YT, Tseng SC. Niche regulation of corneal epithelial stem cells at the limbus. Cell Res. 2007 Jan;17(1):26-36.

Li F, Zhao SZ. Mesenchymal stem cells: Potential role in corneal wound repair and transplantation. World J Stem Cells. 2014 Jul 26;6(3):296-304.

Liang L, Li W, Ling S, Sheha H, Qiu W, Li C, Liu Z. Amniotic membrane extraction solution for ocular chemical burns. Clin Experiment Ophthalmol. 2009 Dec;37(9):855-63. (a)

Liang L, Sheha H, Tseng SC. Long-term outcomes of keratolimbal allograft for total limbal stem cell deficiency using combined immunosuppressive agents and correction of ocular surface deficits. Arch Ophthalmol. 2009 Nov;127(11):1428-34. (b)

Liu CY, Zhu G, Westerhausen-Larson A, Converse R, Kao CW, Sun TT, Kao WW. Cornea-specific expression of K12 keratin during mouse development. Curr Eye Res. 1993 Nov;12(11):963-74.

Ma Y, Xu Y, Xiao Z, Yang W, Zhang C, Song E, Du Y, Li L. Reconstruction of chemically burned rat corneal surface by bone marrow-derived human mesenchymal stem cells. Stem Cells. 2006 Feb;24(2):315-21.

Majo F, Rochat A, Nicolas M, Jaoude GA, Barrandon Y. Oligopotent stem cells are distributed throughout the mammalian ocular surface. Nature 2008 Nov 13; 456(7219):250-4.

Mariappan I, Maddileti S, Savy S, Tiwari S, Gaddipati S, Fatima A, Sangwan VS, Balasubramanian D, Vemuganti GK. In vitro culture and expansion of human limbal epithelial cells. Nat Protoc. 2010 Aug;5(8):1470-9.

Maruyama K, Yamada J, Sano Y, Kinoshita S. Th2-biased immune system promotion of allogeneic corneal epithelial cell survival after orthotopic limbal transplantation. Invest Ophthalmol Vis Sci. 2003 Nov;44(11):4736-41.

Masaki Y, Hirasawa A, Okuyama S, Tsujimoto G, Iwaya M, Li XK, Yokoi Y, Nakamura S, Baba S, Miyamoto M, et al. Microchimerism and heart allograft acceptance. Transplant Proc. 1995 Feb;27(1):148-50.

Matic M, Petrov IN, Chen S, Wang C, Dimitrijevich SD, Wolosin JM. Stem cells of the corneal epithelium lack connexins and metabolite transfer capacity. Differentiation. 1997 May;61(4):251-60.

Meek KM, Dennis S, Khan S. Changes in the refractive index of the stroma and its extrafibrillar matrix when the cornea swells. Biophys J. 2003 Oct;85(4):2205-12.

Meller D, Pires RT, Mack RJ, Figueiredo F, Heiligenhaus A, Park WC, Prabhasawat P, John T, McLeod SD, Steuhl KP, Tseng SC. Amniotic membrane transplantation for acute chemical or thermal burns. Ophthalmology. 2000 May;107(5):980-9.

Meyer-Blazejewska EA, Call MK, Yamanaka O, Liu H, Schltzer-Schrehardt U, Kruse FE, Kao WW. From hair to cornea: toward the therapeutic use of hair follicle-derived stem cells in the treatment of limbal stem cell deficiency. Stem Cells. 2011 Jan;29(1):57-66.

Mills RA, Coster DJ, Williams KA. Effect of immunosuppression on outcome measures in a model of rat limbal transplantation. Invest Ophthalmol Vis Sci. 2002 Mar;43(3):647-55.

Miri A, Al-Deiri B, Dua HS. Long-term outcomes of autolimbal and allolimbal transplants. Ophthalmology. 2010 Jun;117(6):1207-13.

Miri A, Said DG, Dua HS. Donor site complications in autolimbal and living-related allolimbal transplantation. Ophthalmology. 2011 Jul;118(7):1265-71.

Miyazaki D, Inoue Y, Yao YF, Okada AA, Shimomura Y, Hayashi K, Tano Y, Ohashi Y. T-cell-mediated immune responses in alloepithelial rejection after murine keratoepithelioplasty. Invest Ophthalmol Vis Sci. 1999 Oct;40(11):2590-7.

Moore JE, McMullen CB, Mahon G, Adamis AP. The corneal epithelial stem cell. DNA Cell Biol. 2002 May-Jun;21(5-6):443-51.

Müller LJ, Pels E, Vrensen GF. The specific architecture of the anterior stroma accounts for maintenance of corneal curvature. Br J Ophthalmol. 2001 Apr;85(4):437-43.

Nagasaki T, Zhao J. Centripetal movement of corneal epithelial cells in the normal adult mouse. Invest Ophthalmol Vis Sci. 2003 Feb;44(2):558-66.

Nakamura T, Ang LP, Rigby H, Sekiyama E, Inatomi T, Sotozono C, Fullwood NJ, Kinoshita S. The use of autologous serum in the development of corneal and oral epithelial equivalents in patients with Stevens-Johnson syndrome. Invest Ophthalmol Vis Sci. 2006 Mar;47(3):909-16.

Nakamura T, Endo K, Cooper LJ, Fullwood NJ, Tanifuji N, Tsuzuki M, Koizumi N, Inatomi T, Sano Y, Kinoshita S. The successful culture and autologous transplantation of rabbit oral mucosal epithelial cells on amniotic membrane. Invest Ophthalmol Vis Sci. 2003 Jan;44(1):106-16.

Nakamura T, Kinoshita S. Ocular surface reconstruction using cultivated mucosal epithelial stem cells. Cornea. 2003 Oct;22(7 Suppl):S75-80.

Nakamura T, Takeda K, Inatomi T, Sotozono C, Kinoshita S. Long-term results of autologous cultivated oral mucosal epithelial transplantation in the scar phase of severe ocular surface disorders. Br J Ophthalmol. 2011 Jul;95(7):942-6.

Nauta AJ, Fibbe WE. Immunomodulatory properties of mesenchymal stromal cells. Blood 2007; 110: 3499-506.

Nelson J, Cameron J. The conjunctiva: anatomy and physiology. In: Krachmer JH, Manis MJ, Holland EJ (Eds). Cornea: fundamentals, diagnosis and management. 3rd ed. Philadelphia: Elsevier-Mosby; 2011. pp. 25-31. ISBN 9780323063876.

Neuss S, Stainforth R, Salber J, Schenck P, Bovi M, Knchel R, Perez-Bouza A. Long-term survival and bipotent terminal differentiation of human mesenchymal stem cells (hMSC) in combination with a commercially available three-dimensional collagen scaffold. Cell Transplant. 2008;17(8):977-86.

Niederkorn JY. Effect of cytokine-induced migration of Langerhans cells on corneal allograft survival. Eye (Lond). 1995;9 (Pt 2):215-8.

Nishida K, Kinoshita S, Ohashi Y, Kuwayama Y, Yamamoto S. Ocular surface abnormalities in aniridia. Am J Ophthalmol. 1995 Sep;120(3):368-75.

Nishida K, Yamato M, Hayashida Y, Watanabe K, Yamamoto K, Adachi E, Nagai S, Kikuchi A, Maeda N, Watanabe H, Okano T, Tano Y. Corneal reconstruction with tissue-engineered cell sheets composed of autologous oral mucosal epithelium. N Engl J Med. 2004 Sep 16;351(12):1187-96.

Nishida T. Cornea. In: Krachmer JH, Mannis MJ, Hollan EJ (Eds). Cornea. Fundamentals, diagnosis and management, 2nd ed. Philadelphia: Elsevier-Mosby, 2005. pp. 3-26. ISBN 0323032150.

Notara M, Bullett NA, Deshpande P, Haddow DB, MacNeil S, Daniels JT. Plasma polymer coated surfaces for serum-free culture of limbal epithelium for ocular surface disease. J Mater Sci Mater Med. 2007 Feb;18(2):329-38.

Nur-E-Kamal A, Ahmed I, Kamal J, Schindler M, Meiners S. Three-dimensional nanofibrillar surfaces promote self-renewal in mouse embryonic stem cells. Stem Cells. 2006 Feb;24(2):426-33.

O'Callaghan AR, Daniels JT. Concise review: limbal epithelial stem cell therapy: controversies and challenges. Stem Cells. 2011 Dec;29(12):1923-32.

O'Donnell C, Efron N. Corneal hydration control in contact lens wearers with diabetes mellitus. Optom Vis Sci. 2006 Jan;83(1):22-6.

Oh JY, Kim MK, Shin MS, Lee HJ, Ko JH, Wee WR, Lee JH. The anti-inflammatory and anti-angiogenic role of mesenchymal stem cells in corneal wound healing following chemical injury. Stem Cells. 2008 Apr;26(4):1047-55.

Ono K, Yokoo S, Mimura T, Usui T, Miyata K, Araie M, Yamagami S, Amano S. Autologous transplantation of conjunctival epithelial cells cultured on amniotic membrane in a rabbit model. Mol Vis. 2007 Jul 13;13:1138-43.

Ordonez P, Di Girolamo N. Limbal epithelial stem cells: role of the niche microenvironment. Stem Cells. 2012 Feb;30(2):100-7.

O'Sullivan F, Clynes M. Limbal stem cells, a review of their identification and culture for clinical use. Cytotechnology. 2007 Apr;53(1-3):101-6.

Pajoohesh-Ganji A, Pal-Ghosh S, Simmens SJ, Stepp MA. Integrins in slow-cycling corneal epithelial cells at the limbus in the mouse. Stem Cells. 2006 Apr;24(4):1075-86.

Park KS, Lim CH, Min BM, Lee JL, Chung HY, Joo CK, Park CW, Son Y. The side population cells in the rabbit limbus sensitively increased in response to the central cornea wounding. Invest Ophthalmol Vis Sci. 2006 Mar;47(3):892-900.

Pellegrini G, Dellambra E, Golisano O, Martinelli E, Fantozzi I, Bondanza S, Ponzin D, McKeon F, De Luca M. p63 identifies keratinocyte stem cells. Proc Natl Acad Sci U S A. 2001 Mar 13;98(6):3156-61.

Pellegrini G, Traverso CE, Franzi AT, Zingirian M, Cancedda R, De Luca M. Long-term restoration of damaged corneal surfaces with autologous cultivated corneal epithelium. Lancet. 1997 Apr 5;349(9057):990-3.

Pellegrini G., Golisano O., Paterna P., Lambiase A., Bonini S., Rama P., De Luca M. Location and clonal analysis of stem cells and their differentiated progeny in the human ocular surface. J Cell Biol. 1999 May 17;145(4):769-82.

Pels E, van der Gaag R: HLA-A,B,C, and HLA-DR antigens and dendritic cells in fresh and organ culture preserved corneas. Cornea. 1984-1985;3(4):231-9.

Phillips TJ, Gilchrest BA. Clinical applications of cultured epithelium. Epithelial Cell Biol. 1992 Jan;1(1):39-46.

Pindjáková J, Vítová A, Krulová M, Zajícová A, Filipec M, Holáň V. Corneal rat-to-mouse xenotransplantation and the effects of anti-CD4 or anti-CD8 treatment on cytokine and nitric oxide production. Transpl Int. 2005 Jul;18(7):854-62.

Pittenger MF, Mackay AM, Beck SC, Jaiswal RK, Douglas R, Mosca JD, Moorman MA, Simonetti DW, Craig S, Marshak DR. Multilineage potential of adult human mesenchymal stem cells. Science. 1999 Apr 2;284(5411):143-7.

Prabhasawat P, Ekpo P, Uiprasertkul M, Chotikavanich S, Tesavibul N. Efficacy of cultivated corneal epithelial stem cells for ocular surface reconstruction. Clin Ophthalmol. 2012;6:1483-92.

Prabhasawat P, Tesavibul N, Prakairungthong N, Booranapong W. Efficacy of amniotic membrane patching for acute chemical and thermal ocular burns. J Med Assoc Thai. 2007 Feb;90(2):319-26.

Priya CG, Arpitha P, Vaishali S, Prajna NV, Usha K, Sheetal K, Muthukkaruppan V. Adult human buccal epithelial stem cells: identification, ex-vivo expansion, and transplantation for corneal surface reconstruction. Eye (Lond). 2011 Dec;25(12):1641-9.

Puangsricharern V, Tseng SC. Cytologic evidence of corneal diseases with limbal stem cell deficiency. Ophthalmology. 1995 Oct;102(10):1476-85.

Qi X, Xie L, Cheng J, Zhai H, Zhou Q. Characteristics of immune rejection after allogeneic cultivated limbal epithelial transplantation. Ophthalmology. 2013 May;120(5):931-6.

Rama P, Bonini S, Lambiase A, Golisano O, Paterna P, De Luca M et al. Autologous fibrin-cultured limbal stem cells permanently restore the corneal surface of patients with total limbal stem deficiency. Transplantation 2001; 72:1478-85.

Rama P, Matuska S, Paganoni G, Spinelli A, De Luca M, Pellegrini G. Limbal stem-cell therapy and long-term corneal regeneration. N Engl J Med 2010; 363:147-55.

Ramirez-Miranda A, Nakatsu MN, Zarei-Ghanavati S, Nguyen CV, Deng SX. Keratin 13 is a more specific marker of conjunctival epithelium than keratin 19. Mol Vis. 2011;17:1652-61.

Rao SK, Rajagopal R, Sitalakshmi G, Padmanabhan P. Limbal autografting: comparison of results in the acute and chronic phases of ocular surface burns. Cornea 1999; 18:164-71.

Reinshagen H, Auw-Haedrich C, Sorg RV, Boehringer D, Eberwein P, Schwartzkopff J, Sundmacher R, Reinhard T. Corneal surface reconstruction using adult mesenchymal stem cells in experimental limbal stem cell deficiency in rabbits. Acta Ophthalmol. 2011 Dec;89(8):741-8.

Reinhard T, Spelsberg H, Henke L, Kontopoulos T, Enczmann J, Wernet P, Berschick P, Sundmacher R, Bhringer D. Long-term results of allogeneic penetrating limbo-keratoplasty in total limbal stem cell deficiency. Ophthalmology. 2004 Apr;111(4):775-82.

Rheinwald JG, Green H. Serial cultivation of strains of human epidermal keratinocytes: the formation of keratinizing colonies from single cells. Cell. 1975 Nov;6(3):331-43.

Ren H, Wilson G. Apoptosis in the corneal epithelium. Invest Ophthalmol Vis Sci. 1996 May;37(6):1017-25.

Resnikoff S, Pascolini D, Mariotti SP, Pokharel GP. Global magnitude of visual impairment caused by uncorrected refractive errors in 2004. Bull World Health Organ. 2008 Jan;86(1):63-70.

Reza HM, Ng BY, Gimeno FL, Phan TT, Ang LP. Umbilical cord lining stem cells as a novel and promising source for ocular surface regeneration. Stem Cell Rev. 2011 Nov;7(4):935-47.

Ricardo JR, Cristovam PC, Filho PA, Farias CC, de Araujo AL, Loureiro RR, Covre JL, de Barros JN, Barreiro TP, dos Santos MS, Gomes JA. Transplantation of conjunctival epithelial cells cultivated ex vivo in patients with total limbal stem cell deficiency. Cornea. 2013 Mar;32(3):221-8.

Rolando M, Zierhut M. The ocular surface and tear film and their dysfunction in dry eye disease. Surv Ophthalmol. 2001 Mar;45 Suppl 2:S203-10.

Romano AC, Espana EM, Yoo SH, Budak MT, Wolosin JM, Tseng SC. Different cell sizes in human limbal and central corneal basal epithelia measured by confocal microscopy and flow cytometry. Invest Ophthalmol Vis Sci. 2003 Dec;44(12):5125-9.

Sangwan VS, Basu S, Vemuganti GK, Sejpal K, Subramaniam SV, Bandyopadhyay S, Krishnaiah S, Gaddipati S, Tiwari S, Balasubramanian D. Clinical outcomes of xeno-free autologous cultivated limbal epithelial transplantation: a 10-year study. Br J Ophthalmol. 2011 Nov;95(11):1525-9.

Sangwan VS, Jain R, Basu S, Bagadi AB, Sureka S, Mariappan I, Macneil S. Transforming ocular surface stem cell research into successful clinical practice. Indian J Ophthalmol. 2014 Jan;62(1):29-40.

Sangwan VS, Vemuganti GK, Singh S, Balasubramanian D. Successful reconstruction of damaged ocular outer surface in humans using limbal and conjuctival stem cell culture methods. Biosci Rep. 2003 Aug;23(4):169-74.

Sato K, Ozaki K, Oh I, Meguro A, Hatanaka K, Nagai T, Muroi K, Ozawa K. 2007. Nitric oxide plays a critical role in suppression of T-cell proliferation by mesenchymal stem cells. Blood. 2007 Jan 1;109(1):228-34.

Shaharuddin B, Ahmad S, Ali S, Meeson A. Limbal side population cells: a future treatment for limbal stem cell deficiency. Regen Med. 2013 May;8(3):319-31.

Shanmuganathan VA, Foster T, Kulkarni BB, Hopkinson A, Gray T, Powe DG, Lowe J, Dua HS. Morphological characteristics of the limbal epithelial crypt. Br J Ophthalmol. 2007 Apr;91(4):514-9.

Sharma S, Mohanty S, Gupta D, Jassal M, Agrawal AK, Tandon R. Cellular response of limbal epithelial cells on electrospun poly--caprolactone nanofibrous scaffolds for ocular surface bioengineering: a preliminary in vitro study. Mol Vis. 2011;17:2898-910.

Shi W, Wang T, Zhang J, Zhao J, Xie L. Clinical features of immune rejection after corneoscleral transplantation. Am J Ophthalmol. 2008 Nov;146(5):707-13.

Shimano K, Satake M, Okaya A, Kitanaka J, Kitanaka N, Takemura M, Sakagami M, Terada N, Tsujimura T. Hepatic oval cells have the side population phenotype defined by expression of ATP-binding cassette transporter ABCG2/BCRP1. Am J Pathol. 2003 Jul;163(1):3-9.

Shimazaki J, Higa K, Morito F, Dogru M, Kawakita T, Satake Y, Shimmura S, Tsubota K. Factors influencing outcomes in cultivated limbal epithelial transplantation for chronic cicatricial ocular surface disorders. Am J Ophthalmol. 2007 Jun;143(6):945-53.

Schindler M, Ahmed I, Kamal J, Nur-E-Kamal A, Grafe TH, Young Chung H, Meiners S. A synthetic nanofibrillar matrix promotes in vivo-like organization and morphogenesis for cells in culture. Biomaterials. 2005 Oct;26(28):5624-31.

Schlötzer-Schrehardt U, Kruse FE. Identification and characterization of limbal stem cells. Exp Eye Res. 2005 Sep;81(3):247-64.

Schlötzer-Schrehardt U, Dietrich T, Saito K, Sorokin L, Sasaki T, Paulsson M, Kruse FE. Characterization of extracellular matrix components in the limbal epithelial stem cell compartment. Exp Eye Res. 2007 Dec;85(6):845-60.

Schwab IR. Cultured corneal epithelia for ocular surface disease. Trans Am Ophthalmol Soc. 1999;97:891-986.

Schwab IR, Isseroff RR. Bioengineered corneas–the promise and the challenge. N Engl J Med. 2000 Jul 13;343(2):136-8.

Schwab IR, Johnson NT, Harkin DG. Inherent risks associated with manufacture of bioengineered ocular surface tissue. Arch Ophthalmol. 2006 Dec;124(12):1734-40.

Schwab IR, Reyes M, Isseroff RR. Successful transplantation of bioengineered tissue replacements in patients with ocular surface disease. Cornea. 2000 Jul;19(4):421-6.

Shortt AJ, Secker GA, Notara MD, Limb GA, Khaw PT, Tuft SJ, Daniels JT. Transplantation of ex-vivo cultured limbal epithelial stem cells: a review of current techniques and clinical results. Surv Ophthalmol. 2007 Sep-Oct;52(5):483-502.

Shortt AJ, Tuft SJ, Daniels JT. Ex vivo cultured limbal epithelial transplantation. A clinical perspective. Ocul Surf. 2010 Apr;8(2):80-90.

Shortt AJ, Bunce C, Levis HJ, Blows P, Doré CJ, Vernon A, Secker GA, Tuft SJ, Daniels JT. Three-year outcomes of cultured limbal epithelial allografts in aniridia and Stevens-Johnson syndrome evaluated using the Clinical Outcome Assessment in Surgical Trials assessment tool. Stem Cells Transl Med. 2014 Feb;3(2):265-75.

Singh R, Joseph A, Umapathy T, Tint NL, Dua HS. Impression cytology of the ocular surface. Br J Ophthalmol. 2005 Dec;89(12):1655-9.

Skeens HM, Brooks BP, Holland EJ. Congenital aniridia variant: minimally abnormal irides with severe limbal stem cell deficiency. Ophthalmology. 2011 Jul;118(7):1260-4.

Slegers TP, Broersma L, van Rooijen N, Hooymans JM, van Rij G, van der Gaag R. Macrophages play a role in the early phase of corneal allograft rejection in rats. Transplantation. 2004 Jun 15;77(11):1641-6.

Sloper CM, Powell RJ, Dua HS. Tacrolimus (FK506) in the management of high-risk corneal and limbal grafts. Ophthalmology. 2001 Oct;108(10):1838-44.

Smith LA, Liu X, Hu J, Wang P, Ma PX. Enhancing osteogenic differentiation of mouse embryonic stem cells by nanofibers.Tissue Eng Part A. 2009 Jul;15(7):1855-64.

Smith RS, John SWM, Nishina PM, Sundberg JP. The anterior segment and ocular adnexae. In: Smith RS, editor. Systematic Evaluation of the Mouse Eye, Anatomy, Pathology, and Biomethods. CRC Press; Boca Raton, FL: 2002. pp. 3-24. ISBN 084930864X.

Strestíková P, Plsková J, Filipec M, Farghali H. FK 506 and aminoguanidine suppress iNOS induction in orthotopic corneal allografts and prolong graft survival in mice. Nitric Oxide. 2003 Sep;9(2):111-7.

Svobodova E, Krulova M, Zajicova A, Pokorna K, Prochazkova J, Trosan P, Holan V. The role of mouse mesenchymal stem cells in differentiation of naive T-cells into anti-inflammatory regulatory T-cell or proinflammatory helper T-cell 17 population. Stem Cells Dev. 2012 Apr 10;21(6):901-10.

Sugrue S, Zieske J. ZO1 in corneal epithelium: association to the zonula occludens and adherens junctions. Exp Eye Res. 1997 Jan;64(1):11-20.

Sun TT, Green H. Cultured epithelial cells of cornea, conjunctiva and skin: absence of marked intrinsic divergence of their differentiated states. Nature. 1977 Oct 6;269(5628):489-93.

Sun TT, Tseng SC, Lavker RM. Location of corneal epithelial stem cells. Nature 2010 Feb 25;463(7284):E10-11.

Talbot M, Carrier P, Giasson CJ, Deschambeault A, Gurin SL, Auger FA, Bazin R, Germain L. Autologous transplantation of rabbit limbal epithelia cultured on fibrin gels for ocular surface reconstruction. Mol Vis. 2006 Feb 1;12:65-75.

Tan DT, Ficker LA, Buckley RJ. Limbal transplantation. Ophthalmology. 1996 Jan;103(1):29-36.

Tan DT, Dart JK, Holland EJ, Kinoshita S. Corneal transplantation. Lancet. 2012 May 5;379(9827):1749-61.

Tanioka H, Kawasaki S, Yamasaki K, Ang LP, Koizumi N, Nakamura T, Yokoi N, Komuro A, Inatomi T, Kinoshita S. Establishment of a cultivated human conjunctival epithelium as an alternative tissue source

for autologous corneal epithelial transplantation. Invest Ophthalmol Vis Sci. 2006 Sep;47(9):3820-7.

Thoft RA, Friend J, Murphy HS. Ocular surface epithelium and corneal vascularization in rabbits. I. The role of wounding. Invest Ophthalmol Vis Sci. 1979 Jan;18(1):85-92.

Thoft RA, Friend J. The X, Y, Z hypothesis of corneal epithelial maintenance. Invest Ophthalmol Vis Sci 1983 Oct; 24(10):1442-3.

Thoft RA, Sugar J. Graft failure in keratoepithelioplasty. Cornea. 1993 Jul;12(4):362-5.

Thomas PB, Liu YH, Zhuang FF, Selvam S, Song SW, Smith RE, Trousdale MD, Yiu SC. Identification of Notch-1 expression in the limbal basal epithelium. Mol Vis. 2007 Mar 1;13:337-44.

Townsend WM. The limbal palisades of Vogt. Trans Am Ophthalmol Soc. 1991;89:721-56.

Treseler PA, Foulks GN, Sanfilippo F. Expression of ABO blood group, hematopoietic, and other cell-specific antigens by cells in the human cornea. Cornea. 1985-1986;4(3):157-68.

Tsai RJ, Li LM, Chen JK. Reconstruction of damaged corneas by transplantation of autologous limbal epithelial cells. N Engl J Med. 2000 Jul 13;343(2):86-93.

Tsai RJ, Sun TT, Tseng SC. Comparison of limbal and conjunctival autograft transplantation in corneal surface reconstruction in rabbits. Ophthalmology. 1990 Apr;97(4):446-55.

Tsai RJ, Tseng SC. Effect of stromal inflammation on the outcome of limbal transplantation for corneal surface reconstruction. Cornea. 1995 Sep;14(5):439-49.

Tseng SC. Concept and application of limbal stem cells. Eye (Lond). 1989;3 (Pt 2):141-57.

Tsubota K, Satake Y, Kaido M, Shinozaki N, Shimmura S, Bissen-Miyajima H, Shimazaki J. Treatment of severe ocular-surface disorders with corneal epithelial stem-cell transplantation. N Engl J Med. 1999 Jun 3;340(22):1697-703.

Tsubota K, Toda I, Saito H, Shinozaki N, Shimazaki J. Reconstruction of the corneal epithelium by limbal allograft transplantation for severe ocular surface disorders. Ophthalmology. 1995 Oct;102(10):1486-96.

Uccelli A, Moretta L, Pistoia V. Mesenchymal stem cells in health and disease. Nat Rev Immunol. 2008 Sep;8(9):726-36.

Umemoto T, Yamato M, Nishida K, Kohno C, Yang J, Tano Y, Okano T. Rat limbal epithelial side population cells exhibit a distinct expression of stem cell markers that are lacking in side population cells from the central cornea. FEBS Lett. 2005 Dec 5;579(29):6569-74.

Umemoto T, Yamato M, Nishida K, Yang J, Tano Y, Okano T. Limbal epithelial side-population cells have stem cell-like properties, including quiescent state. Stem Cells. 2006 Jan;24(1):86-94.

Van Buskirk EM. The anatomy of the limbus. Eye (Lond). 1989;3 (Pt 2):101-8.

Vemuganti GK, Kashyap S, Sangwan VS, Singh S. Ex-vivo potential of cadaveric and fresh limbal tissues to regenerate cultured epithelium. Indian J Ophthalmol. 2004 Jun;52(2):113-20.

Vemuganti GK, Sangwan VS. Interview: Affordability at the cutting edge: stem cell therapy for ocular surface reconstruction. Regen Med. 2010 May;5(3):337-40.

Vítová A, Filipec M, Zajícová A, Krulová M, Holáň V. Prevention of corneal allograft rejection in a mouse model of high risk recipients. Br J Ophthalmol. 2004 Oct;88(10):1338-42.

Wallgren AC, Karlsson-Parra A, Korsgren O. The main infiltrating cell in xenograft rejection is a $CD4^+$ macrophage and not a T lymphocyte. Transplantation. 1995 Sep 27;60(6):594-601.

Watanabe K, Nakagawa S, Nishida T. Stimulatory effects of fibronectin and EGF on migration of corneal epithelial cells. Invest Ophthalmol Vis Sci. 1987 Feb;28(2):205-11.

Watanabe K, Nishida K, Yamato M, Umemoto T, Sumide T, Yamamoto K, Maeda N, Watanabe H, Okano T, Tano Y. Human limbal epithelium contains side population cells expressing the ATP-binding cassette transporter ABCG2. FEBS Lett. 2004 May 7;565(1-3):6-10.

Watt FM, Hogan BL. Out of Eden: Stem cells and their niches. Science. 2000 Feb 25;287(5457):1427-30.

Watt FM. Epidermal stem cells as targets for gene transfer. Hum Gene Ther. 2000 Nov 1;11(16):2261-6.

Welge-Lüssen U, May CA, Neubauer AS, Priglinger S. Role of tissue growth factors in aqueous humor homeostasis. Curr Opin Ophthalmol. 2001 Apr;12(2):94-9.

West-Mays JA, Dwivedi DJ. The keratocyte: corneal stromal cell with variable repair phenotypes. Int J Biochem Cell Biol. 2006;38(10):1625-31.

Williams KA, Brereton HM, Aggarwal R, Sykes PJ, Turner DR, Russ GR, Coster DJ. Use of DNA polymorphisms and the polymerase chain reaction to examine the survival of a human limbal stem cell allograft. Am J Ophthalmol. 1995 Sep;120(3):342-50.

Williams KA, Coster DJ. The immunobiology of corneal transplantation. Transplantation. 2007 Oct 15;84(7):806-13.

Williams KA, Coster DJ. The role of the limbus in corneal allograft rejection. Eye (Lond). 1989;3 (Pt 2):158-66.

Wolosin JM, Xiong X, Schtte M, Stegman Z, Tieng A. Stem cells and differentiation stages in the limbo-corneal epithelium. Prog Retin Eye Res. 2000 Mar;19(2):223-55.

Xu KP, Wu Y, Zhou J, Zhang X. Survival of rabbit limbal stem cell allografts after administration of cyclosporin A. Cornea. 1999 Jul;18(4):459-65.

Yang X, Moldovan NI, Zhao Q, Mi S, Zhou Z, Chen D, Gao Z, Tong D, Dou Z. Reconstruction of damaged cornea by autologous transplantation of epidermal adult stem cells. Mol Vis. 2008 Jun 5;14:1064-70.

Yao L, Li ZR, Su WR, Li YP, Lin ML, Zhang WX, Liu Y, Wan Q, Liang D. Role of mesenchymal stem cells on cornea wound healing induced by acute alkali burn. PLoS One. 2012;7(2):e30842.

Yao YF, Inoue Y, Miyazaki D, Shimomura Y, Ohashi Y, Tano Y. Ocular resurfacing and alloepithelial rejection in a murine keratoepithelioplasty model. Invest Ophthalmol Vis Sci. 1995 Dec;36(13):2623-33.

Ye J, Yao K, Kim JC. Mesenchymal stem cell transplantation in a rabbit corneal alkali burn model: engraftment and involvement in wound healing. Eye (Lond). 2006 Apr;20(4):482-90.

Yeung AM, Schlötzer-Schrehardt U, Kulkarni B, Tint NL, Hopkinson A, Dua HS. Limbal epithelial crypt: a model for corneal epithelial maintenance and novel limbal regional variations. Arch Ophthalmol. 2008 May;126(5):665-9.

Yeung AM, Tint NL, Kulkarni BB, Mohammed I, Suleman H, Hopkinson A, Dua HS. Infant limbus: an immunohistological study. Exp Eye Res. 2009 Jun;88(6):1161-4.

Yi X, Wang Y, Yu FS. Corneal epithelial tight junctions and their response to lipopolysaccharide challenge. Invest Ophthalmol Vis Sci 2000. 41(13): 4093-100.

Yin JQ, Liu WQ, Liu C, Zhang YH, Hua JL, Liu WS, Dou ZY, Lei AM. Reconstruction of damaged corneal epithelium using Venus-labeled limbal epithelial stem cells and tracking of surviving donor cells. Exp Eye Res. 2013 Oct;115:246-54.

Zannettino AC, Paton S, Arthur A, Khor F, Itescu S, Gimble JM, Gronthos S. Multipotential human adipose-derived stromal stem cells exhibit a perivascular phenotype in vitro and in vivo. J Cell Physiol. 2008 Feb;214(2):413-21.

Zhang Q, Shi S, Liu Y, Uyanne J, Shi Y, Shi S, Le AD. Mesenchymal stem cells derived from human gingiva are capable of immunomodulatory functions and ameliorate inflammation-related tissue destruction in experimental colitis. J Immunol. 2009 Dec 15;183(12):7787-98.

Zhao S, Wehner R, Bornhauser M, Wassmuth R, Bachmann M, et al. Immunomodulatory properties of mesenchymal stromal cells and their therapeutic consequences for immune-mediated disorders. Stem Cells Dev 2010; 19: 607-14.

Zhou S, Schuetz JD, Bunting KD, Colapietro AM, Sampath J, Morris JJ, Lagutina I, Grosveld GC, Osawa M, Nakauchi H, Sorrentino BP. The ABC transporter Bcrp1/ABCG2 is expressed in a wide variety of stem cells and is a molecular determinant of the side-population phenotype. Nat Med. 2001 Sep;7(9):1028-34.

8 APPENDICES

Full text publications representing the forming thesis

8.1 Publication 1

Graft survival and cytokine production profile after limbal transplantation in the experimental mouse model.

Lenčová A, Pokorná K, Zajícová A, Krulová M, Filipec M, Holáň V.

Transpl Immunol. 2011 Apr 15;24(3):189-94. (IF 1.912)

Transplant Immunology 24 (2011) 189–194

Contents lists available at ScienceDirect

Transplant Immunology

journal homepage: www.elsevier.com/locate/trim

Graft survival and cytokine production profile after limbal transplantation in the experimental mouse model

Anna Lenčová [a,b], Kateřina Pokorná [a,c], Alena Zajícová [a], Magdaléna Krulová [a,c], Martin Filipec [b], Vladimír Holáň [a,c,*]

[a] Institute of Molecular Genetics, Academy of Sciences, Videnska 1083, 142 20 Prague, Czech Republic
[b] European Eye Clinic Lexum, U Spolecenske zahrady 3, 140 00 Prague, Czech Republic
[c] Faculty of Natural Sciences, Charles University, Vinicna 7, 128 44 Prague, Czech Republic

ARTICLE INFO

Article history:
Received 6 September 2010
Received in revised form 18 November 2010
Accepted 23 November 2010

Keywords:
Limbal transplantation
Graft survival
Cytokine response
Anti-CD4 treatment

ABSTRACT

Limbal transplantation or limbal stem cell (LSC) transfer represents the only way to treat severe ocular surface damage or LSC deficiency. However, limbal allografts are promptly rejected in spite of extensive immunosuppressive therapy. To characterize immune response after limbal transplantation, we established an experimental model of limbal transplantation in the mouse. Syngeneic, allogeneic and xenogeneic (rat) limbal grafts were grafted orthotopically in BALB/c mice and graft survival was evaluated. The presence of graft donor cells and the expression of IL-2, IL-4, IL-10, IFN-γ and inducible nitric oxide synthase (iNOS) mRNA in the grafts were detected by real-time PCR. While syngeneic grafts survived permanently, allografts were rejected in 9.0 ± 1.8 days and xenografts in 6.5 ± 1.1 days. The manifestation of clinical symptoms of rejection correlated with the disappearance of donor cells in the graft and in the recipient cornea. Intragraft expression of iNOS mRNA and distinct expression patterns of Th1 (IL-2, IFN-γ) and Th2 (IL-4, IL-10) cytokines were detected during rejection of limbal allografts and xenografts. The limbal graft rejection was prevented with anti-CD4, but not anti-CD8 monoclonal antibody therapy. The results indicate that limbal grafts do not enjoy immune privilege of the eye and are promptly rejected by Th1 (allografts) or by a combined Th1 and Th2 (xenografts) type of immune response involving $CD4^+$ cells and iNOS expression. Targeting this pathway may be an effective way to prevent and treat limbal graft rejection.

1. Introduction

The studies in experimental models and clinical observations in patients have shown that a wounded or otherwise damaged corneal surface is healed by cells which originate from limbal stem cells (LSC) located in the basal layer of the limbus [1,2]. If the source of LSC is destroyed, either due to an inherited disease or as a result of ocular surface damage, corneal surface does not heal properly and the cornea is overgrown by cells originating from the conjunctiva. This process leads to corneal neovascularization, chronic inflammation and persistent epithelial defects. The impairment of corneal transparency may result in a loss of vision [3]. Although recent studies on the mouse [4] and human [5,6] indicate that the corneal epithelium possesses some degree of self-renewing capacity, the only way to treat LSC deficiency remains to be limbal transplantation or LSC transfer [7,8]. Indeed, the beneficial effects of limbal transplantation have been shown in several clinical studies [9,10].

However, success of limbal allotransplantation is very low due to a strong immune reaction against the graft donor antigens. The severe allograft rejection occurs despite the potent and extensive immunosuppressive therapy [11–14]. Therefore research and development of novel therapies to prevent and treat limbal allograft rejection is mandatory. So far, there is a limited number of experimental studies that address this issue. Mills et al. [15] introduced a method to orthotopically transplant segments of the limbus. This model was used to study effects of immunosuppressive therapy in rats [15] and on modulation the delayed-type hypersensitivity (DTH) reaction after limbal transplantation in mice [16]. These studies in inbred strains of rodents, as well as the older work performed in outbred rabbit models [17], demonstrated a donor antigen specific immune response that promptly rejects limbal allografts, and that is difficult to suppress rejection reaction by traditional immunosuppressive regiments.

Cellular and molecular mechanisms of limbal allograft rejection have to be recognized in order to develop a successful strategy to manage immune reaction in limbal transplant patients. We have used our previous experience with corneal allo- and xenotransplantation in mice [18–20] to develop and characterize a murine model of orthotopic limbal transplantation. For the first time we also demonstrate a detailed chronology of the fate of limbal xenografts.

* Corresponding author. Institute of Molecular Genetics, Academy of Science of the Czech Republic, Videnska 1083, 142 20 Prague 4, Czech Republic. Tel.: +420 241063226; fax: +420 224310955.
E-mail address: holan@img.cas.cz (V. Holáň).

0966-3274/$ – see front matter © 2010 Elsevier B.V. All rights reserved.
doi:10.1016/j.trim.2010.11.005

We found that rejection of limbal allografts and xenografts is accompanied by different intragraft cytokine responses and by a significant expression of the gene for the inducible nitric oxide synthase (iNOS). Since our previous studies on corneal [20] and skin [21] transplantation have shown the important role of $CD4^+$ cells and macrophages expressing iNOS in graft rejection, we targeted $CD4^+$ cells for immunosuppressive therapy also after limbal transplantation. The results have suggested that anti-CD4 treatment could be an effective way to suppress rejection reaction after limbal transplantation.

2. Materials and methods

2.1. Animals

Mice of both sexes of the inbred strains BALB/c and C57BL/6 (B6) at the age of 7–10 weeks and rats of the inbred strain Lewis at the age of 7–8 weeks were used for the experiments. The mice were from the breeding unit of the Institute of Molecular Genetics, Prague; rats were purchased from the Institute of Physiology, Academy of Sciences, Prague. All experiments were approved by the local Animal Ethics Committee (according to Tenets of the Declaration Helsinki).

2.2. Technique of limbal transplantation

The mice were anesthetized before the operation by intramuscular injection with a mixture of xylasine (Rometar, Spofa, Prague, Czech Republic) and ketamine (Calypsol, Gedeon Richter Ltd., Budapest, Hungary). The surgery method was a slight modification of the transplantation method described by Maruyama et al. [16]. In brief, donor limbal lenticule was circularly cut out from conjunctiva without scleral tissue and around the cornea and was embedded into balanced salt solution. The rest of the corneal endothelium on the back side was removed to eliminate a possible rest of corneal tissue in limbal graft. The width of the limbal graft was approximately 1.0 mm. The corneal epithelium of the recipient ocular surface was debrided by sharp needle (G23) and the limbus was cut out with Vannas scissors (Duckworth and Kent, Baldock, England). The donor limbal graft was placed orthotopically and was secured with 5 interrupted sutures with 11.0 Ethilon (Ethicon, Johnson and Johnson, Livingston, UK). The ophthalmic ointment compound containing bacitracin and neomycin (Ophthalmo-Framykoin, Zentiva, Prague, Czech Republic) was applied on the ocular surface and the eyelids were closed for 72 h by tarsoraphy using 7.0 Resolon suture (Resorba, Nuernberg, Germany). Mice with complications such as cataracts, hemorrhage etc. were excluded from the experiments. Only the right eye was operated on.

In all experiments BALB/c mice were used as the recipients and BALB/c mice (syngeneic grafts), B6 mice (allografts) or Lewis rat (xenografts) as the graft donors. To detect survival of allogeneic cells, limbal grafts from B6 male mice were grafted into BALB/c female recipients and the presence of cells expressing Sry (male-specific) antigen was detected by real-time PCR.

2.3. Clinical evaluation of graft survival

Postoperatively (from day 3, when the tarsoraphy was removed) the ocular surface was observed daily using the operating microscope. The reepithelization of cornea was followed by fluorescein staining. The cornea was scored for opacity and neovascularization, and limbal graft was evaluated for edema. A scoring scale ranging from 0 to 4 for corneal opacity was used to evaluate the rejection [16]. The corneal opacity was graded: 0) clear cornea, 1) lenticular or regional corneal epithelial edema, opacity with clearly visible iris vessels, 2) diffuse epithelial edema, opacity or both, obscuring iris vessels, 3) diffuse epithelial edema, opacity or both, iris vessels not visible and 4) anterior chamber not visible due to epithelial edema, corneal opacity, or both. If the opacity score reached value 2 or more, the graft was considered as rejected. The following scoring system was used to evaluate limbal edema: 0) no edema, 1) focal slight limbal edema, 2) diffuse mild limbal edema, 3) moderate diffuse limbal edema, 4) severe diffuse limbal edema. The corneal neovascularization was graded as follows: 0) no vessels 1) incipient vessels reaching only the periphery of the cornea, 2) one-quarter of the cornea vascularized, 3) half of the cornea vascularized and 4) the entire cornea vascularized.

2.4. RNA isolation and reverse transcription

Total RNA was extracted from the samples of limbal grafts using TRI Reagent (Molecular Research Center, Cincinnati, OH) according to the manufacturer's instructions. The grafts were cut out by Vannas scissors, embedded in TRI Reagent and homogenized. Two μg of total RNA was treated using deoxyribonuclease I (Sigma, St. Louis, MO) and used for subsequent reverse transcription. The first-strand cDNA was synthesized using random hexamers (Promega, Madison, WI) in a total reaction volume of 25 μl using M-MLV Reverse Transcriptase (Promega).

2.5. DNA isolation

Male B6 cells were detected according to the presence of the Sry gene [22] by analyzing DNA from limbal grafts of male origin. Genomic DNA was extracted from B6 male limbal grafts in BALB/c female recipients using NucleoSpin Tissue XS extraction kit (Macherey-Nagel, Dueren, Germany) according to the manufacturer's instructions.

2.6. Quantitative real-time polymerase chain reaction

Quantitative real-time RT-PCR was performed on the iCycler (BioRad, Hercules, CA) and the data were analyzed on the iCycler Detection system (Version 3.1). The specificity of the amplified products was checked by the melting analyses. iQ SYBR Green Supermix (BioRad) was used for all experiments. Experiments were conducted in triplicates and the relative quantification model was applied to calculate expression of target gene in comparison to GADPH used as the housekeeping gene. The list of primers is described in Table 1. The PCR parameters for 25 μl reactions included denaturation at 95 °C for 3 min, then 40 cycles at 95 °C for 10 s, annealing at 60 °C for 20 s and elongation at 72 °C for 20 s. Fluorescence data were collected at each cycle after elongation step at 80 °C for 5 s.

2.7. Antibody treatment

Monoclonal antibodies (mAb) anti-CD4 (clone GK1.5) [23] and anti-CD8 (clone TIB 150) [24] were prepared in the form of ascites in nu/nu mice and were injected intraperitoneally at a dose of 200 μg/mouse/day. The treatment started on the day of grafting and continued every other day until the rejection. FACS analysis performed 1 week after the beginning of the treatment revealed

Table 1
Primer sequences used for real-time PCR.

Gene	Sense primer	Antisense primer
GAPDH	AGA ACA TCA TCC CTG CAT CC	ACA TTG GGG GTA GGA ACA C
RT1-M3	TCT TGG GTG AAG GGT CAC A	TCC TGC AGA ATG GAA AAG AGA
SRY	AGC CTC ATC GGA GGG CTA	AGG CAA CTG CAG GCT GTA AA
IL-2	GCT GTT GAT GGA CCT ACA GGA	TTC AAT TCT GTG GCC TGC TT
IL-4	GAG AGA TCA TCG GCA TTT TGA	TCT GTG GTG TTC TTC GTT GC
IL-10	CAG AGC CAC ATG CTC CTA GA	TGT CCA GCT GGT CCT TTG TT
IFN-γ	ATC TGG AGG AAC TGG CAA AA	TTC AAG ACT TCA AAG AGT CTG AGG
iNOS	CTT TGC CAC GGA CGA GAC	TCA TTG TAC TCT GAG GGC TGA C

that the numbers of cells of targeted cell population was reduced in both spleen and lymph nodes to less than 1.5% of value in control untreated animals and this selective lymphopenia was sustained for the duration of the treatment (data not shown). Control group was treated with physiological solution.

2.8. Statistical analysis

The statistical significance of differences in graft survival between experimental and control groups was calculated using the Mann–Whitney *U* test; differences in gene expression were calculated using the Student's *t* test. A *p* value less than 0.05 was considered statistically significant.

3. Results

3.1. Clinical evaluation of limbal grafts and recipient cornea

To monitor kinetic of rejection reaction after limbal transplantation, we evaluated the appearance and clinical characteristics (edema, neovascularization and opacity) of the grafted limbal tissue. In addition, we also scored and evaluated clinical characteristics of the recipient's cornea, because the corneal transparency and appearance of the corneal surface depend on the presence of the functional limbus and reflect limbal rejection [16].

When the limbal grafts were evaluated clinically and scored, the most remarkable differences were observed in xenografts which developed edema more strongly than allografts or syngeneic grafts (Fig. 1). The edema in allografts and syngeneic grafts developed only slightly and disappeared within 2 weeks (Fig. 2A). The neovascularization and opacity of the limbal graft were most apparent in xenografts, less in allografts and only slightly and temporary in syngeneic grafts (Fig. 1).

The corneal neovascularization significantly developed after limbal transplantation in allogeneic and xenogeneic models, but remained minimal after transplantation of syngeneic limbal grafts (Fig. 2B). In addition, corneal opacity clearly developed after limbal allo- and xenotransplantation, but only slightly and temporally after syngeneic transplantation. On the basis of preliminary experiments, the opacity score 2 or more was considered as limbal graft rejection. As demonstrated in Fig. 2C, all corneas in recipients of limbal allografts reached score 2 or more between days 7 and 12 after transplantation (the average 9.0 ± 1.8 days, $n = 14$). Opacity score 2 or more in corneal xenografts was reached in 5 to 8 days (the average 6.5 ± 1.1 days, $n = 10$) after grafting.

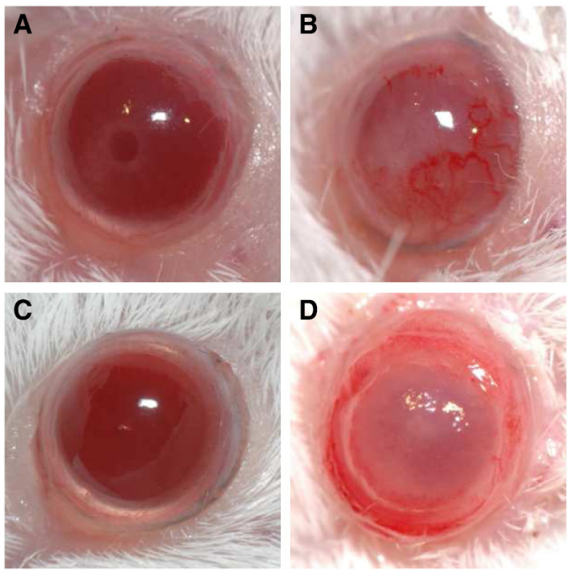

Fig. 1. The appearance of limbal grafts and recipient cornea. (A) Syngeneic graft on day 14 after grafting, (B) allograft on day 9 and (D) xenograft on day 5 after transplantation. While syngeneic grafts are clear with a minimum of neovascularization in the limbal region, apparent corneal opacity and corneal and limbal neovascularization can be seen in allograft and xenograft. These signs of rejection are absent in surviving limbal allografts on day 17 in the recipients treated with mAb anti-CD4 (C).

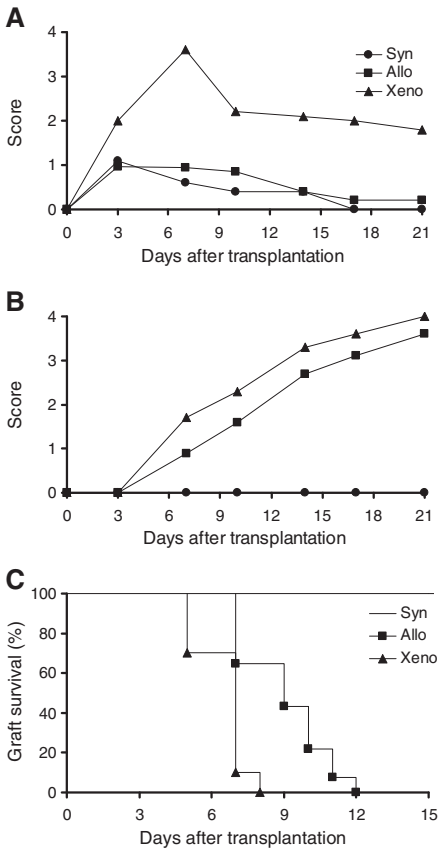

Fig. 2. The kinetic of development of limbal edema, corneal neovascularization and corneal opacity after limbal transplantation in the mouse. Limbal grafts from BALB/c mice (Syn), B6 mice (Allo) or Lewis rats (Xeno) were transplanted in BALB/c recipients and limbal edema (A), corneal neovascularization (B) or corneal opacity (C) were evaluated. When the opacity reached score 2 or more, the graft was considered as rejected. Each point represents the average score from 12 to 14 mice per group.

The opacity in the cornea of recipients of syngeneic limbal grafts did not reach score 2 in any case ($n = 10$).

3.2. Survival of donor cells in the limbal graft and in recipient cornea

Using PCR we were able to detect allogeneic and xenogeneic donor cells in the limbal graft and in the recipient cornea until the day of graft rejection as evaluated by clinical criteria. Allogeneic cells were detected till day 14 after limbal transplantation; xenogeneic cells were present in the graft on day 8, but not on day 12 after grafting (Fig. 3). Similar kinetic of donor cells was seen in the recipient cornea (Fig. 3). When syngeneic grafts from male donors were grafted into female recipients, the male cells were still detected in the graft on day 28 after grafting (data not shown). It shows survival of grafted limbal cells and suggests that the male-specific antigen does not induce rejection of limbal graft in BALB/c mice. The mean survival time of male allografts in female recipients was the same like that of the allografts the same gender (data not shown).

3.3. Intragraft cytokine response

Limbal allografts and xenografts were removed at the day of graft rejection (or syngeneic grafts on days 8–12 after grafting) and the expression of genes for IL-2, IL-4, IL-10, IFN-γ and iNOS was detected by real-time PCR. As demonstrated in Fig. 4, a significant expression of genes for Th1 cytokines IL-2 and IFN-γ was found in allografts, but the expression of genes for Th2 cytokines IL-4 and IL-10 did not exceed the levels in syngeneic grafts. Rejection of limbal xenografts was accompanied by the high expression of genes for both Th1 (IL-2 and IFN-γ) and Th2 (IL-4, IL-10) cytokines. The gene for iNOS was significantly expressed in both allografts and xenografts (Fig. 4).

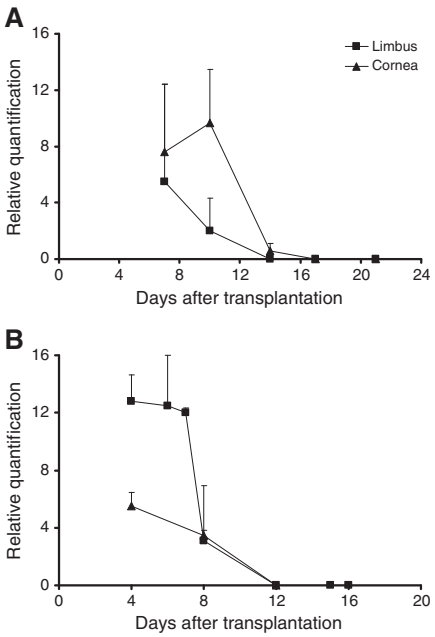

Fig. 3. Detection of the graft donor cells in the limbal graft and recipient cornea. Limbal tissue from male B6 donors (A) or Lewis rat (B) donors was grafted in BALB/c female recipients. The grafted tissue (and the recipient's cornea) were removed at indicated time after transplantation and subjected to real-time PCR analysis to detect DNA for the male-specific antigen Sry in allogeneic model (A) or mRNA for the rat MHC class I (RT1) molecule in xenogeneic model (B). Each point represents the mean ± SD from 2 to 3 determinations.

3.4. Effects of anti-CD4 and anti-CD8 treatment on survival of limbal allografts and xenografts

The BALB/c recipients of B6 limbal allografts and Lewis limbal xenografts were either saline-treated or treated with mAb anti-CD4 or anti-CD8. The opacity of the recipient's cornea was scored and evaluated. As demonstrated in Fig. 5A, all limbal allografts in saline-treated recipients or recipients treated with mAb anti-CD8 were rejected within 13 days after grafting. The average graft survival time in saline-treated recipients was 9.5 ± 1.2 days (n = 6) and in recipients treated with mAb anti-CD8 10.9 ± 1.2 days (n = 8). Treatment of limbal allograft recipients with mAb anti-CD4 postponed the appearance of signs of rejection (corneal opacity) and resulted in a significant ($P<0.001$, Mann–Whitney *U* test) prolongation of graft survival (the average 22.8 ± 4.2 days, n = 8). Limbal xenografts in saline-treated and anti-CD8 treated recipients were rejected within 7 days after grafting (the average times 6.0 ± 0.8 and 6.3 ± 0.2 days, respectively, n = 6 for each group). Treatment of xenograft recipients with mAb anti-CD4 significantly ($P<0.01$) prolonged graft survival (the average 9.5 ± 1.8 days, n = 6), but all xenografts were rejected within 12 days after transplantation (Fig. 5B).

4. Discussion

Transplantation of limbal tissue or LSC is the only way to treat LSC deficiency and thus improve or restore the vision in patients with severe limbal damages. Beneficial effects of limbal transplantation in patients with LSC deficiency have been reported [9,11–14], but the major problem of limbal allotransplantation is a high risk of immune rejection and a necessity of systemic immunosuppression [10,14]. By contrast corneal allografts often survive with only topical preventive immunosuppressive treatment. This stark contrast between incidence of rejection in corneal and limbal allografts may be, in part, due to a stronger vascular supply, and a higher density of antigen-presenting cells, such as Langerhans' cells, in the limbal region [25].

Experimental limbal transplantation in animal models confirmed high incidence of rapid rejection similar to that observed in patients [15,16]. Allogeneic cells of donor origin were not detectable in the recipient after 2 weeks after transplantation indicating a potent and rapid immune rejection [15]. To address this issue we have established and characterized a novel murine model of limbal allo-

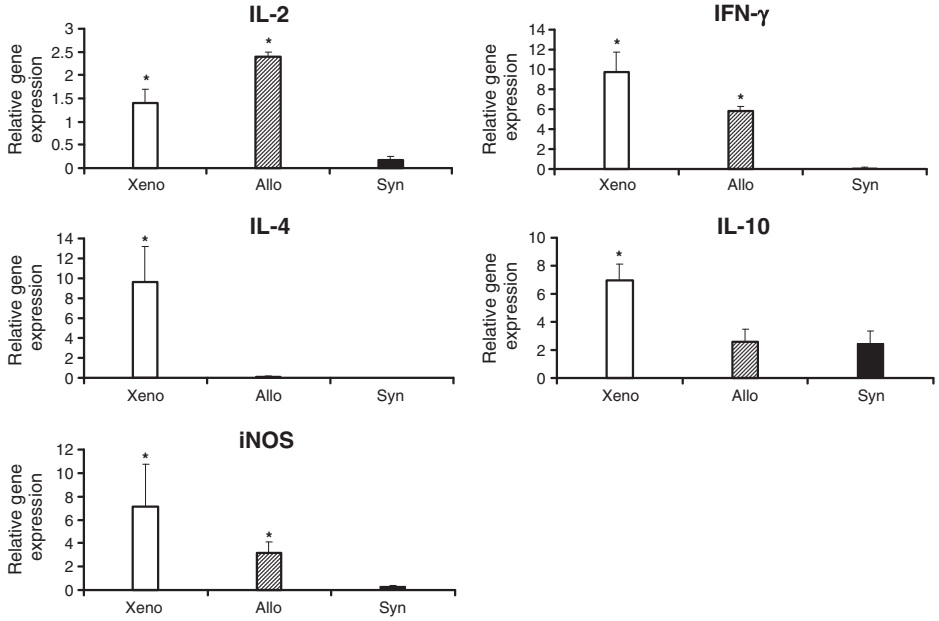

Fig. 4. Expression of genes for IL-2, IFN-γ, IL-4, IL-10 and iNOS in syngeneic limbal grafts (Syn), limbal allografts (Allo) and xenografts (Xeno). Syngeneic grafts were harvested on days 8–12 after grafting, allografts and xenografts at the time of the graft rejection (allografts on days 9–11 and xenografts on days 6–8 after transplantation). Expression of particular gene was normalized to GAPDH. Each bar represents the mean value ± SD from 2 to 3 determinations. Values with asterisk are significantly ($p<0.05$) different from syngeneic control.

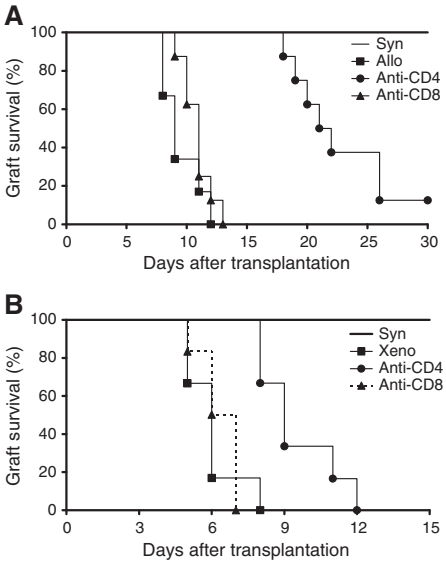

Fig. 5. Effects of anti-CD4 and anti-CD8 treatment on limbal allograft and xenograft survival. BALB/c recipients of B6 limbal allografts (A) or limbal xenograft (B) were treated from the day of transplantation every other day with saline, mAb anti-CD4 or mAb anti-CD8. Survival of limbal grafts was scored and evaluated according to the corneal opacity. Each group of animals contained 6–8 mice. Treatment with mAb anti-CD4 induced statistically significant prolongation of both limbal allograft ($P<0.001$) or limbal xenograft ($P<0.01$) survival.

and xenotransplantation, and conducted series of studies to elucidate immunological mechanisms responsible for the low survival rates of limbal transplants. We have observed that rejection of limbal allografts is characterized by neovascularization in the graft and in the recipient cornea, and by a significant corneal opacity. Detection of corneal opacity coincided with the complete disappearance of allogeneic donor cells from both the limbus and corneal epithelium at 7–12 days after transplantation. To test a possibility that the limbal graft failure is due to a technical issue, male limbal cells were transplanted into female recipients. No clinical signs of rejetion of H-Y incompatible limbal grafts were observed and donor male cells were detected in BALB/c female recipients as long as 4 weeks after the surgery. Therefore, this weak incompatibility in the male-specific antigen does not induce limbal graft rejection. Similarly, H-Y incompatible corneal grafts were not rejected in BALB/c mice [26] and H-Y incompatible skin grafts are not rejected in BALB/c female recipients (our unpublished observations). In contrast, limbal grafts incompatible in another relatively weak antigen, enhanced green fluorescent protein, were rejected by the rat recipients [27]. These differences may reflect interspeciese differences or suggest that BALB/c female mice are non responder to the male-specific antigen. Detection of donor male cells in the female recipients as long as 4 weeks after the surgery indicates that the prompt rejection of allogeneic limbal cells is not due to the surgical failure. Transplantation of limbal xenograft (from the rat to the mouse) evoked the strongest rejection reaction characterized by graft neovascularization, opacity and edema and by neovascularization and opacity in the recipient's cornea. All limbal xenografts were rejected within 8 days after transplantation and no xenogeneic cells were detected by the real-time PCR beyond this period. These data suggest that limbal allografts and xenografts are promptly rejected and do not enjoy immune privilege of the anterior part of the eye.

Rejection of limbal allografts was associated with a strong Th1 cytokine response characterized by the expression of genes for IL-2 and IFN-γ in the rejected grafts. Expression of the gene for IL-4 was not detected in rejected limbal allografts and also expression of the gene for IL-10, another Th2 cytokine, did not exceed the baseline levels in syngeneic limbal grafts. On the contrary, a strong expression of genes for Th2 cytokines IL-4 and IL-10, in addition to Th1 cytokines, was detected in rejected limbal xenografts. This pattern of cytokine expression during limbal graft rejection resembles cytokine profiles after corneal allo- and xenotransplantation, but the role of the Th2 cytokines in the rejection of xenografts is unclear [20]. Macrophages and their product nitric oxide (NO) have been shown to play a more important role in graft rejection. Mills et al. [15] observed a significant infiltration of limbal allografts in rats by macrophages and we found a strong expression of the gene for iNOS in both rejected limbal allografts and xenografts. It has been already shown in various allo- and xenotransplantation models, including corneal transplantation, that the inhibition of iNOS activity may prolong graft survival [21,28]. The production of NO by graft infiltrating macrophages depends on the availability of IFN-γ which was also detected during rejection of both limbal allo- and xenografts and is key factor in DTH reaction. This suggests that strategies directed to inhibit IFN-γ (Th1 response), NO production and the DTH reaction should be beneficial in promotion of limbal graft survival. Indeed, Maruyama et al. [16] have shown that the Th2-biased immune system and the suppression of the DTH reaction may support the survival of limbal allografts in the mouse. We showed here that targeting of $CD4^+$ cells results in a suppression of the rejection reaction and in a significant prolongation of limbal allograft and xenograft survival. The effect of anti-CD4 therapy may be due to elimination of $CD4^+$ T cells which mediate the DTH reaction and are the important source of IFN-γ for iNOS expression [21]. In addition, anti-CD4 antibody can inactivate $CD4^+$ macrophages which play a role in both afferent phase of transplantation reaction as antigen-presenting cells and in the effector phase as cytotoxic macrophages [27–29]. It has been shown that a subpopulation of macrophages expresses CD4 molecules, and these $CD4^+$ macrophages have been shown to be involved in graft rejection [30]. Nevertheless, anti-CD4 monotherapy did not ensure a permanent limbal allograft survival. The rejections observed in the anti-CD4 treated recipients may be due to the activity of other $CD4^+$ cell-independent mechanisms (such as $CD8^+$ cell-activated macrophages, cytotoxic T cells, etc.). The results also showed that anti-CD8 treatment was not effective in the prevention of limbal allograft rejection, similarly as in the case of corneal transplantation [19,31].

For the first time our study demonstrates intragraft cytokine response in orthotopic limbal allo- and xenograft recipients and indicates the key role of Th1 response and $CD4^+$ cells in the limbal graft rejection. Therefore, the strategies targeting $CD4^+$ cells as the main mediators of Th1 response and activators of macrophages for NO production were suggested to prevent limbal graft rejection. This suggestion was confirmed by the effectiveness of anti-CD4 treatment in suppression of graft rejection in allogeneic limbal transplantation in the mouse model.

Acknowledgements

This work was supported in part by grant KAN200520804 from the Grant Agency of the Academy of Sciences, projects 1M0506, MSM0021620806 and MSM0021620858 from the Ministry of Education of the Czech Republic, grant 310/08/H077 from the Grant Agency of the Czech Republic and project AVOZ50520514 from the Academy of Sciences of the Czech Republic. The authors thank Mr. Ivan Kolín for the help with photo documentation.

References

[1] Tseng SC. Regulation and clinical implications of corneal epithelial stem cells. Mol Biol Rep 1996;23:47–58.
[2] Daniels JT, Dart JK, Tuft SJ, Khaw PT. Corneal stem cells in review. Wound Repair Regen 2001;9:483–94.

[3] Huang AJ, Tseng SC. Corneal epithelial wound healing in the absence of limbal epithelium. Investig Ophthalmol Vis Sci 1991;32:96–105.
[4] Majo F, Rochat A, Nicolas M, Jaoude GA, Barrandon Y. Oligopotent stem cells are distributed throughout the mammalian ocular surface. Nature 2008;456:250–4.
[5] Chang C-Y, Green CR, McGhee CNJ, Sherwin T. Acute wound healing in the human central corneal epithelium appears to be independent of limbal stem cell influence. Investig Ophthalmol Vis Sci 2008;49:5279–86.
[6] Dua HS, Miri A, Alomar T, Yeung AM, Said DG. The role of limbal stem cells in corneal epithelial maintenance: testing the dogma. Ophthalmology 2009;116: 856–63.
[7] Tan DT, Ficker LA, Buckley RJ. Limbal transplantation. Ophthalmology 1996;103: 29–36.
[8] Pellegrini G, Traverso CE, Franzi AT, Zingirian M, Canceda R, De Luca M. Long term restoration of damaged corneal surfaces with autologous cultivated corneal epithelium. Lancet 1997;349:990–3.
[9] Dua HS, Azuara-Blanco A. Allo-limbal transplantation in patients with limbal stem cell deficiency. Br J Ophthalmol 1999;83:414–9.
[10] Tsubota K, Satake Y, Kaido M, Shinozaki N, Shimmura S, Bissen-Miyajima H, et al. Treatment of severe ocular surface disorders with corneal epithelial stem-cell transplantation. N Engl J Med 1999;340:1697–703.
[11] Holland EJ. Epithelial transplantation for the management of severe ocular surface disease. Trans Am Ophthalmol Soc 1996;94:677–743.
[12] Cauchi PA, Ang GS, Azuara-Blanco A, Burr JM. A systematic literature review of surgical interventions for limbal stem cell deficiency in humans. Am J Ophthalmol 2008;146:251–9.
[13] Thoft RA, Sugar J. Graft failure in keratoepithelioplasty. Cornea 1993;12:362–5.
[14] Daya SM, Bell RW, Habib NE, Powel-Richards A, Dua HS. Clinic and pathologic findings in human keratolimbal allograft rejection. Cornea 2000;19:443–50.
[15] Mills RA, Coster DJ, Williams KA. Effect of immunosuppression on outcome measures in a model of rat limbal transplantation. Investig Ophthalmol Vis Sci 2002;43:647–55.
[16] Maruyama K, Yamada J, Sano Y, Kinoshida S. Th2-biased immune system promotion of allogeneic corneal epithelial cell survival after orthotopic limbal transplantation. Investig Ophthalmol Vis Sci 2003;44:4736–41.
[17] Swift GJ, Aggarwal RK, Davis GJ, Coster DJ, Williams KA. Survival of rabbit limbal stem cell allografts. Transplantation 1996;62:568–74.
[18] Holan V, Haskova Z, Filipec M. Transplantation immunity and tolerance in the eye. Rejection and acceptance of orthotopic corneal allografts in mice. Transplantation 1996;62:1050–4.
[19] Vítova A, Filipec M, Zajicova A, Krulova M, Holan V. Prevention of corneal allograft rejection in a mouse model of high-risk recipients. Br J Ophthalmol 2004;88: 1338–42.
[20] Pindjakova J, Vitova A, Krulova M, Zajicova A, Filipec M, Holan V. Corneal rat-to mouse xenotransplantation and the effects of anti-CD4 or anti-CD8 treatment on cytokine and nitric oxide production. Transpl Int 2005;18:854–62.
[21] Krulova M, Zajicova A, Fric J, Holan V. Alloantigen-induced, T-cell-dependent production of nitric oxide by macrophages infiltrating skin allografts in mice. Transpl Int 2002;15:108–16.
[22] Masaki Y, Hirasawa A, Okuyama S, Tsujimoto G, Iwaya M, Li XK, et al. Microchimerism and heart allograft acceptance. Transplant Proc 1995;27:148–50.
[23] Dialynas DP, Wilde DB, Marrack P, Pierres A, Wall KA, Havran W, et al. Characterization of the murine antigenic determinant designated L3T4a, recognized by monoclonal antibody GK1.5: expression of L3T4a by functional T cell clones appears to correlate primarily with class II MHC antigen-reactivity. Immunol Rev 1983;74:29–56.
[24] Gottlieb PD, Marshak-Rothstein A, Auditore-Hargreaves K. Construction and properties of new Lyt-congeneic strains and anti-Lyt-2.2 and anti-Lyt-3.1 monoclonal antibodies. Immunogenetics 1980;10:545–52.
[25] Gillette TE, Chandler JW, Greiner JV. Langherhans cells of the ocular surface. Ophthalmology 1982;89:700–11.
[26] Haskova Z, Filipec M, Holan V. The significance of gender incompatibility in donors and recipients and the role of minor histocompatibility antigens in corneal transplantation. Cesk Slov Oftalmol 1997;53:128–35.
[27] Keijser S, de Keizer RJ, Prins FA, Tanke HJ, van Rooijen N, Vrensen GF, et al. A new model for limbal transplantation using E-GFP for follow-up of transplant survival. Exp Eye Res 2006;83:188–95.
[28] Strestikova P, Plskova J, Filipec M, Farghali H. FK 506 and aminoguanidine suppress iNOS induction in orthotopic corneal allografts and prolong graft survival in mice. Nitric Oxide 2003;9:111–7.
[29] Siegers TP, Broersma L, van Rooijen N, Hooymans JM, van Rij G, van der Gaag R. Macrophages play a role in the early phase of corneal allograft rejection in rats. Transplantation 2004;77:1641–6.
[30] Wallgren AC, Karlsson-Parra A, Korsgren O. The main infiltrating cell in xenograft rejection is a CD4+ macrophage and not a T lymphocyte. Transplantation 1995;60:594–601.
[31] He YG, Ross J, Niederkorn JY. Promotion of murine orthotopic corneal allograft survival by systemic administration of anti-CD4 monoclonal antibody. Investig Ophthalmol Vis Sci 1991;32:2723–7.

8.2 Publication 2

A rapid separation of two distinct populations of mouse corneal epithelial cells with limbal stem cell characteristics by centrifugation on Percoll gradient.

Krulova M, Pokorna K, Lencova A, Fric J, Zajicova A, Filipec M, Forrester JV, Holan V.

Invest Ophthalmol Vis Sci. 2008 Sep;49(9):3903-8. (IF 3.528)

A Rapid Separation of Two Distinct Populations of Mouse Corneal Epithelial Cells with Limbal Stem Cell Characteristics by Centrifugation on Percoll Gradient

Magdalena Krulova,[1,2] *Katerina Pokorna,*[1,2] *Anna Lencova,*[1,3] *Jan Fric,*[1,2] *Alena Zajicova,*[1] *Martin Filipec,*[3] *John V. Forrester,*[4] *and Vladimir Holan*[1,2]

Purpose. To detect and isolate cells with stem cell (SC) characteristics in the limbus of the mouse.

Methods. Limbal tissues from BALB/c mice were trypsin-dissociated and separated on the gradient Percoll (Fluka, Buchs, Switzerland). Several fractions were isolated and characterized by real-time PCR for the presence of limbal SC markers and differentiation markers of corneal epithelial cells by flow cytometry for the determination of the side-population (SP) phenotype and growth properties in vitro.

Results. Cells retained in the lightest fraction (40% Percoll) and in the densest fraction (80% Percoll) of the gradient were both enriched for populations with a high expression of the SC markers ABCG2 and Lgr5 and also expressing the SP phenotype. However, the lightest fraction (representing approximately 12% of total limbal cells) contained cells with the strongest spontaneous proliferative capacity and expressed the corneal epithelial differentiation marker K12. In contrast the densest fraction (<7% of original cells) was K12 negative and contained small nonspontaneously proliferating cells, which instead were positive for p63. Unexpectedly, cells from this fraction had the highest proliferative activity when cultured on a 3T3 feeder cell monolayer.

Conclusions. These findings demonstrate the presence of two distinct populations of corneal epithelial cells with limbal SC characteristics, based on differential expression of the keratin-specific marker K12 and transcription factor p63, and suggest a difference in developmental stage of the two populations, with the $K12^{-}p63^{+}$ population being closer to the primitive limbal SC. (*Invest Ophthalmol Vis Sci.* 2008;49:3903–3908) DOI:10.1167/iovs.08-1987

From the [1]Institute of Molecular Genetics, Academy of Sciences of the Czech Republic, Prague, Czech Republic; the [2]Faculty of Natural Sciences, Charles University, Prague, Czech Republic; the [3]Eye Clinic Lexum, Prague, Czech Republic; and the [4]Department of Ophthalmology, University of Aberdeen, Aberdeen, Scotland.

Supported by Grant KAN200520804 from the Grant Agency of the Academy of Sciences, projects 1M0506, MSM0021620806, and MSM0021620858 from the Ministry of Education of the Czech Republic; Grant 310/08/H077 from the grant Agency of the Czech Republic; and project AVOZ50520514 from the Academy of Sciences of the Czech Republic.

Submitted for publication March 6, 2008; revised April 10 and 24, 2008; accepted July 14, 2008.

Disclosure: **M. Krulova**, None; **K. Pokorna**, None; **A. Lencova**, None; **J. Fric**, None; **A. Zajicova**, None; **M. Filipec**, None; **J.V. Forrester**, None; **V. Holan**, None

The publication costs of this article were defrayed in part by page charge payment. This article must therefore be marked "*advertisement*" in accordance with 18 U.S.C. §1734 solely to indicate this fact.

Corresponding author: Vladimir Holan, Institute of Molecular Genetics, Academy of Sciences of the Czech Republic, Videnska 1083, 142 20 Prague 4, Czech Republic; holan@img.cas.cz.

The corneal surface is renewed under normal physiological conditions or during healing after injury by cells that migrate from the limbus. These cells originate from limbal stem cells (SCs) which reside in the basal layer of the limbus and represent a minor fraction of a heterogeneous limbal cell population.[1–3] When the limbal SC population is damaged or depleted (e.g., after injuries such as alkaline burns or genetically as in the Pax6 heterozygotic mouse),[4,5] healing of the corneal surface is prevented, and the cornea is invaded by cells from conjunctival epithelia resulting in poor epithelialization, vascularization, and corneal scarring, potentially leading to blindness. In such cases, transplantation of limbal SCs may be the only way to treat various eye surface injuries or diseases.[6–8]

To study the biological properties and to provide a potential source of limbal SCs, methods are needed to isolate or at least enrich limbal SCs from the heterogenous population of limbal cells. The absence of a definitive biological or phenotypic marker contributes a degree of uncertainty to the unequivocal isolation and characterization of limbal SCs. So far, a variety of SC markers have been proposed to identify this population of cells. Among the major characteristics proposed for SCs are small size[9,10]; slow-cycling properties[11]; the expression of intracellular markers such as drug resistance transporter ABCG2, the transcription factor p63, the integrin $\alpha 9$, and the cytokeratin K19[12–18]; and the absence of corneal differentiation markers K3 and K12 or connexin 43.[1,19–21] Recently, the leucine-rich-repeat–containing G-protein-coupled receptor, Lgr5, has been suggested to mark of SCs in multiple adult tissues.[22] SCs express the side-population (SP) phenotype based on the ability to efflux the DNA-binding dye Hoechst 33342.[18,23] Although SCs are in vivo in a quiescent state and are only slowly dividing, in vitro they possess the highest colony-forming unit efficacy and growth properties on feeder cell monolayers.[10,24,25] Some of these characteristics, mainly the SP phenotype and small cell size, have been used in attempts to isolate SCs from human and rabbit limbuses or limbal cell cultures.[10,12,24] Another approach to enriching human limbal epithelial cells with SC properties is based on their differential adhesiveness to collagen type IV.[26] To date, probably due to the small size of the mouse eye, no attempt to isolate and characterize limbal SCs in the mouse has been reported. We show here for the first time that two distinct populations of corneal epithelial cells with limbal SC characteristics can be isolated from the mouse limbus by centrifugation on a Percoll gradient (Fluka, Buchs, Switzerland). These cells share characteristics of SCs with human or rabbit limbal SCs and can be used for the study of limbal SC properties and for studies of limbal SC deficiency in experimental mouse models such as the $Pax6^{+/-}$ mouse.

Material and Methods

Mice

Mice of the inbred strain BALB/c of both sexes at the age of 2 to 4 months were used in these experiments. The animals were obtained from the breeding unit of the Institute of Molecular Genetics (Prague,

Czech Republic). The use of animals was approved by a local Ethics Committee of the Institute of Molecular Genetics, and all animals were handled in full accordance with the ARVO Statement for the Use of Animals in Ophthalmic and Vision Research.

Isolation of Limbal Cells

Limbal tissue was obtained by scissor dissection of the eyes of killed mice guided by an operating microscope. Limbal tissues from 10 to 12 BALB/c mice were pooled and cut into small pieces in RPMI 1640 medium (Sigma-Aldrich, St. Louis, MO). The tissue was centrifuged (8 minutes at 250*g*), and the pellet was subjected to digestion with trypsin from porcine pancreas (Sigma-Aldrich). The procedure consisted in 10 trypsinization cycles (300 μL of 0.5% trypsin solution per 10 limbuses, 10 minutes incubation in 37°C). The supernatants (tissue-free solution) from each trypsinization step were harvested into an excess (30 mL) of RPMI 1640 medium with 10% fetal calf serum (FCS; Sigma-Aldrich) on ice, and the trypsinization procedure was repeated on the residual pellet. After the last trypsinization step, the harvested cell suspension was filtrated through a nylon mesh and centrifuged for 8 minutes at 250*g*. The pellet was resuspended in 1.2 mL of RPMI 1640 medium, and the number of cells was determined by hemocytometry.

Percoll Gradient Centrifugation

To prepare a stock solution, nine parts Percoll was mixed with one part 10× concentrated phosphate buffered saline (PBS). From the stock solution, a 40%, 50%, 60%, 70%, or 80% Percoll solution was prepared by dilution in 1× PBS. A Percoll gradient was prepared in a 10-mL test tube by overlaying of 1.0 mL of each Percoll dilution 80% through 40%. Finally, 1.0 mL of suspension of trypsin-dissociated limbal cells was gently overlaid on the top of the Percoll gradient. The gradient was centrifuged for 10 minutes at 300*g* at 4°C.

After centrifugation, the separated layers of cells on individual Percoll concentrations could be directly visualized, and individual cell layers (as well as the cell pellet) were harvested into RPMI 1640 medium with 5% of FCS and washed three times by centrifugation (8 minutes at 250*g*). After the last washing, the cells were resuspended in 500 μL of RPMI 1640 medium containing 10% of FCS, 10 mM HEPES buffer, antibiotics (100 U/mL of penicillin, 100 μg/mL of streptomycin) and 5×10^{-5} M 2-mercaptoethanol (hereinafter called complete RPMI 1640 medium). The number of cells in each fraction was then determined.

Quantitative Real-Time Polymerase Chain Reactions

The expression of genes for mouse ABCG2, Lgr5, the α isoform of DeltaNp63 (p63), and K12 was determined by quantitative real-time PCR. Total RNA was isolated from unseparated limbal cells or cells from individual Percoll fractions (TRI Reagent; Molecular Research Center, Cincinnati, OH). One microgram of total RNA was reverse transcribed into cDNA in 20-μL reaction mixture, as described previously.[27]

Quantitative real-time PCR was performed (iCycler; Bio-Rad, Hercules, CA), and the data were analyzed (iCycler Detection System, ver. 3.1; Bio-Rad). The specificity of the amplified products was checked by the melting analyses. Master mix (iQ SYBR Green Supermix; Bio-Rad) was used in all experiments. Each single experiment was performed in triplicate, and the reaction efficiency for each gene was estimated by the dilution curve method. The relative quantification model with efficiency correction was applied to calculate expression of target genes in comparison to GADPH, which was used as the housekeeping gene. The primers are described in Table 1. The PCR parameters for 25-μL reactions included denaturation at 95°C for 3 minutes, then 40 cycles at 95°C for 10 seconds, annealing at 60°C for 20 seconds, and elongation at 72°C for 20 seconds. Fluorescence data were collected at each cycle after an elongation step at 80°C for 5 seconds.

Light-Scattering Measurements

Trypsin-dissociated unseparated limbal cells or limbal cells from individual Percoll fractions were resuspended in PBS with 5% FCS and 2 μg/mL of propidium iodide (Sigma-Aldrich) for 20 minutes at 4°C. The light-scattering properties of the cells were measured in a flow cytometer (BD LSRII; BD Biosciences, Franklin Lakes, NY), with an Argon laser (488 nm) providing the probing beam, and the FSC/SSC density plots of viable cells were generated.

Hoechst 33342 Exclusion Assay

Freshly isolated unseparated limbal cells or cells of individual fractions from a Percoll gradient were resuspended at a concentration of 1×10^6 cells/mL in Dulbecco;1 Dulbecco's Modified Eagle's Medium (DMEM) containing 2% FCS and incubated with 5 μg/mL Hoechst 33342 (Sigma-Aldrich) dye. To determine the effect of verapamil on the Hoechst 33342 efflux, the cells were preincubated with verapamil (80 μM; Sigma-Aldrich) for 5 minutes before the addition of the Hoechst 33342 dye. After the incubation for 60 minutes at 37°C, propidium iodide (2 μg/mL) was added to exclude dead cells from the analysis, and the cells were then analyzed on a flow cytometer (FACSVantage SE; BD Biosciences), as described by Goodell et al.[28] Briefly, Hoechst 33342 was excited at 350 nm with a UV laser (Enterprise II-621; Coherent, Santa Clara, CA), and fluorescence emission was detected through 450-nm band-pass (Hoechst blue) and 660-nm long-pass (Hoechst red) filters.

Spontaneous Proliferation of Limbal Cells In Vitro

Unseparated limbal cells or cells from individual fractions from the Percoll gradient were diluted to a concentration of 5×10^4 cells/mL in complete RPMI 1640 medium. One hundred microliters per well of cell suspension was incubated in triplicate in 96-well tissue culture plates (Nunc, Roskilde, Denmark). Cell proliferation was determined by adding 1 μCi/well of [^{3}H]thymidine (Nuclear Research Institute, Rez, Czech Republic) for the last 8 hours of the 96-hour incubation period. The cells were harvested (Automasch 2000 harvester; Dynatech, Burlington, MA), and [^{3}H]thymidine activity was determined.

Cell Proliferation on Feeder 3T3 Fibroblasts

Irradiated (150 Gy) mouse 3T3 fibroblasts were seeded as feeder cells at a concentration of 10^4 cells/well in a volume of 50 μL of complete RPMI 1640 medium into wells of 96-well tissue culture plates (Nunc) and incubated overnight. Unseparated limbal cells or cells from individual Percoll gradient fractions (5×10^3 cells in 50 μL) were then added in triplicate into wells with feeder cells. The cultures were incubated for 96 hours, [^{3}H]thymidine (1 μCi/well) was added for the

TABLE 1. Mouse Primer Sequences Used for Real-Time PCR

Gene	Sense Primer	Antisense Primer
GADPH	GGG TGT GAA CCA CGA GAA AT	ACA CAT TGG GGG TAG GAA CA
ABCG2	GCC TTG GAG TAC TTT GCA TCA	AAA TCC GCA GGG TTG TTG TA
p63	TGG AAA ACA ATG CCC AGA CT	CTG CTG GTC CAT GCT GTT C
Lgr5	CTT CAC TCG GTG CAG TGC T	CAG CCA GCT ACC AAA TAG GTG
K12	CTG TGG AGG CCT CTT TTC TG	ATT CCA GCT ATC CCC AAT CC

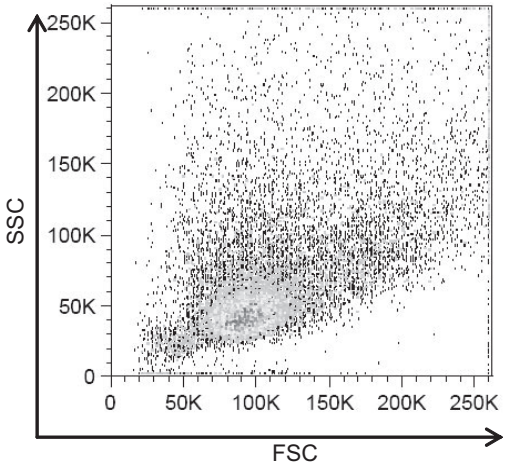

FIGURE 1. Flow cytometry analysis (light-scattering profile) of freshly isolated, unseparated mouse limbal cells. Limbal tissue from normal BALB/c mice was trypsin-dissociated, and single cell suspensions were analyzed according to their size (FSC) and granularity (SSC) profiles. A representative dot-plot is shown.

last 8 hours of the incubation period, and the incorporated radioactivity was determined as just described.

Statistical Analysis

The statistical significance of differences between individual groups was calculated by Student's *t*-test.

RESULTS

Limbal Cell Isolation and Percoll Gradient Separation

Trypsin-dissociation of limbal tissue from one BALB/c mouse yielded on average 0.5 to 1 $\times$ 10^5 cells that were heterogeneous in both size and morphology, as determined by the light-scattering profile (Fig. 1). Accordingly, limbal cells obtained by trypsin digestion (see the Methods section) from 10 BALB/c mice were pooled and separated on the Percoll gradient. The proportion of cells retained in individual Percoll gradient fractions and the recovery of original cells are shown in Table 2. While the lightest fraction (40% Percoll) contained predominantly large and more heterogeneous cells with a smaller nucleus/cytoplasm ratio, the fraction retained on the 80% Percoll (densest fraction) was enriched in small dense cells with a higher ratio nucleus/cytoplasm. The pelleted fraction contained dead cells, cell debris, and fragments of corneal tissue and thus was not included in the analyses.

Phenotype Characterization

The expression of genes for the putative SC markers ABCG2, Lgr5, and p63 and for corneal epithelial cell differentiation marker K12 was determined by using real-time PCR in unseparated limbal cells and limbal cell fractions isolated from Percoll gradient. As demonstrated in Figure 2, both the lightest (40% Percoll) and densest (80% Percoll) fractions were enriched in cells expressing the SC markers ABCG2 and Lgr5, whereas the fraction from the middle region of the Percoll gradient had a lower expression of these markers compared to unseparated limbal cells. The marker of primitive and SCs p63 was expressed selectively in the dense (80% Percoll) cell fraction (Fig. 2). The corneal differentiation marker K12 was expressed predominantly in larger cells retained on 40% or 50% Percoll and was absent in small cells of the dense fractions (Fig. 2).

Identification of the SP Phenotype on the Basis of the Efflux of Hoechst 33342 Dye

Using flow cytometry we first demonstrated that normal fresh mouse limbus contains a small population of cells (SP cells) that can be detected by verapamil-sensitive disappearance of a unique tail of a low Hoechst 33342 blue-red fluorescence (Figs. 3A, 3B). This population represented 2.3% to 5.4% of total mouse limbal cells. Analysis of individual fractions from the Percoll gradient showed that SP cells were enriched in light and dense fractions (40% and 80% Percoll) and were relatively decreased in cells from the intermediate fractions of the Percoll gradient (Figs. 3C–H).

Forward-scattering analysis was performed to determine the relative cell size and granularity of SP cells from unseparated total limbal cells (Fig. 4A) or of the fractions from the 40% (Fig. 4B) and the 80% (Fig. 4C) Percoll gradients. The SP cells from the 40% gradient fraction were apparently more heterogeneous with respect to granularity than were the small and more uniform SP cells in the 80% fraction.

Growth Properties of Limbal Cell Fractions

To evaluate the proliferative capacity of the various cell fractions, we seeded the cells at a concentration of 5 $\times$ 10^3 cells/well into 96-well tissue culture plates (in a volume of 100 μL complete RPMI 1640 medium/well). Cell proliferation was determined by incorporation of [^{3}H]thymidine. As demonstrated in Figure 5A, the 40% Percoll gradient cell fraction proliferated with a significantly higher intensity than did the unseparated limbal cells, whereas cells from the 70% or 80% fractions had very limited proliferative activity.

We also assessed the proliferative capacity of individual cell populations on irradiated 3T3 fibroblast feeder cells in 96-well tissue culture plates. The proliferative activity of limbal cells was determined according to the incorporation of radioactivity. The results are expressed as the ratio of the proliferative activity of limbal cells on a 3T3 feeder layer to the proliferation of the same cells in wells without feeder cells. As demonstrated

TABLE 2. Recovery of Original Limbal Cells and the Proportion of Cells in Individual Fractions after Percoll Gradient Centrifugation

	% of Original Cells in the Percoll Fraction						
Exp.	40	50	60	70	80	Bottom	Cell Recovery (%)
1	14.2	17.2	16.3	22.8	7.2	8.0	85.7
2	10.4	17.3	27.1	13.5	3.1	8.4	79.8
3	13.0	11.6	23.1	17.3	7.7	9.7	82.4
4	10.2	13.3	22.1	21.7	6.1	4.2	77.6
5	14.6	16.3	20.0	20.3	7.1	8.4	86.7

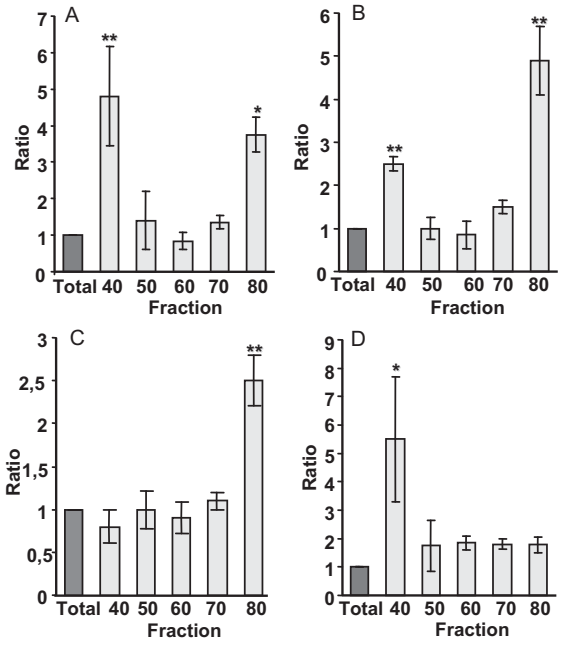

FIGURE 2. Expression of genes for SC markers ABCG2 (**A**), Lgr5 (**B**), and p63 (**C**), and for corneal differentiation marker K12 (**D**) in unseparated limbal cells and in individual fractions from a Percoll gradient. Real-time PCR was performed on unseparated limbal cells (total) and cells retained on 40%, 50%, 60%, 70%, and 80% gradients. Data are the mean ± SD of three separate experiments. The comparative C_t method was used to determine the change in targeted gene expression normalized by the internal control gene GAPDH. $^*P < 0.05$, $^{**}P < 0.01$.

in Figure 5B, in this experimental setting, the strongest proliferative activity was observed in the small cell population retained in the 70% and 80% Percoll gradient fractions, while the proliferative capacity of cells from the 40% and 50% fractions was not increased over spontaneous proliferation levels without feeder cells.

DISCUSSION

SCs for the renewal of the corneal surface epithelium are located in the basal layer of the limbal epithelium. These cells, which are characterized by small size; a low rate of replication; expression of certain markers such as a transporter ABCG2, p63, integrin α9, or K19; and by the expression of the SP phenotype have been described in human,[10,12–14] rabbit,[24,29] and rat[23] corneas. To date, there are no reports of isolation and characterization of limbal SCs in the mouse.

We have shown that cells sharing morphologic, phenotypical, and functional characteristics with human and rabbit limbal SC can also be found in the mouse limbus. To dissociate the limbal tissue into a single cell suspension, we compared various enzymatic digestion protocols including dispase treatment, combination of dispase, and trypsin or trypsin digestion alone. Repeated short trypsin digestions were the optimal method, allowing recovery of 0.5 to 1 × 10^5 limbal cells per one BALB/c mouse. These cells were heterogeneous with respect to the size, granularity, and the ratio of cytoplasm to nucleus and could be separated into six subpopulations on a 40% to 80% discontinuous Percoll gradient. The densest fraction (80% Percoll), representing approximately 7% of original limbal cells, was enriched in cells showing morphologic characteristics described for the human and rabbit limbal SCs: small size, dense cells, and a low ratio of cytoplasm to nucleus. Further analysis of this fraction showed that this population was enriched in cells expressing the SP phenotype (>30% of SP cells in comparison to 2%–5% of cells expressing the SP phenotype in the whole limbus) and the fraction also had significantly enhanced expression of the SC markers ABCG2, Lgr5, and p63 in comparison with unseparated limbal cells. In addition, these cells were in a nonproliferative quiescent state as demonstrated by their very low spontaneous uptake of radioactive thymidine in vitro. However, when cultured on a feeder cell layer, they demonstrated considerable proliferative capacity. All these characteristics resemble properties of limbal SC described in human or rabbit limbal tissue.[12–14,24,29]

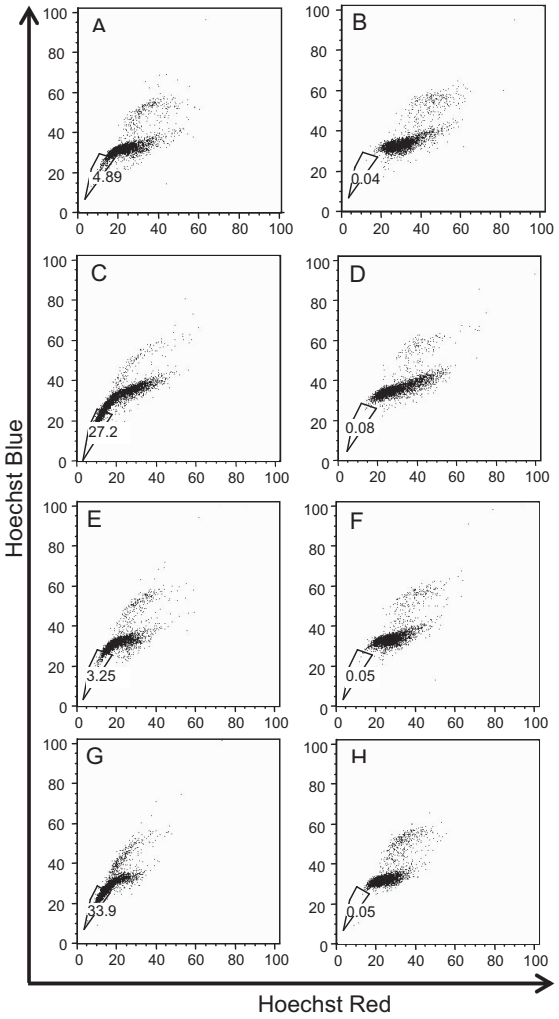

FIGURE 3. SP profile of freshly isolated unseparated mouse limbal cells and cells from the Percoll gradient fractions. Unseparated limbal cells (**A**, **B**) or cells from fraction 40% (**C**, **D**), 60% (**E**, **F**), or 80% (**G**, **H**) gradients were subjected to Hoechst 33342 exclusion assay. The cells were analyzed by flow cytometry (**A**–**H**), and the dye efflux from the SP was blocked by verapamil (**B**, **D**, **F**, **H**).

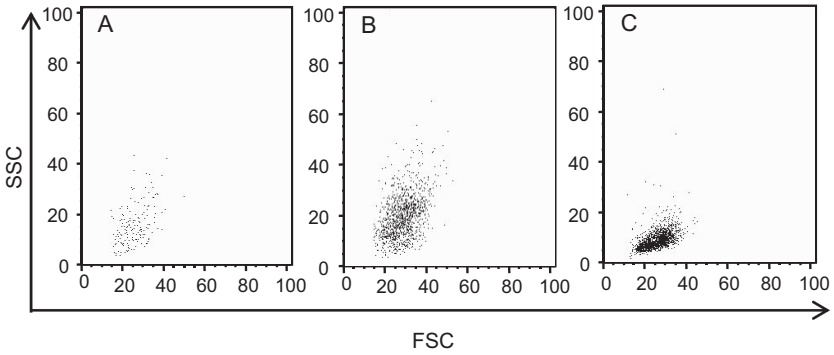

FIGURE 4. Light-scattering profile of SP cells from unseparated freshly isolated mouse limbal cells (**A**), or from the top (40% Percoll) (**B**) and the bottom (80% Percoll) (**C**) fraction. Shown are the light-scattering properties of cells denoted by each enclosed area in Figures 3A, 3C, and 3G.

A second cell fraction showing at least some characteristics of limbal SCs was detected in the lightest cell population (40% Percoll gradient) and represented approximately 12% of the total limbal cell population. These cells expressed genes for the SC markers ABCG2 and Lgr5, and over 20% of the cells expressed the SP phenotype, a property of SCs.[30,31] However, unlike the dense cell population (80% gradient) which also expressed the SP phenotype and SC markers, the light cell population was positive for corneal differentiation marker K12 and had the highest spontaneous proliferative capacity (significantly higher than unseparated limbal cells) and their proliferation response did not increase when they were cultured on a feeder cell monolayer. Thus, two separable populations of mouse limbal cells which have SC characteristics (ABCG2 and Lgr5 expression, the SP phenotype) can be obtained by centrifugation on Percoll gradient. The cells retained in the intermediate layer of the gradient (60% Percoll) had lower expression levels of SC markers and a lower percentage of cells expressing the SP phenotype than original unseparated limbal cells.

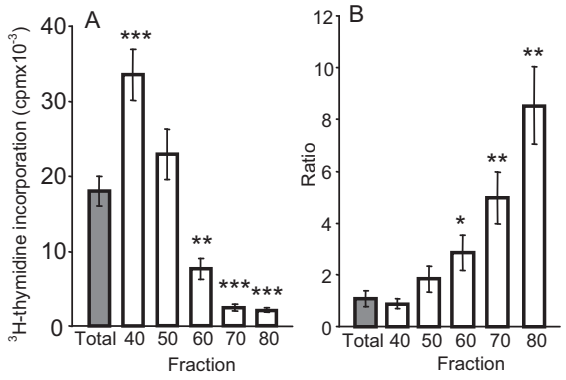

FIGURE 5. Growth properties of unseparated, freshly dissociated mouse limbal cells and cells from individual fractions obtained after Percoll gradient centrifugation. Unseparated limbal cells (total cell population) or cells retained on 40%, 50%, 60%, 70%, and 80% Percoll gradient fractions were seeded into wells of 96-well tissue culture plates (5,000 cells/well) (**A**) or into wells containing a 3T3 fibroblast feeder layer (**B**). Cell proliferation was determined by incorporation of [^{3}H]thymidine added to the cultures for the last 6 hours of the 96-hour incubation period. The results are expressed by the counts per minute of incorporated [^{3}H]thymidine (**A**) or as the increase in the proliferation of particular cell population cultivated on the 3T3 feeder layer in comparison to proliferation of the same cells cultivated without the 3T3 feeder cells. Each bar represents the mean ± SE of results in three independent experiments. $^*P < 0.05$, $^{**}P < 0.01$, $^{***}P < 0.001$, significantly different from the control (unseparated limbal cells).

The results thus demonstrated that two distinct populations of limbal cells with SC characteristics can be isolated in the mouse. Both populations contained cells expressing the SP phenotype based on the efflux of Hoechst 33342 dye. However, forward-scattering analysis of SP cells from the top and bottom fractions showed that both populations differ in their size and granularity. The number of SP cells in the unseparated mouse limbus was 3.8% (average from five experiments) of total limbal cells, substantially higher than the number of slow-cycling corneal epithelial cells found at the mouse limbus[32] or the number of SP cells in human, rabbit, and rat limbal epithelia,[13,23,24] but corresponds to the number of SP cells found in the rat cornea.[23] Although it has been shown that the SP phenotype is associated with ABCG2 expression,[33] the corollary is not necessarily true (i.e., not all cells expressing ABCG2 exhibit the SP phenotype). The studies of Umemoto and coworkers in humans,[16] rabbits,[29] and rats[23] showed that although the number of cells exhibiting the SP phenotype was less than 2% in the limbus, immunochemistry revealed that a larger proportion (approximately 10%) of limbal basal epithelial cells expressed ABCG2 transporter.[23] Similarly, Budak et al.[18] suggested the existence of a significantly higher number of ABCG2$^+$ cells than SP cells. This discrepancy was explained by the differences in the transport activity of ABCG2. Umemoto et al.[23] also showed that in the rat, unlike the human and rabbit, the central cornea contains cells with the SP phenotype but that these cells expressed significantly lower levels of putative SC markers than did the SP cells in the limbus. In addition, SP cells found in the rat cornea had a different profile on forward scatter analyses than SP cells in the limbus. Our study showed that mouse limbal cells with the SP phenotype from the light cell fraction of the Percoll gradient had distinctive light-scattering properties from SP cells from the dense cell fraction. It appears that the light cell fraction resembles the SP cells described by Umemoto et al.[23] in the rat central cornea rather than the basal limbal SCs. A high expression of the corneal epithelial cell differentiation marker K12 in the light cell population supports this analysis. It is therefore apparent that interspecies differences exist in the distribution and properties of corneal epithelial cells with limbal SC characteristics and that the mouse may, in this respect, represent a unique species different from human, rabbit, or rat.

The limbal cells isolated in the dense cell fraction (80% Percoll) mimicked more closely the limbal SCs described in the human and rabbit by both SC characteristics (small cell size, expression of ABCG2, p63 and Lgr5, the SP phenotype) and by growth properties. These cells occurred in a quiescent state and did not proliferate within the first 3 days in tissue culture, as has been described for SP cells in the rabbit.[24] Budak et al.[18] showed that SP cells remained quiescent for at least 72 hours after seeding, whereas the non-SP cells began to divide within

24 to 48 hours. However, when we cultured the dense cell population on a 3T3 feeder cell monolayer, they exhibited a strong proliferative activity. Similarly, de Paiva et al.[13] showed that human limbal SP cells proliferate better on feeder cells than do non-SP cells. To evaluate growth properties of individual cell fractions, we cultured these cells at low cell concentrations. The cells from the light fraction formed colonies of fibroblast-like cells and their growth was enhanced in the presence of epidermal or fibroblast growth factor. On the contrary, the cells from the dense fraction did not grow in cultures without feeder cells, even in the presence of the growth factors. A similar pattern of proliferation and responsiveness to the growth factors was observed in the cells from the light fraction when cultured on a 3T3 cell monolayer. However, the cells from the dense fractions that did not proliferate in cultures without feeder cells, formed on the 3T3 cell monolayer colonies of spheric cells, and their growth was not significantly influenced by epidermal or fibroblast growth factor. It is possible that quiescent, slowly dividing limbal SCs (separated in the dense fraction) require a specific niche (feeder cells) to support their proliferation.

This study showed that there are two distinct populations of corneal epithelial cells with SC characteristics (expression of ABCG2 and Lgr5, an SP phenotype) that can be isolated from the mouse limbus and that Percoll gradient centrifugation is a convenient method of enriching and harvesting such cells for the study of their characteristics, growth requirements, and use to treat various limbal SC deficiencies in experimental models.

References

1. Schermer A, Galvin S, Sun TT. Differentiation-related expression of a major 64 K corneal keratin in vivo and in culture suggests limbal location of corneal epithelial stem cells. *J Cell Biol*. 1986;103:49–62.
2. Tseng SC. Regulation and clinical implication of corneal epithelial stem cells. *Mol Biol Rep*. 1996;23:47–58.
3. Daniels JT, Dart JKG, Tuft SJ, et al. Corneal stem cells in review. *Wound Rep Reg*. 2001;9:483–494.
4. Gomes JA, dos Santos MS, Cunha MC, Mascaro VL, Barros Jde N, de Sousa LB. Amniotic membrane transplantation for partial and total limbal stem cell deficiency secondary to chemical burn. *Ophthalmology*. 2003;110:466–473.
5. Collinson JM, Chanas SA, Hill RE, West JD. Corneal development, limbal stem cell function, and corneal epithelial cell migration in the Pax6$^{+/-}$ mouse. *Invest Ophthalmol Vis Sci*. 2004;45:1101–1108.
6. Pellegrini G, Traverso CE, Franzi AT, Zingirian M, Cancedda R, De Luca M. Long-term restoration of damaged corneal surfaces with autologous cultivated corneal epithelium. *Lancet*. 1997;349:990–993.
7. Samson CM, Nduaguba C, Baltatzis S, Foster CS. Limbal stem cell transplantation in chronic inflammatory eye disease. *Ophthalmology*. 2002;109:862–868.
8. Du Y, Chen J, Funderburgh JL, Zhu X, Li L. Functional reconstruction of rabbit corneal epithelium by human limbal cells cultured on amniotic membrane. *Mol Vis*. 2003;9:635–643.
9. Romano AC, Espana EM, Yoo SH, Budak MT, Wolosin JM, Tseng SC. Different cell sizes in human limbal and central corneal basal epithelia measured by confocal microscopy and flow cytometry. *Invest Ophthalmol Vis Sci*. 2003;44:5125–5129.
10. de Paiva CS, Pflugfelder SC, Li D-Q. Cell size correlates with phenotype and proliferative capacity in human corneal epithelial cells. *Stem Cells*. 2006;24:368–375.
11. Cotsarelius G, Cheby SZ, Dong G, et al. Existence of slow-cycling limbal epithelial basal cells that can be preferentially stimulated to proliferate: implications on epithelial stem cells. *Cell*. 1989;57:201–209.
12. Chen Z, de Paiva CS, Luo L, Kretzer FL, Pflugfelder SC, Li DQ. Characterization of putative stem cell phenotype in human limbal epithelia. *Stem Cells*. 2004;22:355–366.
13. de Paiva C, Chen Z, Corrales RM, Pflugfelder SC, Li D-Q. ABCG2 transporter identifies a population of clonogenic human limbal epithelial cells. *Stem Cells*. 2005;23:63–73.
14. Schlotzen-Schrehardt U, Kruse FE. Identification and characterization of limbal stem cells. *Exp Eye Res*. 2005;81:247–264.
15. Pellegrini G, Dellambra E, Colisano O, et al. p63 identifies keratinocyte stem cells. *Proc Nat Acad Aci USA*. 2001;98:3156–3161.
16. Watanabe K, Nishida K, Yamato M, et al. Human limbal epithelium contains side population cells expressing the ATB-binding cassette transporter ABCG2. *FEBS Lett*. 2004;565:6–10.
17. Kasper M. Patterns of cytokeratins and vimentin in guinea pig and mouse eye tissue: evidence for regional variations in intermediate filament expression in limbal epithelium. *Acta Histochem*. 1992;93:319–332.
18. Budak MT, Alpdogan OS, Zhou M, Laver RM, Skunci MAM, Wolosin JM. Ocular surface epithelia contain ABCG2-dependent side population cells exhibiting features associated with stem cells. *J Cell Sci*. 2005;118:1715–1724.
19. Liu CY, Zhu G, Converse R, et al. Characterization and chromosomal localization of the cornea-specific murine keratin gene Krt1.12. *J Biol Chem*. 1994;260:24627–24636.
20. Chen WY, Mui MM, Kao WW, Liu CY, Tseng SC. Conjunctival epithelial cells do not transdifferentiate in organotypic cultures: expression of K12 keratin is restricted to corneal epithelium. *Curr Eye Res*. 1994;13:765–778.
21. Matic M, Petrov IN, Chen S, Wang C, Dimitrijevich SD, Wolosin JM. Stem cells of the corneal epithelium lack connexins and metabolite transfer capacity. *Differentiation*. 1997;61:251–260.
22. Barker N, van Es JH, Kuipers J, et al. Identification of stem cells in small intestine and colon by marker gen Lgr5. *Nature*. 2007;449:1003–1007.
23. Umemoto T, Yamato M, Nishida K, et al. Rat limbal epithelial side population cells exhibit a distinct expression of stem cell markers that are lacking in side population cells from the central cornea. *FEBS Lett*. 2005;579:6559–6574.
24. Park K-S, Lim CH, Min B-M, et al. The side population cells in the rabbit limbus sensitively increased in response to the central cornea wounding. *Invest Ophthalmol Vis Sci*. 2006;47:892–900.
25. Lavker RM, Dong G, Cheng SZ, Kudoh K, Cotsarelis G, Sun TT. Relative proliferative rates of limbal and corneal epithelia: implications of corneal epithelial migration, circadian rhythm, and suprabasally located DNA-synthesizing keratinocytes. *Invest Ophthalmol Vis Sci*. 1991;32:1864–1875.
26. Li DQ, Chen Y, Song XJ, De Paiva CS, Kim HS, Pflugfelder SC. Partial enrichment of a population of human limbal epithelial cells with putative stem cell properties based on collagen type IV adhesiveness. *Exp Eye Res*. 2005;80:581–590.
27. Holáň V, Kuffová L, Zajícová A, et al. Urocanic acid enhances IL-10 production in activated CD4^{+} T cells. *J Immunol*. 1998;161:3237–3241.
28. Goodell MA, Brose K, Paradis G, Paradis G, Commer AS, Mulligan RC. Isolation and functional properties of murine hematopoietic stem cells that are replicating in vivo. *J Exp Med*. 1996;183:1797–1806.
29. Umemoto T, Yamato M, Nishida K, Yang J, Tano Y, Okano T. Limbal epithelial side-population cells have stem cell-like properties, including quiescent state. *Stem Cells*. 2006;24:86–94.
30. Shimano K, Satane M, Okata A, et al. Hepatic oval cells have the side population phenotype defined by expression of ATP-binding cassette transporter ABCG2/BCRP1. *Am J Pathol*. 2003;163:3–9.
31. Zhou S, Schuetz JD, Bunting KD, et al. The ABC transporter is expressed in a wide variety of stem cells and is a molecular determinant of the side-population phenotype. *Nat Med*. 2001;7:1028–1034.
32. Pajoohesh-Ganji A, Pal-Ghosh S, Siemmens SJ, Stepp MA. Integrins in slow-cycling corneal epithelial cells at the limbus in the mouse. *Stem Cells*. 2006;24:1075–1086.
33. Kim M, Turnquist H, Jackson J, et al. The multidrug resistance transporter ABCG2 (breast cancer resistance protein 1) effluxes Hoechst 33342 and is overexpressed in hematopoietic stem cells. *Clin Cancer Res*. 2002;8:22–28.

8.3 Publication 3

Treatment of ocular surface injuries by limbal and mesenchymal stem cells growing on nanofiber scaffolds

Zajicova A, Pokorna K, Lencova A, M Krulova M, Svobodova E, Kubinova S, Sykova E, Pradny M, Michalek J, Svobodova J, Munzarova M, Holan V.

Cell Transplant. 2010;19(10):1281-90. (IF 6.204)

Cell Transplantation, Vol. 19, pp. 1281–1290, 2010

0963-6897/10 $90.00 + .00
DOI: 10.3727/096368910X509040
E-ISSN 1555-3892
www.cognizantcommunication.com

Treatment of Ocular Surface Injuries by Limbal and Mesenchymal Stem Cells Growing on Nanofiber Scaffolds

Alena Zajicova,* Katerina Pokorna,*† Anna Lencova,* Magdalena Krulova,*† Eliska Svobodova,*† Sarka Kubinova,‡ Eva Sykova,‡ Martin Pradny,§ Jiri Michalek,§ Jana Svobodova,¶ Marcela Munzarova,¶ and Vladimir Holan*†

*Institute of Molecular Genetics, Academy of Sciences, Prague, Czech Republic
†Faculty of Science, Charles University, Prague, Czech Republic
‡Institute of Experimental Medicine, Academy of Sciences, Prague, Czech Republic
§Institute of Macromolecular Chemistry, Academy of Sciences, Prague, Czech Republic
¶Elmarco, Liberec, Czech Republic

Stem cell (SC) therapy represents a promising approach to treat a wide variety of injuries, inherited diseases, or acquired SC deficiencies. One of the major problems associated with SC therapy remains the absence of a suitable matrix for SC growth and transfer. We describe here the growth and metabolic characteristics of mouse limbal stem cells (LSCs) and mesenchymal stem cells (MSCs) growing on 3D nanofiber scaffolds fabricated from polyamide 6/12 (PA6/12). The nanofibers were prepared by the original needleless electrospun Nanospider technology, which enables to create nanofibers of defined diameter, porosity, and a basis weight. Copolymer PA6/12 was selected on the basis of the stability of its nanofibers in aqueous solutions, its biocompatibility, and its superior properties as a matrix for the growth of LSCs, MSCs, and corneal epithelial and endothelial cell lines. The morphology, growth properties, and viability of cells grown on PA6/12 nanofibers were comparable with those grown on plastic. LSCs labeled with the fluorescent dye PKH26 and grown on PA6/12 nanofibers were transferred onto the damaged ocular surface, where their seeding and survival were monitored. Cotransfer of LSCs with MSCs, which have immunosuppressive properties, significantly inhibited local inflammatory reactions and supported the healing process. The results thus show that nanofibers prepared from copolymer PA6/12 represent a convenient scaffold for growth of LSCs and MSCs and transfer to treat SC deficiencies and various ocular surface injuries.

Key words: Limbal stem cells (LSCs); Mesenchymal stem cells (MSCs); Nanofiber scaffolds; Ocular surface injuries; Inflammation; Tissue regeneration

INTRODUCTION

Stem cell (SC) therapy represents a promising approach to treating various inherited diseases or tissue injuries associated with SC deficiency. Adult (tissue-specific) SCs benefit from the ability to differentiate into the cell type for which they are committed and even from their ability to differentiate into other cell types (9,12). In addition, a population of SCs derived from bone marrow, called mesenchymal stem cells (MSCs), has immunosuppressive properties and thus can contribute to the healing process by inhibiting local inflammatory reactions (3,16,21).

One of the major problems associated with SC therapy remains the absence of a suitable carrier for the transfer of SCs to precise tissue locations. So far, various materials and scaffolds have been tested for the transportation of SCs. For example, macroporous hydrogels have been used to deliver MSCs for spinal cord injury repair (29) or self-assembling peptide nanofibers have been tested for myoblast transplantation in infarcted myocardium (7). To treat severe ocular surface damage and a deficiency in limbal SCs (LSCs), which are irreplaceable for corneal healing, various carriers for the culturing of LSCs and for their transplantation onto the recipient eye have been tested. They include fibrin glue (24), polymers or collagen sponges (26), and human amniotic membrane (30).

In the last years, promising scaffolds for the growth and transfer of various types of SCs have been offered

Received October 23, 2009; final acceptance May 11, 2010. Online prepub date: June 23, 2010.
Address correspondence to Vladimir Holan, Ph.D., Institute of Molecular Genetics, Academy of Sciences of the Czech Republic, Videnska 1083, 142 20 Prague 4, Czech Republic. Tel: +420-241063226; Fax: +420-224310955; E-mail: holan@img.cas.cz

by nanotechnology. Electrospinning processes can fabricate nanofibers with a diameter ranging from a few tens to hundreds of nanometers and with a defined porosity. The three-dimensional structure of nanofibrous materials has an extremely large surface area, and nanofibers can mimic the structure of extracellular matrix proteins, which provide support for cell growth and function. Nanofiber scaffolds can create specific niches where SCs can reside and maintain their unique properties. It has been shown that embryonic SCs or MSCs grow and differentiate on nanofibers comparably or even better than on plastic surfaces (10,20,27,33,34). We sought to determine whether adult tissue-specific SCs can also be grown on nanofiber scaffolds and whether these scaffolds can be used as carriers for cell transplantation in tissue regeneration.

Using the original Nanospider electrospinning technology we prepared nanofiber scaffolds from a panel of natural and synthetic polymers and tested them for their biocompatibility and their ability to support the growth of various cell types (S. Kubinova et al., manuscript submitted for publication). On the basis of the stability of its nanofibrous architecture in aqueous solutions and its optimal biocomptibility, we selected copolymer polyamide 6/12 (PA6/12) for further studies. We characterized the growth properties of LSCs and MSCs on these nanofibers and used PA6/12 scaffolds for the transfer of LSCs and MSCs to treat ocular surface injuries in an experimental mouse model.

MATERIALS AND METHODS

Mice

Mice of the inbred strains BALB/c and C57BL/10Sn of both sexes at the age of 2–4 months were used in the experiments. The animals were obtained from the breeding unit of the Institute of Molecular Genetics, Prague. The use of animals was approved by the local Animal Ethics Committee of the Institute of Molecular Genetics. The animals were treated in accordance with the Principles of Laboratory Animal Care.

Materials and Nanofiber Preparation

The copolymer PA6/12 was purchased from Chemopharma (Wien, Austria). This material (10 wt%) was dissolved in 85 wt% formic acid (Penta Company, Fairfield, NJ) and heated at 50°C for 6 h. After reducing the temperature to room temperature, the material was used for electrospinning. A modified needleless Nanospider™ technology (U.S. patent No. WO205024101.2005), in which polymeric jets are spontaneously formed from liquid surfaces on a rotating spinning electrode, was used for the preparation of the nanofibers. This Nanospider technology flexibly enables the formation of fibers tens of nanometers to tens of micrometers in diameter. All nanofibrous samples used during this study were prepared at a basis weight of 3–5 g/m^2 and had nanofiber diameter ranging from 290 to 539 nm.

To test the stability of nanofibers in aqueuos solutions, the nanofibrous samples were cut into small pieces and soaked in deionized water in petri dishes. The water was exchanged every day. After a 7- or 14-day period of soaking the samples were dried at room temperature, and their nanofibrous architecture was analyzed using scanning electron microscopy (SEM).

LSCs, MSCs, Corneal Epithelial and Endothelial Cell Lines

LSCs were obtained by enzyme digestion from limbal tissues as we have recently described (13). In brief, limbal tissues from 10–12 BALB/c mice were cut with scissors and subjected to 10 short (10 min each) trypsinization cycles. The released cells were harvested after each cycle, centrifuged (8 min at $250 \times g$) and resuspended in RPMI-1640 medium (Sigma, St. Louis, MO) containing 10% fetal calf serum (FCS, Sigma), antibiotics (100 U/ml of penicillin, 100 μg/ml of streptomycin), 10 mM HEPES buffer, and 2×10^{-5} M 2-mercaptoethanol. The cells were seeded into 12-well tissue culture plates (Nunc, Roskilde, Netherlands) and after 1 week expanded in 25-cm^2 tissue culture flasks (Corning, Schipol-Rijk, Netherlands). For the growth on nanofibers, cells growing in vitro for 2–3 weeks were used.

MSCs were isolated from femurs and tibias of BALB/c mice. The bone marrow was flushed out, a single-cell suspension was prepared by homogenization, and the cells were seeded at a concentration of 4×10^6 cells/ml in complete RPMI-1640 medium in 25-cm^2 tissue culture flasks (Corning). On the following day the nonadherent cells were washed out and the adherent cells were cultured with a regular exchange of the medium and passaging of the cells to maintain their optimal concentration. After 3 weeks of culturing, the cells were characterized phenotypically by flow cytometry (over 90% of them were MHC class II$^-$, CD86$^-$, and CD11b$^-$, but the majority was CD105$^+$) and for their ability to differentiate into adipocytes (data not shown).

Mouse corneal epithelial and endothelial cell lines, prepared by the immortalization of mouse corneal epithelial and endothelial cells (11), were also tested for their growth on nanofiber scaffolds.

Demonstration of the Immunosuppressive Properties of MSC In Vitro

Spleen cells (0.5×10^6/ml) from BALB/c mice were cultured in 200 μl of RPMI-1640 medium containing 10% FCS in 96-well tissue culture plates (Nunc), either

unstimulated or were stimulated with 1.0 μg/ml of concanavalin A (Con A, Sigma). MSC were added to these cultures at a ratio of MSCs to spleen cells of 1:2, 1:4, or 1:8. Cell proliferation was determined by incorporation of [^{3}H]thymidine (1 μCi/well, Nuclear Research Institute, Rez, Czech Republic) added to the cultures for the last 6 h of a 72-h incubation period. The cells were harvested using an Automash 2000 cell harvestor (Dynex, Chantilly, VA) and the radioactivity was determined. The presence of IFN-γ in the supernatants was assessed by an enzyme-linked immunosorbent assay (ELISA) using capture and detection anti-cytokine antibodies purchased from PharMingen (San Diego, CA) and following the instructions of the manufacturer.

Morphology of Cells Growing on Nanofibers and Plastic

LSCs or MSCs were cultured at various cell concentrations on nanofibers fixed in the inserts or on plastic surfaces. Nanofiber scaffolds were cut into squares (approximately 1.5×1.5 cm) and fixed into CellCrownTM^{24} inserts (Scaffdex, Tampere, Finland). The inserts with nanofibers were sterilized by UV light, soaked in sterile destilled water, washed in culture medium, and transferred into 24-well tissue culture plates (Corning). Fifty thousand cells in a volume of 700 μl of culture RPMI-1640 medium with 10% of FCS was transferred into each well. One or 2 days after seeding, the cells were fixed for 15 min in 4% paraformaldehyde, washed with phosphate-buffered saline (PBS), and treated with Chemiblocker (1:20, Chemicon, Temecula, CA) and Triton X-100 (0.2%, Sigma). To label F-actin, the cells were incubated with Alexa fluor 568 Phalloidin (Molecular Probes, Invitrogen, Paisley, UK) diluted 1:300 in PBS containing 1% bovine serum albumin (Sigma) and 0.5% Triton X-100 (Sigma) overnight at room temperature. The nuclei were vizualized by using 4′,6-diamidino-2-phenylindole (DAPI) fluorescent dye (Invitrogen). Images were taken by a laser scanning confocal microscope (Zeiss, Jena, Germany).

Determination of Cell Proliferation

The proliferation of cells growing on plastic or nanofibers was determined according to [^{3}H]thymidine incorporation. The cells (50×10^3/well/700 μl of culture medium) were seeded into the wells of 24-well tissue culture plates (Corning) with or without inserts containing nanofibers. The plates were incubated for 24 or 48 h and cell proliferation was determined by adding [^{3}H]thymidine (3 μCi/well, Nuclear Research Institute) for the last 6 h of the incubation period. The radioactivity incorporated in cells growing on plastic or nanofibers was measured using a Tri-Carb 2900TR scintilation counter (Packard, Meridien, CT).

Determination of Metabolic Cell Activity

The metabolic activity of living cells was determined by the WST assay. The assay is based on the ability of living cells to cleave by mitochondrial dehydrogenases tetrazolium salts into water soluble formazan, which is then measured by spectrophotometry. Fifty thousand cells in 700 μl of RPMI-1640 culture medium were cultured in the wells of 24-well tissue culture plate (Corning) with or without inserts containing nanofibers for 24 h at 37°C in an atmosphere of 5% CO_2. WST-1 reagent (Roche, Mannheim, Germany) (10 μl/100 μl of the medium) was added to each well, and the plates were incubated for another 4 h to form formazan. Formazan-containing medium (100 μl) was transferred from each well into the wells of a 96-well tissue culture plate (Corning) and the absorbance was measured using a Sunrise Remote ELISA Reader (Grödig, Austria) at a wavelength of 450 nm.

A Model of the Damaged Ocular Surface and Cell Transfers

The recipient BALB/c mice were deeply anesthetized by an intramuscular injection of a mixture of xylazine and ketamine (Rometar, Spofa, Prague, Czech Republic). The surface (corneal region) of the right eye was damaged by epithelial debridement with a sharp needle (G23) and the limbus was cut out with Vannas scissors (Duckworth and Kent, Baldock, UK). To induce a stronger immune reaction in the anterior segment of the eye, an allogeneic limbus from C57BL/6 donors was grafted orthotopically to the recipients with a removed limbus according to the technique of Maruyama et al. (17). A 4-mm-diameter nanofiber circle (with or without SCs) was used to cover the limbal and corneal region and was sutured with four interrupted sutures using 11.0 Ethilon (Ethicon, Johnson & Johnson, Livingston, England) on the damaged ocular surface. The nanofibers with growing cells were transferred with the cell side facing down towards the ocular surface. For the cell transfer, equal numbers of LSCs and MSCs growing on the nanofiber scaffold were transferred, approximately 4×10^4 cells of each type. The eyelids were closed by tarsorhapy using one suture of Resolon 7.0 (Resorba, Nuremberg, Germany) for 72 h. An ophthalmic ointment compound containing bacitracin and neomycin (Ophthalmo-Framykoin, Zentiva, Prague, Czech Republic) was applied on the ocular surface for 3 days. The nanofiber scaffolds were removed from the ocular surface on day 3 after the operation.

To trace the fate and survival of LSCs after their

transfer onto the ocular surface, the cells were labeled with the fluorescent vital dye PKH26 (PKH26 Red Fluorescent Cell Linker Kit, Sigma) according to the instructions of the manufacturer, cultured for 24 h on a nanofiber scaffold, and transferred on the damaged eye surface as described above. The recipients were killed 2, 7, or 14 days after cell transfer and the whole globes were dissected and placed for 1 h into 4% paraformaldehyde. Then the globes were transferred into a 15% sucrose solution in PBS for 24-h fixation; subsequently, cryosections at a thickness of 7 μm were prepared using a Leica CM 3050 S cryostat (Leica, Wetzlar, Germany). The nuclei were stained with DAPI. The presence of stained cells was analyzed using a fluorescent microscope.

Determination of Inflammatory Reaction by Real-Time PCR

The expression of genes for IL-2 and IFN-γ and for inducible nitric oxide synthase (iNOS) in cells from the ocular surface was detected by real-time PCR. The whole ocular surface (including the cornea and limbal region) was removed using Vannas scissors on day 7 after the operation and transferred into Eppendorf tubes containing 200 μl of TRI Reagent (Molecular Research Center, Cincinnati, OH). Total RNA was extracted using TRI Reagent according to the manufacturer's instructions. Total RNA (2 μg) was treated using deoxyribonuclease I (Sigma) and used for subsequent reverse transcription. The first-strand cDNA was synthesized using random hexamers (Promega, Madison, WI) in a total reaction volume of 25 μl using M-MLV Reverse Transcriptase (Promega). Quantitative real-time PCR was performed in an iCycler (BioRad, Hercules, CA) using the primers described in Table 1. iQ SYBR Green Supermix (BioRad) was used in all experiments. The PCR parameters included denaturation at 95°C for 3 min, then 40 cycles at 95°C for 20 s, annealing at 60°C for 30 s, and elongation at 72°C for 30 s. Fluorescence data were collected at each cycle after an elongation step at 80°C for 5 s and were analyzed on the iCycler Detection system, Version 3.1. Each single experiment was done in triplicate. The relative quantification model was applied to calculate the expression of the target gene in comparison to GAPDH used as an endogenous control.

Statistical Analysis

Analysis of data showed normal distribution and the results are expressed as mean ± SE. Comparisons between two groups were analyzed by Student *t*-test, and multiple comparisons were analyzed by ANOVA followed by Bonferroni post hoc test. A value of $p < 0.05$ was considered statistically significant.

RESULTS

Comparison of Metabolic Activity and Growth Properties of Cells Growing on PA6/12 Nanofibers or on Plastic Surfaces

LSCs, MSCs, and corneal epithelial or corneal endothelial cells were grown for 24 or 48 h on nanofibers (fixed in inserts) or on a plastic surface in 24-well tissue culture plates and their metabolic and proliferative activities were determined. As demonstrated in Figure 1, all four cell types had comparable metabolic activities and proliferative capacities irrespective of whether they grew on the plastic surface or on nanofibers. The growth of LSCs and MSCs on nanofibers was confirmed when the metabolic activity that corresponds to the number of living cells was determined at different time intervals. As shown in Figure 2, the metabolic activity of SCs gradually increased during the 48-h incubation period.

The Morphology of Cells Growing on Nanofibers

The shape of the cells and the organization of the actin cytoskeleton of LSCs growing on PA6/12 nanofibers were compared with those of cells growing on plastic surfaces. Figure 3 shows that the shape of the cells and the organization and thickness of the actin filaments formed in adherent cells were comparable between cells growing on nanofibers and plastic surfaces. Confocal and electron microscopy showed the penetration of LSCs into the nanofibrous structure and the growth of pseudopodia among the nanofibers (data not shown).

Transfer of LSCs and MSCs Using Nanofiber Scaffolds Onto the Damaged Ocular Surface

To prove that LSCs can be transferred using a nanofiber scaffold onto the ocular surface and that they can subsequently migrate from the scaffold onto the dam-

Table 1. Mouse Primer Sequences Used for Real-Time PCR

Gene	Sense Primer	Antisense Primer
GADPH	AGAACATCATCCCTGCATCC	ACATTGGGGGTAGGAACAC
IL-2	GCTGTTGATGGACCTACAGGA	TTCAATTCTGTGGCCTGCTT
IFN-γ	ATCTGGAGGAACTGGCAAAA	TTCAAGACTTCAAAGAGTCTGAGG
iNOS	CTTTGCCACGGACGAGAC	TCATTGTACTCTGAGGGCTGAC

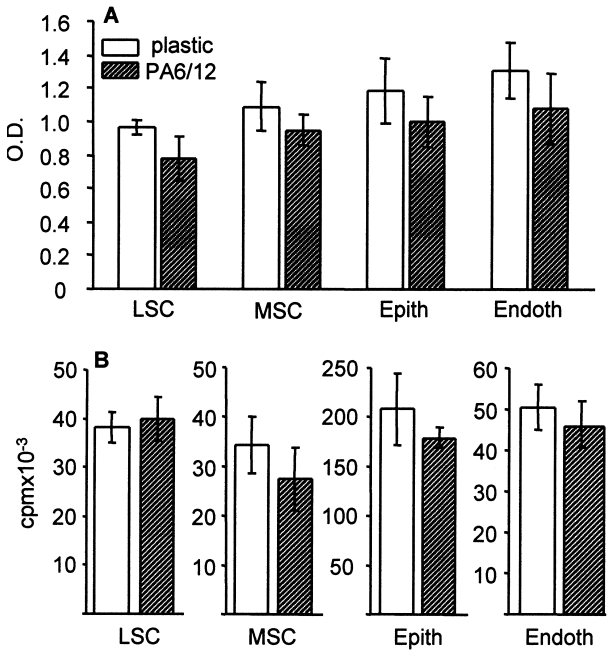

Figure 1. Metabolic and proliferative activities of LSCs, MSCs, and corneal epithelial and corneal endothelial cells growing on plastic or nanofibers. The same number of cells was seeded on plastic (24-well tissue culture plate) or PA6/12 nanofibers fixed in inserts. (A) The metabolic activity was determined by adding WST-1 reagent to the cultures for the last 4 h of a 24-h incubation period. (B) The proliferative activity was determined by adding [^{3}H]thymidine into the culture medium for the last 6 h of a 24-h incubation period. Each bar represents the mean ± SE from three to four determinations.

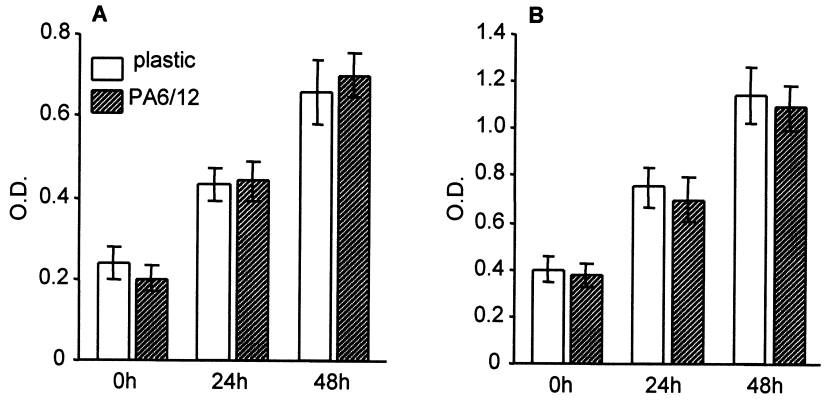

Figure 2. Comparison of the growth of LSCs and MSCs on plastic or nanofibers. Equal numbers of MSCs (A) or LSCs (B) were seeded into the wells of a 24-well tissue culture plate or onto PA6/12 nanofibers fixed in inserts and the metabolic activity of the living cells was determined at the beginning of culture (0 h) and after 24- or 48-h incubation. Each bar represents the mean ± SE from three determinations.

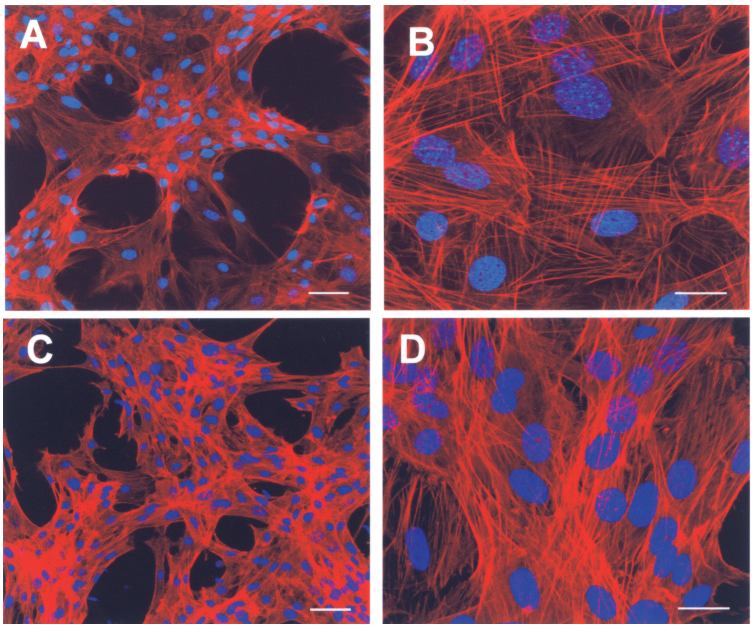

Figure 3. The morphology of LSCs growing on a glass surface or on PA6/12 nanofibers. The cells were cultured for 24 h on poly-L-lysine-coated glass inserts in 24-well tissue culture plates or on nanofibers fixed in inserts and were stained for F-actin with phalloidin (red filaments). The nuclei are blue (DAPI staining). (A, B) LSCs growing on the glass surface at two different magnifications. (C, D) LSCs growing on nanofiber scaffolds. Scale bars: (A, C) 50 μm; (B, D) 20 μm.

aged ocular surface, we labeled LSCs with the fluorescent dye PKH26, cultured them on PA6/12 nanofibers, and transferred them onto the damaged ocular surface. The globes were harvested at different time intervals after cell transfer and cryosections were prepared. As demonstrated in Figure 4, PKH26-labeled cells were clearly detected on the ocular surface on days 2, 7, and 14 after cell transfer.

Suppression of a Local Inflammatory Reaction by LSCs and MSCs

First, we demonstrated the immunosuppressive properties of MSC in vitro. Mouse spleen cells were stimulated with the T-cell mitogen Con A in the presence or absence of MSCs. As demonstrated in Figure 5, MSCs inhibited cell proliferation (Fig. 5A) and IFN-γ production (Fig. 5B) in a dose-dependent manner. No immunosuppression was observed if LSCs were used instead of MSCs, and the suppression by MSCs was preserved if MSCs were tested in a mixture with LSCs (data not shown).

To demonstrate the suppression of a local inflammatory reaction by the transfer of LSCs and MSCs in vivo, two models of ocular surface damage and treatment were used. In the first model, the ocular surface was mechanically damaged. The second model combined mechanical damage and the transplantation of allogeneic limbus. In the healthy, nondamaged eye, no detectable expression of IL-2, IFN-γ, or iNOS genes was found. The mechanical injury induced a moderate inflammatory reaction associated with the production of IFN-γ and iNOS. This response was inhibited after the transfer of nanofibers containing LSCs and MSCs (data not shown). The ocular surface damage associated with orthotopic limbal allotransplantation induced a strong inflammatory reaction characterized by the expression of the IL-2, IFN-γ, and iNOS genes (Fig. 6). This reaction was slightly inhibited by covering the eye surface with cell-free nanofibers and was significantly attenuated after the transfer of LSCs and MSCs growing on nanofiber scaffold (Fig. 6).

DISCUSSION

A growing body of recent studies has shown that electrospun nanofibers of various polymers allow the adhesion, proliferation, metabolic activity, morphology,

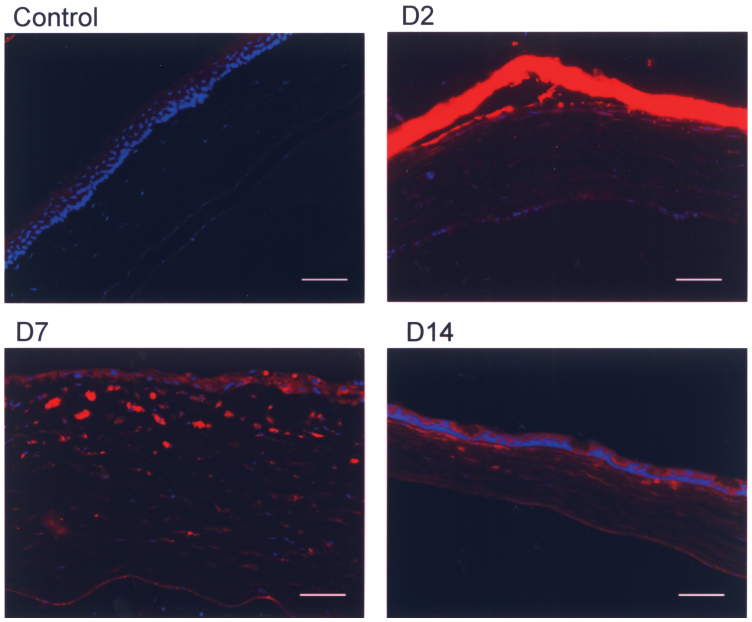

Figure 4. Detection of PKH26-labeled LSCs on the damaged ocular surface after their transfer on a PA6/12 nanofiber scaffold. LSCs were labeled with PKH26 and cultured for 24 h on nanofibers fixed in inserts. The nanofibers with cells were transferred and fixed (with the cell side facing down) for 3 days on the damaged ocular surface. The globes were removed 2, 7, or 14 days after the operation and 7-μm cryosections were prepared. The nuclei were vizualized with DAPI. The cryosections were prepared (A) from the control undamaged eye (without labeled cells), (B) from the eye 2 days after operation (the nanofiber scaffold with labeled LSCs is seen as a red lane, corneal epitheliun is removed), and from the eyes 7 (C) and 14 (D) days after the cell transfer (red stained cells are still present, the corneal epithelium is regenerated). Scale bars: 50 μm.

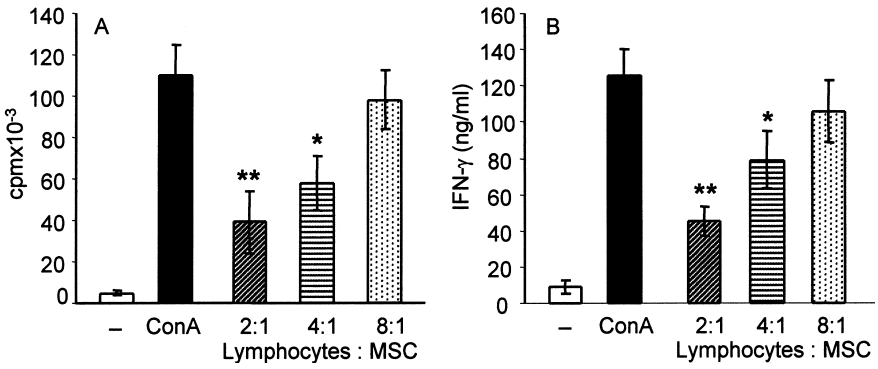

Figure 5. Immunosuppressive properties of MSCs in vitro. Spleen cells from BALB/c mice were cultured either unstimulated or stimulated with Con A (1.0 μg/ml) in the presence or absence of MSCs (at a ratio of 2:1, 4:1, or 8:1). Cell proliferation (A) was determined by [^{3}H]thymidine incorporation after a 72-h incubation period, the production of IFN-γ (B) was measured by ELISA in the supernatants after a 48-h incubation period. Each bar represents the mean ± SE from three experiments. *$p < 0.01$, **$p < 0.001$.

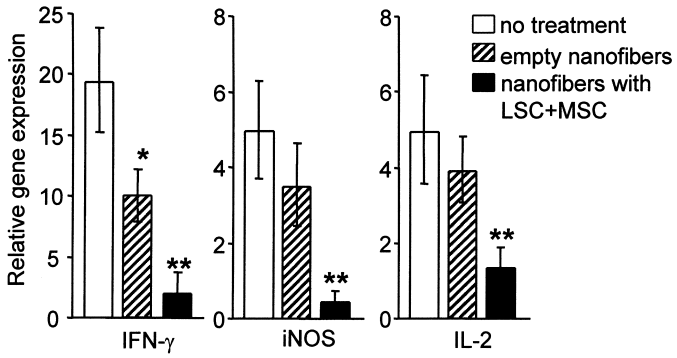

Figure 6. Suppression of the local inflammatory reaction after the transfer of LSCs and MSCs on a nanofiber scaffold. The inflammatory reaction was induced on ocular surface by epithelial debridement and orthotopic limbal allotransplantation. The ocular surface then remained untreated, covered with nanofibers without cells or covered with nanofibers with LSCs and MSCs. On day 7 after cell transfer the ocular surface was removed and the expression of genes for IL-2, IFN-γ, and iNOS was determined by real-time PCR. The comparative Ct method was used to determine the extent of the targeted gene expression normalized to an internal GAPDH control. Each bar represents the mean ± SE from three experiments (two mice in each experiment). $*p < 0.05$ in comparison to uncovered damaged eyes, $**p < 0.001$ in comparison to damaged eyes covered with cell-free (empty) nanofibers.

and organized assembly of different cell types in vitro (2,5,18,25,35). The constructs formed by nanofiber scaffolds and specialized cells have been suggested as perspective and promising tools for tissue engineering (14,15). However, the performance and behavior of nanofibrous materials in vivo are not well understood. Only scarce recent data are available to demonstrate the usefulness of nanofiber scaffolds in vivo.

We described here the preparation of electrospun nanofibers and their use as a scaffold to grow and transfer LSCs and MSCs to treat ocular surface injuries and SC deficiencies. The nanofibers were prepared by the original needleless Nanospider technology, which enables the creation of nanofibers from various polymers and of defined fiber diameter, porosity, and a basis weight. From a large panel of polymers tested in our pilot experiments, we selected copolymer PA6/12. This polymer turned out to be sufficiently biocompatible, forming nanofibers stable in aqueous solutions and suitable for the growth of limbal and mesenchymal SCs. In addition, differentiated corneal epithelial and endothelial cells were grown on PA6/12 nanofibers and their metabolic and proliferative activities were comparable with those of the same cells grown on plastic surfaces.

We have made a successful attempt to use the nanofiber scaffolds for the transfer of LSCs to treat ocular surface injuries or LSC deficiencies in an experimental mouse model. The limbus represents the region in the eye where SCs reside that are responsible for corneal renewal and repair (4,31). We have recently shown that the cells obtained by trypsinization of limbal tissue express the markers and characteristics of LSCs and that these cells can be propagated in vitro in tissue culture (13). Here we have shown that LSCs can be cultured on a polyamide nanofiber scaffold and that their proliferation, metabolic activity, and morphology when grown on nanofibers are comparable with those of cells grown on plastic surfaces. In addition, we have shown that LSCs growing on a nanofiber scaffold can be successfully transferred onto the damaged ocular surface. So far, human amniotic membranes have been used most frequently as a matrix for the growth and transfer of LSCs for therapeutic purposes (26,30). In spite of the use of human allogeneic amniotic material as a scaffold of LSCs for the reconstruction of the ocular surface, the beneficial effects of LSC transplantation have been reported (22). The use of biocompatible synthetic polymers for the preparation of nanofiber scaffolds for the growth and transfer of LSC would have apparent advantages.

We are aware that the limbal cell population that we transferred using the nanofiber scaffold was not a pure SC population. The population contained also differentiated cells originating from LSCs and other cell types of the LSC niche. Analysis of the gene expression of the transferred cells revealed that this cell population contained both differentiated epithelial cells (expressing CK12 and connexin 43) and cells expressing the putative LSC markers ABCG2, p63, and Lgr5 [(13), and unpublished data]. However, such a cultured population of

limbal epihelial cells is generally referred to as LSCs, and their therapeutic potential in the treatment of LSC deficiencies has been documented (22,32).

In addition to LSCs, we also grew on nanofiber scaffolds MSCs, which can differentiate to various cell types including corneal epithelial cells (8,19,23) and that have the ability to inhibit immunological reactions (1,6). We confirmed the immunosuppressive effects of MSCs in vitro by the inhibition of T-lymphocyte proliferation and by the suppression of cytokine production. It has been shown that the transfer of MSCs onto the damaged eye can support the healing process, but the effects of MSCs were attributed to the ability of MSCs to inhibit inflammatory reactions (15,21). In our experiments we cocultured LSCs and MSCs on nanofiber scaffolds and transferred them onto the damaged ocular surface where a local inflammatory reaction characterized by the expression of genes for IL-2, IFN-γ, and iNOS was induced by epithelial debridement and limbal allotransplantation. Analysis of the gene expression in tissue harvested from the damaged ocular surface 1 week after the injury showed that there was a significant suppression of the gene expression of the inflammatory proteins IL-2, IFN-γ, and iNOS, suggesting that the MSCs suppress the inflammatory reaction. This suggestion is supported by previous data showing that MSCs applied to the ocular surface can inhibit the local inflammatory reaction (15,21).

It has been demonstrated previously that embryonic SCs can be grown, propagated, and differentiated on nanofibers (20,28). Our results suggest that nanofiber scaffolds prepared from PA6/12 by electrospinning technology can serve as a convenient matrix for the growth of adult tissue-specific SCs and for their transfer to treat ocular surface injuries. Studies are in progress to test the survival and propagation of cells in terms of the persistance of SC markers and characteristics during their growth on nanofiber scaffolds and to monitor the presence of LSCs after their transfer onto the ocular surface in experimental LSC deficiency models.

ACKNOWLEDGMENTS: This work was supported by grant KAN200520804 from the Grant Agency of the Academy of Sciences, grant 310/08/H077 from the grant Agency of the Czech Republic, projects 1M0506 and MSM0021620858 from the Ministry of Education of the Czech Republic, and project AVOZ50520514 from the Academy of Sciences of the Czech Republic.

REFERENCES

1. Aggarwal, S.; Pittenger, M. F. Human mesenchymal stem cells modulate allogeneic immune cell responses. Blood 105:1815–1818; 2005.
2. Bhattarai, N.; Edmondson, D.; Veiseh, O.; Matsen, F. A.; Zhang, M. Electrospun chitosan-based nanofibers and their cellular compatibility. Biomaterials 26:6176–6184; 2005.
3. Caplan, A. I.; Bruder, S. P. Mesenchymal stem cells: Building blocks for molecular medicine in the 21st century. Trends Mol. Med. 7:259–264; 2001.
4. Daniels, J. T.; Dart, J. K. G.; Tuft, S. J.; Khaw, P. T. Corneal stem cells in review. Wound Repair Regen. 9: 483–494; 2001.
5. Das, H.; Abdulhameed, N.; Joseph, M.; Sakthivel, R.; Mao, H.-Q.; Pompili, V. J. Ex vivo nanofiber expansion and genetic modification of human cord blood-derived progenitor/stem cells enhances vasculogenesis. Cell Transplant. 18:305–318; 2009.
6. Di Nicola, M.; Carlo-Stella, G.; Magni, M.; Milanesi, M.; Londoni, P. D.; Matteucci, P.; Grisanti, S.; Giammi, A. M. Human bone marrow stroma cells suppress T-lymphocyte proliferation induced by cellular and nonspecific mitogenic stimuli. Blood 99:3838–3843; 2002.
7. Dubios, G.; Segers, V. F.; Bellamy, V.; Sabbah, L.; Peyrard, S.; Bruneval, P.; Hagege, A. A.; Lee, R. T.; Menasche, P. Self-assembling peptide nanofibers and skeletal myoblast transplantation in infarcted myocardium. J. Biomed. Mater. Res. B Appl. Biomater. 87:222–228; 2008.
8. Gu, S.; Xing, C.; Han, J.; Tso, M. O. M.; Hong, J. Differentiation of rabbit bone marrow mesenchymal stem cells into corneal epithelial cells in vivo and ex vivo. Mol. Vis. 15:99–107; 2009.
9. Hall, P. A.; Watt, P. M. Stem cells: The regeneration and maintenance of cellular diversity. Development 106:619–633; 1989.
10. Hashemi, S. M.; Soleimani, M.; Zargarian, S. S.; Haddadi-Asi, V.; Ahmadbeigi, N.; Soudi, S.; Gheisari, Y.; Hajarizadeh, A.; Mohammedi, V. In vitro differentiation of human cord blood-derived unrestricted stem cells into hepatocyte-like cells on poly(ypsilon-caprolactone) nanofiber scaffolds. Cells Tissues Organs 190:135–149; 2009.
11. He, Y. G.; Mellon, J.; Niederkorn, J. Y. The effect of oral immunization on corneal allograft survival. Transplantation 61:920–926; 1996.
12. Kortison, S. J.; Shah, N. M.; Anderson, D. J. Regulatory mechanisms in stem cell biology. Cell 88:287–298; 1997.
13. Krulova, M.; Pokorna, K.; Lencova, A.; Zajicova, A.; Fric, J.; Filipec, M.; Forrester, J. V.; Holan, V. A rapid separation of two distinct populations of corneal epithelial cells with limbal stem cell characteristics in the mouse. Invest. Ophthalmol. Vis. Sci. 49:3903–3908; 2008.
14. Li, W. J.; Tuli, R.; Okafor, C.; Derfoul, A.; Danielson, K. G.; Hall, D. J.; Tuan, R. S. A three-dimensional nanofibrous scaffold for cartilage tissue engineering using human mesenchymal stem cells. Biomaterials 26:599–609; 2005.
15. Ma, Y.; Xu, Y.; Xiao, Y.; Yang, W.; Zhang, C.; Song, E.; Du, Y.; Li, L. Reconstruction of chemically burned rat cornea surface by bone marrow-derived human mesenchymal stem cells. Stem Cells 24:315–321; 2006.
16. Ma, Z.; Kotaki, M.; Inai, R.; Ramakrishna, S. Potential of nanofiber matrix as tissue-engineering scaffolds. Tissue Eng. 11:101–109; 2005.
17. Maruyama, K.; Yamada, J.; Sano, Y.; Kinoshita, S. Th2-biased immune system promotion of allogeneic corneal epithelial cell survival after orthotopic limbal transplantation. Invest. Ophthalmol. Vis. Sci. 44:4736–4743; 2003.
18. Min, B.-M.; Lee, G.; Kim, S. H.; Nam, Y. S.; Lee, T. S.; Park, W. H. Electrospinning of silk fibroin nanofibers and its effect on the adhesion and spreading of normal human keratinocytes and fibroblasts in vitro. Biomaterials 25: 1289–1297; 2004.
19. Neuss, S.; Stainforth, R.; Salber, J.; Schneck, P.; Bovi, M.; Knüchel, R.; Perez-Bouza, A. Long-term survival and

bipotent terminal differentiation of human mesenchymal stem cells (hMSC) in combination with a commercially available three-dimensional collagen scaffold. Cell Transplant. 17:977–986; 2008.
20. Nur-E-Kamal, A.; Ahmed, I.; Kamal, J.; Schindler, M.; Meiners, S. Three-dimensional nanofibrillar surfaces promote self-renewal in mouse embryonic stem cells. Stem Cells 24:426–433; 2006.
21. Oh, J. Y.; Kim, M. K.; Shin, M. S.; Lee, H. J.; Ko, J. H.; Wee, W. R.; Lee, J. H. The anti-inflammatory and anti-angeogenic role of mesenchymal stem cells in corneal wound healing following chemical injury. Stem Cells 26: 1047–1055; 2008.
22. Pellegrini, G.; Traverso, C. E.; Franzi, A. T.; Zingirian, M.; Cancedda, R.; De Luca, M. I. Long-term restoration of damaged corneal surface with autologous cultivated corneal epithelium. Lancet 349:990–993; 1997.
23. Pittenger, M. F.; Mackay, A. M.; Beck, S. C.; Jaiswal, R. K.; Souhlas, R.; Mosca, J. D.; Moorman, M. A.; Simonetti, D. W.; Craig, S.; Marshak, D. R. Multilineage potential of adult human mesenchymal stem cells. Science 284:143–147; 1999.
24. Rama, P.; Bonini, S.; Lambiase, A.; Golisano, O.; Paterna, P.; De Luca, M.; Pellegrini, G. Autologous fibrin-cultured limbal stem cells permanently restore the corneal surface of patients with total limbal stem deficiency. Transplantation 72:1478–1485; 2001.
25. Schindler, M.; Ahmed, I.; Kamal, J.; Nur-E-Kamal, A.; Grafe, T. H.; Zouny Chung, H.; Meiners, S. A synthetic nanofibrillar matrix promotes in vivo-like organization and morphogenesis for cells in culture. Biomaterials 26: 5624–5631; 2005.
26. Schwab, I. R.; Johnson, N. T.; Harkim, D. G. Inherent risks associated with manufacture of bioengineered ocular surface tissue. Arch. Ophthalmol. 124:1734–1740; 2006.
27. Shin, Y. R.; Chen, C. N.; Tsai, S. W.; Wang, Y. J.; Lee, O. K. Growth of mesenchymal stem cells on electrospun type I collagen nanofibers. Stem Cells 24:2391–2397; 2006.
28. Smith, L. A.; Liu, X.; Hu, J.; Wang, P.; Ma, P. X. Enhancing osteogenic differentiation of mouse embryonic stem cells by nanofibers. Tissue Eng. Part A 15:1855–1864; 2009.
29. Sykova, E.; Jendelova, P.; Urdzikova, L.; Lesny, P.; Hejcl, A. Bone marrow stem cells and polymer hydrogels—two strategies for spinal cord injury repair. Cell. Mol. Neurobiol. 25:1113–1129; 2006.
30. Tsai, R. J.; Li, L. M.; Chen, J. K. Reconstruction of damaged cornea by transplantation of autologous limbal epithelial cells. N. Engl. J. Med. 343:86–93; 2000.
31. Tseng, S. C. Regulation and clinical implication of corneal epithelial stem cells. Mol. Biol. Rep. 23:47–58; 1996.
32. Tsubota, K.; Satake, Y.; Kaido, M.; Shinozaki, N.; Shimmura, S.; Bissen-Miyajima, H.; Shimazaki, J. Treatment of severe ocular-surface disorders with corneal epithelial stem-cell transplantation. N. Engl. J. Med. 340:1697–1703; 1999.
33. Xie, J.; Willerth, S. M.; Li, X.; Macewan, M. R.; Rader, A.; Sakiyama-Elbert, S. E.; Xioa, Y. The differentiation of embryonic stem cells seeded on electrospun nanofibers into neural lineages. Biomaterials 30:354–362; 2009.
34. Xin, X.; Hussain, M.; Mao, J. J. Continuing differentiation of human mesenchymal stem cells and induced chondrogenic and osteogenic lineages in electrospun PLGA nanofiber scaffold. Biomaterials 28:316–325; 2007.
35. Yoshimoto, H.; Shin, Y. M.; Terai, H.; Vacanti, J. P. A biodegradable nanofiber scaffold by electrospinning and its potential for bone tissue engineering. Biomaterials 24: 2077–2082; 2003.

8.4 Publication 4

Suppression of alkali-induced oxidative injury in the cornea by mesenchymal stem cells growing on nanofiber scaffolds and transferred onto the damaged corneal surface

Cejkova J, Trosan P, Cejka C, Lencova A, Zajicova A, Javorkova E, Kubinova S, Sykova E, Holan V

Exp Eye Res. 2013 Nov;116:312-23. (IF 3.017)

Experimental Eye Research 116 (2013) 312–323

Contents lists available at ScienceDirect

Experimental Eye Research

journal homepage: www.elsevier.com/locate/yexer

Suppression of alkali-induced oxidative injury in the cornea by mesenchymal stem cells growing on nanofiber scaffolds and transferred onto the damaged corneal surface

Jitka Cejkova [a,*], Peter Trosan [a,b], Cestmir Cejka [a,c], Anna Lencova [d], Alena Zajicova [a], Eliska Javorkova [a,b], Sarka Kubinova [a], Eva Sykova [a], Vladimir Holan [a,b]

[a] Institute of Experimental Medicine, Laboratory of Eye Histochemistry and Pharmacology, Academy of Sciences of the Czech Republic, Videnska 1083, 14220 Prague 4, Czech Republic
[b] Faculty of Natural Science, Charles University in Prague, Vinicna 7, 128 43 Prague 2, Czech Republic
[c] Czech Technical University in Prague, Faculty of Biomedical Engineering, Sítná 3105, 272 01 Kladno 2, Czech Republic
[d] European Eye Clinic Lexum, Antala Staska 1670/80, 14000 Prague 4, Czech Republic

ARTICLE INFO

Article history:
Received 29 May 2013
Accepted in revised form 3 October 2013
Available online 18 October 2013

Keywords:
alkali-induced oxidative stress
rabbit cornea
rabbit mesenchymal stem cells
central corneal thickness
immunohistochemistry
real-time PCR

ABSTRACT

The purpose of this study was to investigate whether rabbit bone marrow-derived mesenchymal stem cells (MSCs) effectively decrease alkali-induced oxidative stress in the rabbit cornea. The alkali (0.15 N NaOH) was applied on the corneas of the right eyes and then rinsed with tap water. In the first group of rabbits the injured corneas remained untreated. In the second group MSCs were applied on the injured corneal surface immediately after the injury and eyelids sutured for two days. Then the sutures were removed. In the third group nanofiber scaffolds seeded with MSCs (and in the fourth group nanofibers alone) were transferred onto the corneas immediately after the injury and the eyelids sutured. Two days later the eyelid sutures were removed together with the nanofiber scaffolds. The rabbits were sacrificed on days four, ten or fifteen after the injury, and the corneas were examined immunohistochemically, morphologically, for the central corneal thickness (taken as an index of corneal hydration) using an ultrasonic pachymeter and by real-time PCR. Results show that in untreated injured corneas the expression of malondialdehyde (MDA) and nitrotyrosine (NT) (important markers of lipid peroxidation and oxidative stress) appeared in the epithelium. The antioxidant aldehyde dehydrogenase 3A1 (ALDH3A1) decreased in the corneal epithelium, particularly in superficial parts, where apoptotic cell death (detected by active caspase-3) was high. (In control corneal epithelium MDA and NT are absent and ALDH3A1 highly present in all layers of the epithelium. Cell apoptosis are sporadic). In injured untreated cornea further corneal disturbances developed: The expressions of matrix metalloproteinase 9 (MMP9) and proinflammatory cytokines, were high. At the end of experiment (on day 15) the injured untreated corneas were vascularized and numerous inflammatory cells were present in the corneal stroma. Vascular endothelial growth factor (VEGF) expression and number of macrophages were high. The results obtained in injured corneas covered with nanofiber scaffolds alone (without MSCs) or in injured corneas treated with MSCs only (transferred without scaffolds) did not significantly differ from the results found in untreated injured corneas. In contrast, in the injured corneas treated with MSCs on nanofiber scaffolds, ALDH3A1 expression remained high in the epithelium (as in the control cornea) and positive expression of the other immunohistochemical markers employed was very low (MMP9) or absent (NT, MDA, proinflammatory cytokines), also similarly as in the control cornea. Corneal neovascularization and the infiltration of the corneal stroma with inflammatory cells were significantly suppressed in the injured corneas treated with MSCs compared to the untreated injured ones. The increased central corneal thickness together with corneal opalescency appearing after alkali injury returned to normal levels over the course of ten days only in the injured corneas treated with MSCs on nanofiber scaffolds. The expression of genes for the proinflammatory cytokines corresponded with their immunohistochemical expression. In conclusion, MSCs on nanofiber scaffolds protected the formation of toxic peroxynitrite

* Corresponding author. Tel.: +420 2 241062208; fax: +420 2 241062692.
E-mail address: cejkova@biomed.cas.cz (J. Cejkova).

0014-4835/$ – see front matter
http://dx.doi.org/10.1016/j.exer.2013.10.002

(detected by NT residues), lowered apoptotic cell death and decreased matrix metalloproteinase and pro-inflammatory cytokine production. This resulted in reduced corneal inflammation as well as neovascularization and significantly accelerated corneal healing.

1. Introduction

Alkali injury to the cornea very often causes severe ocular damage resulting in impaired vision. Although more concentrated alkalis are dangerous to the cornea due to the extensive destruction of all its layers, less concentrated alkalis also pose a threat to vision because oxidative stress is a direct result of such injury (Kubota et al., 2011). Oxidative stress is characterized by an increased production of reactive oxygen species (ROS) and/or by a significant decrease in the effectiveness of antioxidant protective mechanisms. Kubota et al. (2011) found enhanced ROS production immediately after an alkali injury in the mouse cornea, as shown by increased dihydroethidium fluorescence indicative of superoxide production and increased levels of nuclear factor kappa-light-chain-enhancer of activated B cells, a protein complex that controls the transcription of DNA. Also, monocyte chemoattractant protein-1 and vascular endothelial growth factor (VEGF) were significantly enhanced, pointing to corneal angiogenesis. Immediate antioxidant therapy of the alkali-injured cornea with H_2-enriched irrigation solution facilitated corneal healing (Kubota et al., 2011).

In this study, we demonstrate the suppression of oxidative injury to the rabbit cornea evoked by alkali using bone marrow mesenchymal stem cells (MSCs) growing on nanofiber scaffolds and transferred onto the alkali-injured corneal surface. Recently, increasing evidence has indicated that MSCs, possessing immunomodulatory and anti-inflammatory properties, can regenerate tissues (e.g., Oh et al., 2010; Zajicova et al., 2010; Joyce et al., 2012; Lan et al., 2012; Pinnamaneni and Funderburgh, 2012; Svobodova et al., 2012). To our knowledge, this is the first study using MSCs for the healing of alkali-induced oxidative stress in the cornea, although MSCs have been described as enabling corneal healing after alkali burns (Ma et al., 2005; Ye et al., 2006, 2008; Arnalich-Montiel et al., 2008; Jiang et al., 2010; Yao et al., 2012). Moreover, the novelty of this study consists in the use of nanofibers as scaffolds for MSC transplantation onto the alkali-injured cornea.

2. Material and methods

2.1. Alkali injuries in experimental animals

Adult female New Zealand white rabbits (2.5–3.0 kg) were used in our experiments. The investigation was conducted according to the ARVO Statement on the Use of Animals in Ophthalmic and Vision Research. Rabbits were anesthetized by an intramuscular injection of Rometar (Xylazinum hydrochloricum, Spofa, Prague, Ccech Republic, 2%, 0.2 ml/1 kg body weight) and Narkamon (Ketaminum hydrochloricum, Spofa, 5%, 1 ml/1 kg body weight).

The right corneas of anesthetized rabbits were injured by dropping 0.15 N NaOH on the corneal surface for 1 min (15 drops, alkali injured the whole cornea including the limbal region), then the eyes were thoroughly rinsed with tap water. The rabbits were divided into four groups. In each experimental group six corneas were investigated. In the first group of rabbits the injured corneas were left without any treatment. In the second group MSCs were applied on the corneal surface and eyelids closed by tarsorhapy using 1 suture of Resolon 7.0 (Resorba, Nuremberg, Germany). After two days the sutures were removed. In the third group nanofiber scaffolds seeded with MSCs were applied on the corneal surface (in the fourth group nanofiber scaffolds alone, without MSCs) and the scaffolds were sutured to the conjunctiva with four interrupted sutures using 11.0 Ethilon (Ethicon, Johnson & Johnson, Livingston, England). The eyelids were closed by tarsorhapy similarly as in the second group of animals. An ophthalmic ointment containing bacitracin and neomycin (Ophthalmo-Framykoin, Zentiva, Prague, Czech Republic) was applied on the sutures. Two days later the sutures and nanofiber scaffolds were removed.

During the experiments the corneas were examined for central corneal thickness using an ultrasonic pachymeter. The animals were sacrificed on days four, ten or fifteen after injury and corneas examined immunohistochemically, morphologically and using real-time PCR.

2.2. Isolation and culture of rabbit MSCs

MSCs were isolated from the bone marrow of adult New Zealand white rabbits and were cultured as described for mouse MSCs (Svobodova et al., 2012). In brief, the bone marrow from the femurs and tibias was flushed out, washed and cultured in Dulbecco's modified Eagle's (DMEM) medium (PAA Laboratories, Pasching, Austria) supplemented with 10% fetal calf serum (FCS, Sigma Co., St. Louis, MO), antibiotics (100 μg/ml of streptomycin, 100 U/ml of penicillin) and 10 mM Hepes buffer. The cells were cultured at a concentration of 4×10^6 cells/ml in 6 ml of culture medium in 25-cm^2 tissue culture flasks (Nunc, Roskilde, Denmark). After a 24-h incubation period the non-adherent cells were removed by washing, and the remaining adherent cells were cultured with a regular exchange of the culture medium and passaging of the cells to maintain an optimal cell concentration. After approximately 3 weeks of culture (2–3 passages) the cells were harvested by gentle scraping and used for transplantation onto the ocular surface. For topical administration, 100 μl media containing 1×10^6 MSCs was employed.

The rabbit MSCs used in our experiments were characterized according to their adherence to plastic surfaces, by a typical fibroblast-like cell morphology, by the expression of CD73, by the absence of CD11b, and by the ability to differentiate into adipogenic and osteogenic lineages (as we have described in details for mouse MSCs, in Svobodova et al., 2012).

2.3. Nanofiber scaffolds for transfer of MSCs

Nanofiber scaffolds were prepared from polymer poly(L-lactid acid) by the original needleless electrospinning procedure as described elsewhere (Zajicova et al., 2010; Holan et al., 2011). Nanofiber scaffolds were cut into squares (approximately 1.5 × 1.5 cm) and fixed into CellCrown™24 inserts (Scaffdex, Tampere, Finland). The inserts with nanofibers were sterilized and transferred into 24-well tissue culture plates (Corning, Schiphol-Rijk, Netherlands). One hundred thousand cells in a volume of 700 μl of culture medium with 10% FCS were transferred into each well. The cells were cultured on nanofiber scaffolds for 24 h. A 10-mm diameter nanofiber circle was cut out from the nanofiber scaffold and was used to cover the limbal and corneal region.

2.4. The measurement of central corneal thickness (taken as an index of corneal hydration)

The central corneal thickness of anesthetized animals was measured using an Ultrasonic Pachymeter SP-100 (Tomey Corporation, Noritake-Shinmachi, Nishi-ku, Nagoya, Japan) in the corneal center. The corneal thickness was measured in the same corneas before alkali injury (corneas of healthy eyes) and on day 2 and 10 after alkali injury. Every cornea was measured four times with the Pachymeter, and the mean value of the thickness and the standard deviation were computed.

2.5. Preparation of cryostat sections, immunohistochemical examinations

After sacrificing the animals on day four or ten after the injury, the eyes were enucleated and the anterior eye segments dissected out and quenched in light petroleum chilled with an acetone-dry ice mixture. Sections were cut on a cryostat and transferred to glass slides. Subsequently, the cryostat sections were fixed in acetone at 4 °C for 5 min. For the immunohistochemical localization of active caspase-3, ALDH3A1, NT, MDA, IL-8, IL-1 β, VEGF and macrophages, the following primary antibodies were used: mouse monoclonal (3CSP03) anti-human caspase-3 (Abcam, Cambridge, UK), mouse polyclonal anti-human ALDH3A1 (Abcam), monoclonal mouse anti-NT (Abcam), polyclonal goat anti-MDA (US Biological, Swampscott, MA), monoclonal mouse anti-IL-8 (Abcam, Cambridge, UK), monoclonal mouse anti-IL-1 β antibody (Abcam), monoclonal mouse anti-macrophage (Abcam) and monoclonal mouse anti-VEGF (Abcam). The binding of the primary antibodies was demonstrated using the HRP/DAB Ultra Vision detection system (Thermo Scientific, Fremont, CA), following the instructions of the manufacturer: hydrogen peroxide block (15 min), ultra V block (5 min), primary antibody incubation (60 min), biotinylated goat anti-mouse or donkey anti-goat (Santa Cruz Biotechnology, Santa Cruz, CA) secondary antibody incubation (10 min) and peroxidase-labeled streptavidin incubation (10 min). Visualization was performed using a freshly prepared DAB substrate-chromogen solution. Cryostat sections in which the primary antibodies were omitted from the incubation media served as negative controls. Some sections were counterstained with Mayer's hematoxylin. To confirm the specificity of the staining for nitrotyrosine, the antibody was incubated with 10 mM nitrotyrosine (Kooy et al., 1997). After the staining procedure, the samples were immediately examined using an Orthoplan Leitz light microscope equipped with a Leica DC 500 digital camera.

2.6. Corneal impression cytologies, immunohistochemical examination

Corneal epithelial cells were obtained using Millicell membranes (Millicell-CM, hydrophilic PTFE, Millipore Corporation, Billerica, MA, USA). For corneal cytology samples, the rabbit corneas of healthy eyes were used (not employed in other experiments) on which nanofiber scaffolds were transferred for one, two or three days. The samples were collected as described previously for conjunctival epithelial cells (Cejkova et al., 2008). Briefly: First, 0.4% oxybuprocaine hydrochloride (single drop) was instilled to the eye. (Corneal impression cytologies were also collected in sleeping intramuscularly anesthetized animals). To remove superficial corneal epithelial cells, strips of Millicell membrane were gently pressed for 5 s onto the corneal surface. The specimens (corneal cells on the Millicells) were stored at −80 °C until they were employed for immunohistochemical examination. The Millicell membranes with corneal epithelial cells were fixed in acetone for 1 min, released from the plastic holder, rinsed with PBS (phosphate buffered saline tablets, Sigma), placed cell side up on round 12 mm coverslips and then (after rinsing with PBS) permeabilised with 0.2% triton (Triton X 100, Sigma) in PBS. For the detection of the urokinase-type plasminogen activator and endothelial nitric oxide synthase, the following primary antibodies were used: Monoclonal mouse anti-u-PA Ab-1 (Neomarkers, Fremont, CA) and monoclonal mouse anti-human e-NOS (Biosciences, Sant Jose, CA). The binding of the primary antibodies was demonstrated using the HRP/DAB Ultra Vision detection system (Thermo Scientific, Fremont, CA) following the instructions of the manufacturer: hydrogen peroxide block (15 min), ultra V block

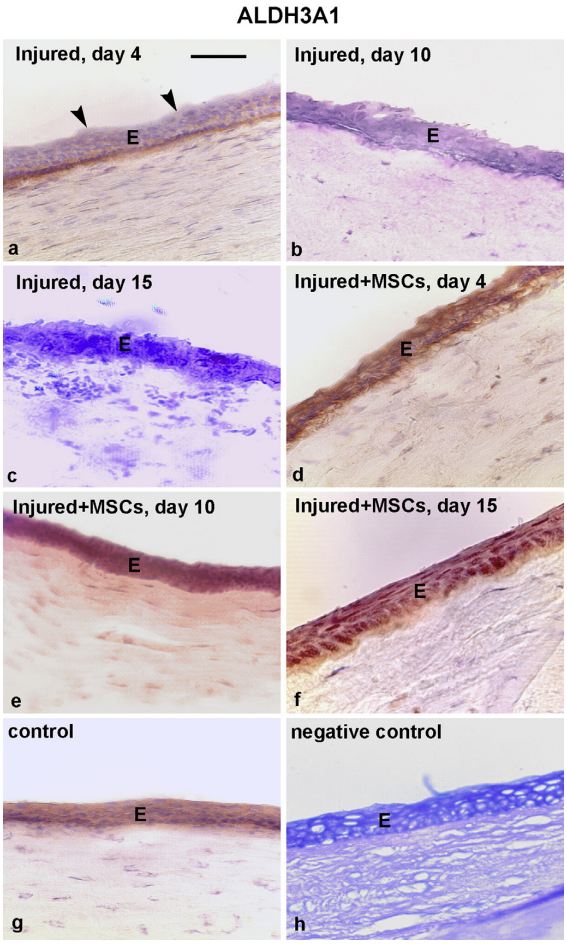

Fig. 1. Expression of ALDH3A1 in corneas on day 4, 10 and 15 after injury. E – corneal epithelium. Scale bar: 10 μM a – ALDH3A1 staining in an injured cornea is decreased in the corneal epithelium, mainly in superficial corneal layers (arrows). b – on day 10 and c – on day 15 after the injury the expression of ALDH3A1 gradually decreased. Compare with the expression of ALDH3A1 in the epithelium of an injured cornea treated with MSCs on nanofiber scaffolds, where it is high in all layers of the corneal epithelium from day 4 (d) to day 10 (e) and day 15 (f) after the injury, similarly as in the epithelium of control cornea (g). h – Using incubation medium from which the primary antibody was omitted, no positive staining is apparent. The section is stained by counterstaining only (as a negative control for ALSH3A1). All sections are counterstained with haematoxylin.

(5 min), primary antibody incubation (60 min), biotinylated goat anti-mouse (Santa Cruz Biotechnology) secondary antibody incubation (10 min) and peroxidase-labeled streptavidin incubation (10 min). Visualization was performed using a freshly prepared DAB substrate-chromogen solution.

Negative controls included the omission of the primary antibody. Some samples were counterstained with Mayers' hematoxylin (Sigma). After the staining procedure, the samples were immediately examined using an Orthoplan Leitz light microscope equipped with a Leica DC 500 digital camera.

For morphological examination, untreated injured corneas or injured corneas treated with MSCs of rabbits sacrificed on day fifteen after injury were examined by Haematoxylin-eosin staining. (Cryostat sections of the corneas were prepared similarly as for the immunohistochemical examinations).

2.7. Detection of gene expression by real-time polymerase chain reaction (PCR)

The expression of genes for the IL-1 β, IL-2, IFN-γ and VEGF in cells from control, alkali injured or injured and MSC-treated corneas was determined by quantitative PCR. The central cornea was excised using Vannas scissors and transferred into Eppendorf tubes containing 500 μl of TRI Reagent (Molecular Research Center, Cincinnati, OH). The details of RNA isolation, transcription and the PCR parameters have been described previously (Trosan et al., 2012). In brief, total RNA was extracted using TRI Reagent according to the manufacturer's instructions. One μg of total RNA was treated using deoxyribonuclease I (Promega, Madison, WI) and subsequently used for reverse transcription. The first-strand cDNA was synthesized using random primers (Promega) in a total

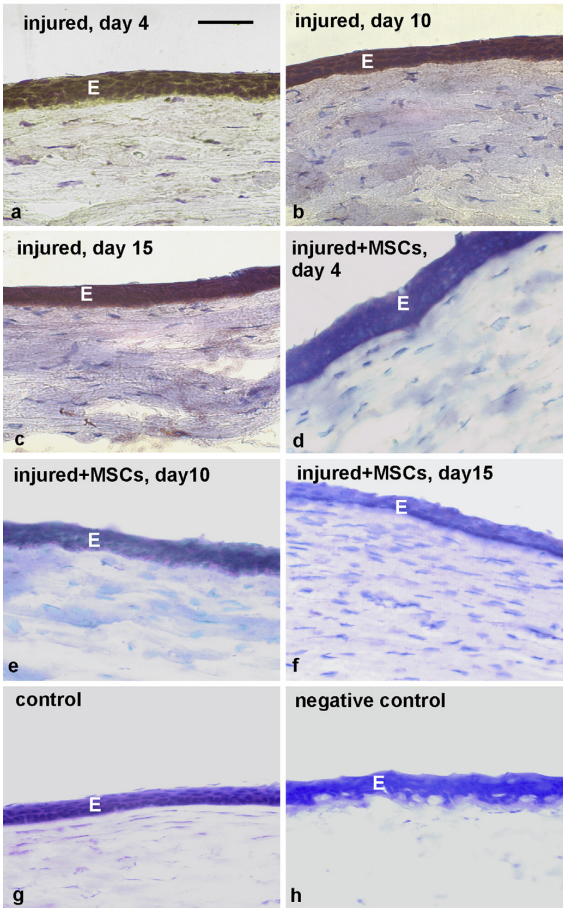

Fig. 2. Expression of NT in corneas on day 4, 10 and 15 after injury. E – corneal epithelium. Scale bar: 10 μM. NT expression is high in the epithelium of an injured cornea on day 4 (a), day 10 (b) and day 15 (c) after the injury. This is in contrast to injured cornea treated with MSCs on nanofiber scaffolds, where NT expression is absent in the epithelium (d, day 4; e, day 10; f, day 15 after the injury), similarly as in the control cornea (g). h – The primary antibody was omitted from the incubation medium. The section is stained by counterstaining only (as a negative control for NT). All sections are counterstained with haematoxylin.

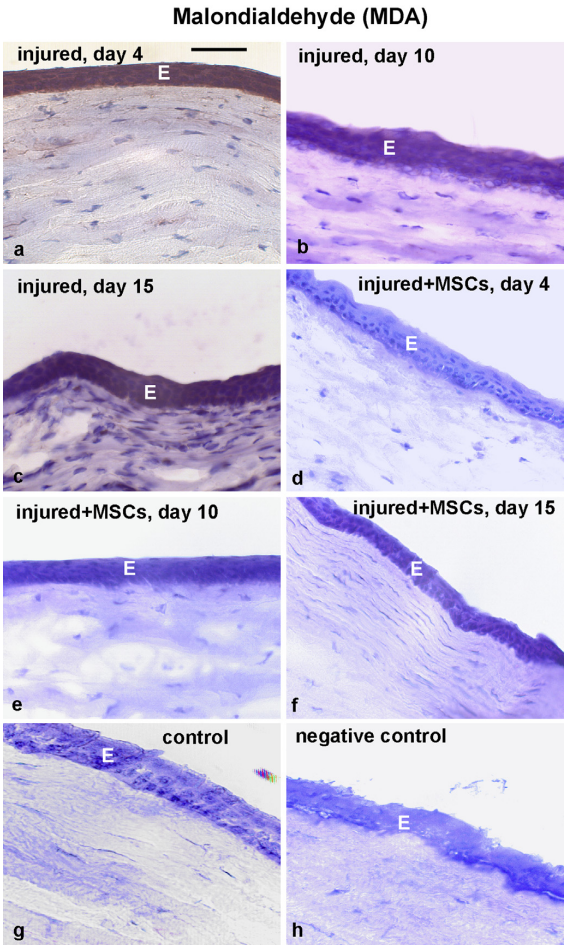

Fig. 3. Expression of MDA in corneas on day 4, 10 and 15 after injury. E – corneal epithelium. Scale bar: 10 μM. MDA expression is high in the epithelium of injured corneas on day 4 (a), day 10 (b) and as well as day 15 (c) after the injury. On day 15 following the injury MDA expression increased in the corneal stroma. In contrast, MDA expression is absent in an injured cornea treated with MSCs on nanofiber scaffolds from day 4 (d), day 10 (e) to day 15 (e) after the injury, similarly as in a control cornea (g). h – The primary antibody was omitted from the incubation medium. The section is stained by counterstaining only (as a negative control for MDA). All sections are counterstained with haematoxylin.

reaction volume of 25 μl using M-MLV Reverse Transcriptase (Promega).

Quantitative real-time PCR was performed in a StepOnePlus real-time PCR system (Applied Biosystems, Foster City, CA). The relative quantification model with efficiency correction was applied to calculate the expression of the target gene in comparison with GAPDH used as the housekeeping gene. The following primers were used for amplification: GAPDH – 5′-cccaacgtgtctgtcgtg (sense), 5′-ccgacccagacgtacagc (antisense), IL-1 β – 5′-ctgcggcagaaagcagtt (sense), 5′-gaaagttctcaggccgtcat (antisense), IL-2 – 5′-tttcaggtca-cagaattgaaacat (sense), 5′-gcacttcctccagaggtttg (antisense), IFN-γ – 5′-gggtaactgtgaatgttcaatgg (sense), 5′-gctcagaaacccagttgcat (antisense), and VEGF – 5′-cgagaccttggtggacatct (sense), 5′-atctg-catggtgacgttgaa (antisense). The PCR parameters included denaturation at 95 °C for 3 min, then 40 cycles at 95 °C for 20 s, annealing at 60 °C for 30 s and elongation at 72 °C for 30 s. Fluorescence data were collected at each cycle after an elongation step at 80 °C for 5 s and were analyzed on the StepOne Software, version 2.2.2 (Applied Biosystems). Each individual experiment was done in triplicate.

2.8. Statistics

The Mann–Whitney *U* test and an unpaired *t*-test were used to analyze the differences between controls and individual experimental groups or between untreated injured corneas and injured corneas treated with MSCs. A P value <0.05 was considered to

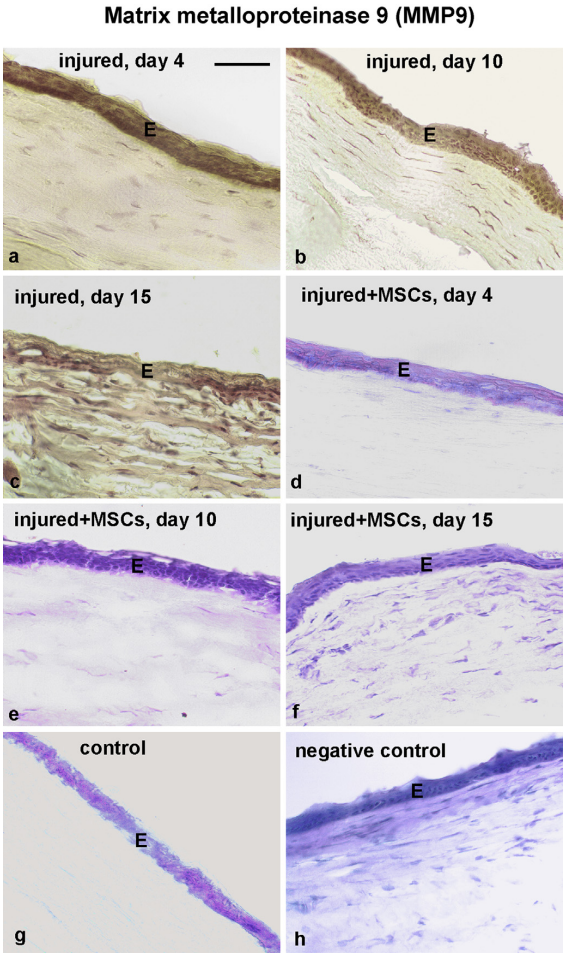

Fig. 4. Expression of MMP9 in corneas on day 4, 10 and 15 after injury. E – corneal epithelium. Scale bar: 10 μM. MMP9 expression is high in the epithelium of an injured cornea from day 4 (a) to day 10 (b) after the injury. On day 15 following the injury (c) the expression of MMP9 increased also in the corneal stroma. In contrast, the expression of MM9 in injured corneas treated with MSCs seeded on nanofiber scaffolds, was very low during 15 days after the injury (d, day 4; e, day 10; f, day 15 following the injury). g – Control cornea. The MMP9 expression is very low in the corneal epithelium. h – The primary antibody is omitted from the incubation medium. The section is stained by counterstaining only (as a negative control for MMP9). The sections are counterstained with haematoxylin.

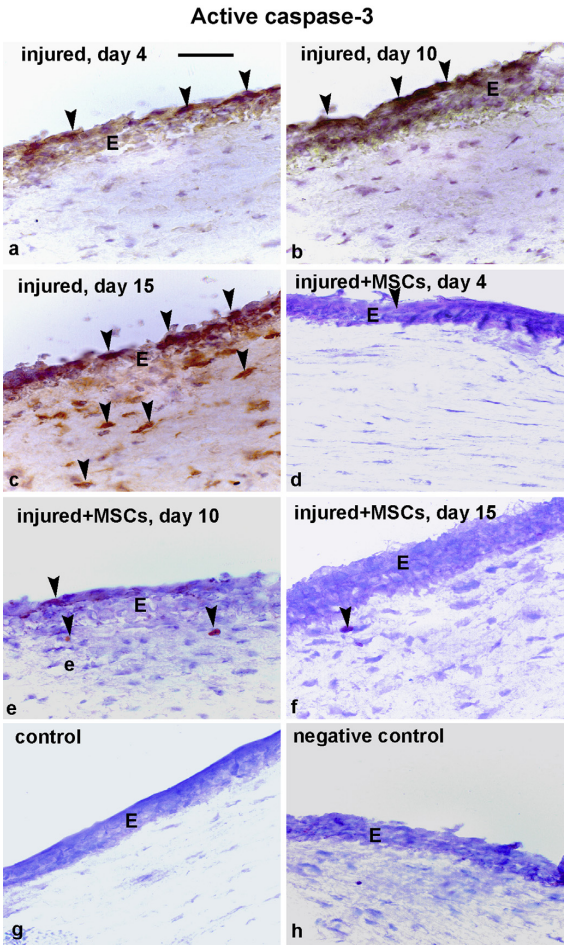

Fig. 5. Active caspase-3 expressions in corneas on day 4, 10 and 15 after the injury. E – corneal epithelium. Scale bar: 10 μM a – Caspase-3 staining is strong in the epithelium (particularly in superficial layers, arrows) of injured corneas on day 4 (a) as well as 10 (b) after the injury (arrows). c – On day 15 after the injury the expression of caspase-3 is present in the corneal epithelium as well as in the corneal stroma (arrows show to the cell apoptosis). d – The expression of caspase-3 is reduced in the epithelium (arrows) of injured corneas treated with MSCs on nanofiber scaffolds from day 4 (d), day 10 (e) as well as day 15 (f) after the injury. Solely apoptosis (arrows) are seen. g - Caspase-3 expression is absent in a control cornea. h – The primary antibody is omitted from the incubation medium. The section is stained by counterstaining only (as a negative control for caspase-3). The sections are counterstained with haematoxylin.

indicate statistical significance. Using the immunohistochemical markers, the number of positively stained cells (and inflammatory cells) was counted in the central as well as the limbal corneal regions over an area 100 μm long and 100 μm wide in sagittal cryostat sections.

For statistical examination of corneal neovascularization, the number of vessels was manually counted in each of 60° sector of the corneal surface. The mean value and standard deviation were counted from six measurements. This procedure was applied for every eye from matching group of six eyes (6 injured untreated, 6 injured MSCs treated). The significancy between groups was analysed using unpaired *t*-test.

For statistical evaluation of the central corneal thickness measured by an ultrasonic Pachymeter, a paired *t*-test was employed to investigate the differences between injured corneas treated with MSCs vs. the same corneas before injury or injured corneas vs. the same corneas before alkali injury.

3. Results

3.1. The effect of MSCs transferred on nanofiber scaffolds on the injured cornea

On day 4 after the injury the expression of ALDH3A1 was decreased in the upper layers of the epithelium of the injured corneas (Fig. 1 a, arrows) and it was nearly absent in the epithelium of the injured cornea on day 10 (Fig. 1b) and day 15 (Fig. 1c). In contrast, the expression of ALDH3A1 was high in the epithelium of injured corneas treated with MSCs from day 4 to day 15 after the injury (Fig. 1d, day 4, Fig. 1e, day 10, Fig. 1f, day 15), similarly as in the epithelium of control cornea (Fig. 1g). The extent of peroxynitrite formation, detected as NT residues, was high in the epithelium of injured corneas on day 4 (Fig. 2a), on day 10 (Fig. 2b), as well as on day 15 (Fig. 2c), whereas in corneas treated with MSCs peroxynitrite formation was absent in the epithelium on day 4 to day 15

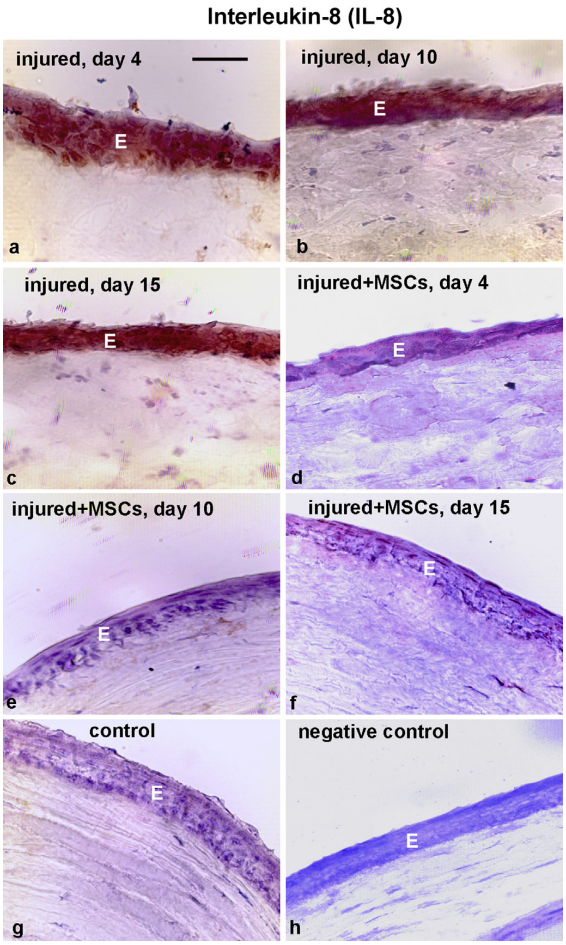

Fig. 6. IL-8 expressions in corneas on day 4, 10 and 15 after the injury. E – corneal epithelium. Scale bar: 10 μM. IL-8 is strongly expressed in the epithelium of injured corneas from day 4 (a), to day 10 (b) and day 15 (c) after the injury. In contrast, the expression of IL-8 is absent in the epithelium of injured corneas treated with MSCs on nanofiber scaffolds from day 4 (d), day 10 (e) and day 15 (f) after the injury. g – IL-8 expression is absent in a control cornea. h – The primary antibody was omitted from the incubation medium. The section is stained by counterstaining only (as a negative control for IL-8). The sections are counterstained with haematoxylin.

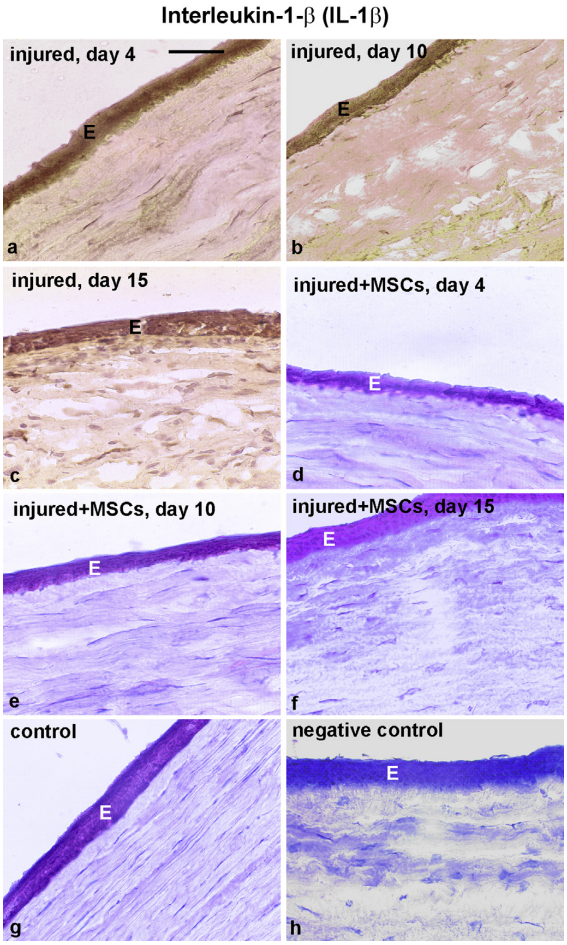

Fig. 7. IL-1 β expressions in corneas on day 4, 10 and 15 after the injury. E – corneal epithelium. Scale bar: 10 μM. The expression of IL-1 β is high in the corneal epithelium on day 4 (a), day 10 (b), as well as day 15 (c) after the injury. On day 15 IL-1 β expression is present also in the corneal stroma. In injured corneas treated with MSCs transferred on nanofiber scaffolds is absent in the cornea (d, day 4; e, day 10; f, day 15 after the injury), similarly as in the control cornea (g). h – The primary antibody was omitted from the incubation medium. The section is stained by counterstaining only (as a negative control for IL-1 β). The sections are counterstained with haematoxylin.

after the injury (Fig. 2d, day 4; Fig. 2e, day 10; Fig. 2f, day 15), similarly as in the epithelium of control corneas (Fig. 2g). Furthermore, MDA expression was high in the epithelium of injured corneas (Fig. 3 a, day 4; Fig. 3b, day 10; Fig. 3c, day 15 after the injury); however, in the epithelium of injured corneas treated with MSCs the MDA expression was absent (Fig. 3d, day 4; Fig. 3e, day 10 and Fig. 3f, day 15 following the injury), very similar as in the epithelium of control corneas (Fig. 3 g). The expression of MMP 9 in untreated injured corneas was high (Fig. 4 a, day 4; Fig. 4b, day 10; Fig. 4c, day 15 after the injury) compared to the levels found in injured corneas treated with MSCs, where the expression of MMP9 was low (Fig. 4d, day 4; Fig. 4e, day 10; Fig. 4f, day 15 after the injury) as in control corneas (Fig. 4 g). The expression of active caspase-3 was high in the epithelium of injured corneas (Fig. 5 a, arrows, day 4 and Fig. 5b, arrows, day 10 after the injury). On day 15 after the injury many apoptotic cells were present in the epithelium and also in the corneal stroma (Fig. 5c, arrows), whereas in the epithelium of injured corneas treated with MSCs the expression of active caspase-3 was very low from day 4 to day 15 after the injury (Fig. 5d, day 4; Fig. 5e, day 10; Fig. 5f, day 15 after the injury). Also, the expression of IL-8 was high in the epithelium of injured corneas (Fig. 6 a, day 4; Fig. 6b, day 10; Fig. 6c, day 15 after the injury). In contrast, IL-8 expression was absent in the epithelium of injured corneas treated with MSCs (Fig. 6d, day 4; Fig. 6e, day 10; Fig. 6F, day 15 after the injury), similarly as in the epithelium of control corneas (Fig. 6g). Very similar results were obtained with the expression of IL-1-β. Its expression was high in the epithelium of injured cornea (Fig. 7 a, day 4; Fig. 7b, day 10 and Fig. 7c, day 15 after the injury). In contrast, in the injured cornea treated with MSCs the expression of IL-1 β was absent in the epithelium (Fig. 7d, day 4; Fig. 7e, day 10; Fig. 7f, day 15 after the injury).

The central thicknesses of injured corneas or injured corneas treated with MSCs were shown in Fig. 8A and compared with macroscopical changes of corneal transparency (Fig. 8 B). Increased corneal hydration together with corneal opalescency after alkali injury returned to normal values during ten days only in those injured corneas treated with MSCs.

3.2. *Corneal neovascularization and inflammatory cells in the corneal stroma detected morphologically and immunohistochemically (day 15 after the injury)*

Corneal neovascularization and a high number of inflammatory cells detected by Haematoxylin-eosin staining were present in untreated injured corneas (Fig. 9 a, arrows point to vessels) compared to injured corneas treated with MSCs (Fig. 9b). VEGF expression was high in the epithelium and stroma (vessels) (Fig. 9c, arrows) of injured corneas. (VEGF in the corneal stroma is better seen in a

A

The thickness of the central cornea two or ten days after alkali injury and treatment with MSCs.

Group	N	Central corneal thickness		
		Before injury	Two days after injury	Ten days after injury
Without MSCs	6	349.99 ± 1.19	665.51 ± 14.32[a]	357.37 ± 3.04[a]
MSCs-treated	6	348.18 ± 1.41	681.62 ± 1.84[a]	349.64 ± 1.38[b]

[a]Significantly ($P < 0.001$) different from the corneal thickness before injury.
[b]Significantly not different ($P > 0.05$) from corneal thickness before injury.

B

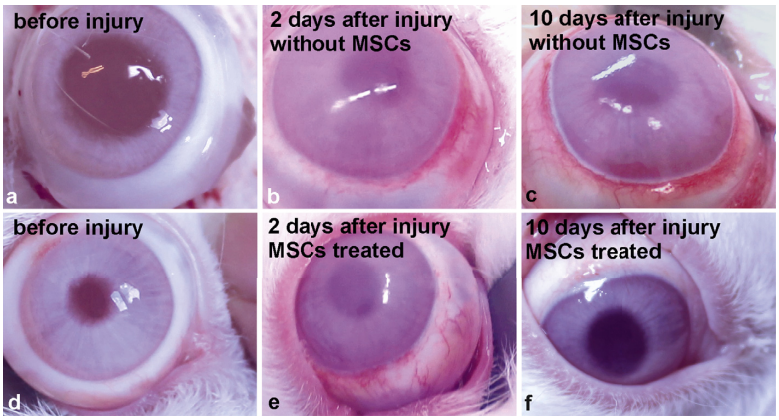

Fig. 8. The central thickness of corneas (taken as an index of corneal hydration) two days after injury with 0.15 N NaOH and covering with nanofiber scaffolds, with or without MSCs, was significantly increased (compared to the central thickness of the corneas before alkali injury) in both groups (A). This was accompanied by corneal opalescency (B, b, e). After an additional eight days (i.e., on day 10 after injury) the central thickness of the corneas was not significantly increased (compared to the central thickness of the corneas before alkali injury) only in those injured corneas treated with MSCs (A). In this case the corneal transparency restored (B, f), whereas in untreated alkali-injured corneas corneal opalescency persisted (B, c).

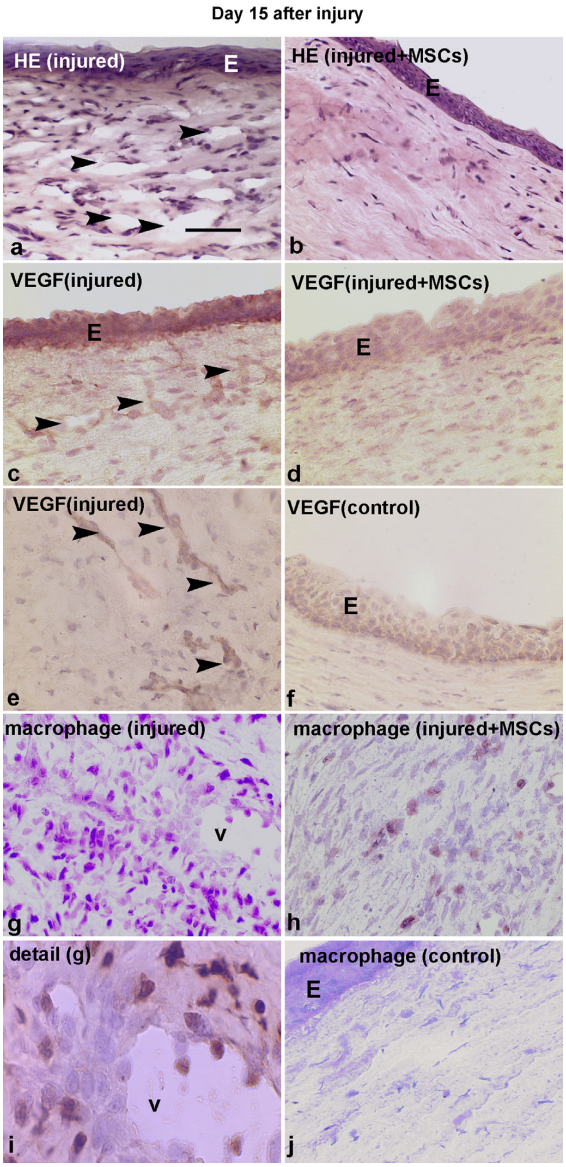

Fig. 9. Haematoxylin-eosin staining (HE), VEGF and macrophage expression in corneas on day fifteen after injury. E (corneal epithelium). Scale bar: 10 μM a – In HE staining of an injured cornea, numerous inflammatory cells are seen in the corneal stroma and the cornea is vascularized (arrows). b – In HE staining of an injured cornea treated with MSCs, corneal neovascularization is absent, and the number of inflammatory cells is suppressed in the corneal stroma. Compare with an injured cornea (a). c – VEGF expression is high in the epithelium and corneal stroma (arrows) of injured corneas. d – VEGF expression is low in the epithelium of injured corneas treated with MSCs and VEGF is not detected in the corneal stroma. e – VEGF expression in the stroma of an injured cornea is better seen in a tangential section. f – VEGF staining is weak in the epithelium of a control cornea. g – A large number of cells detected with anti-macrophage antibody (macrophages, monocytes) is present in the vascularized (v) corneal stroma of an injured cornea. h – In an injured cornea treated with MSCs the number of cells detected with anti-macrophage antibody is low. Compare with an injured cornea (g). i – A detail from (g) with macrophage/monocyte detection (v - vessel). j – A control cornea is stained by counterstaining only. The sections are lightly counterstained with haematoxylin.

tangential section, Fig. 9e, arrows). In contrast, VEGF expression was low in the corneal epithelium of injured corneas treated with MSCs (Fig. 9d), similarly as in the control corneas (Fig. 9f). VEGF expression was absent in the stroma of injured corneas treated with MSCs (Fig. 9d). Using an anti-macrophage antibody, numerous cells (macrophages/monocytes) were detected in the stroma of untreated injured corneas (Fig. 9 g, v – vessel). In Fig. 9 (i) a detail of macrophages/monocytes from Fig. 9(g) is shown.

Nanofiber scaffolds alone (without MSCs) had no significant beneficial effect on the healing of alkali-injured corneas. Also MSCs applied on the corneal surface alone by dropping (without scaffolds) did not show significant positive effects on corneal healing, very probably due to the rapid washing away of MSCs from the corneal surface – earlier than eyelids could be sutured.

Compared to injured untreated corneas, where corneal neovascularization was extensive (grade 4, Fig. 10D or grade 3, Fig. 10E), in injured corneas treated with MSCs corneal neovascularization was suppressed (grade 2, Fig. 10F or grade 1, Fig. 10G). Manual counting of vessels (Fig. 10H) corresponded with quantification of corneal neovascularization with real-time PCR (the expression of genes for VEGF), Fig. 10I.

3.3. Corneal impression cytologies

After one or two days of the presence of nanofiber scaffolds on the ocular surface of healthy eyes (with the eyelids sutured), no expression of u-PA was observed in cytology samples of the corneal epithelial cells (Fig. 11a), similarly as in the cytology samples of the epithelial cells of the control corneas (Fig. 11c), whereas following three days of the presence of nanofiber scaffolds on the ocular surface (with the eyelids sutured), u-PA expression appeared in corneal cytology samples (Fig. 11b). Very similar results were obtained with e-NOS (Fig. 11e–h). The expression of this enzyme was seen in cytology samples of the epithelial cells of healthy corneas on which nanofiber scaffolds were present for three days (with the eyelids sutured) (Fig. 11f).

3.4. Expression of genes for proinflammatory cytokines in control, injured and MSC-treated corneas

The corneas from healthy control eyes, eyes injured by alkali and injured eyes treated with MSCs were harvested on day 10 after injury, and the expression of genes for IL-1 β, IL-2, IFN-γ was determined. The alkali-induced oxidative stress in the cornea induced the significant expression of proinflammatory cytokine and VEGF genes. Treatment of the injury by covering the eye with a nanofiber scaffold seeded with MSCs significantly reduced the local inflammatory reaction and corneal neovascularization, as demonstrated by the significantly decreased expression of genes for proinflammatory cytokines (Fig. 12) and VEGF (Fig. 10).

4. Discussion

Our results show that MSCs effectively reduce alkali-induced oxidative stress in the cornea, leading to the suppression of intracorneal inflammation as well as a decrease in corneal neovascularization, resulting in significantly accelerated healing. To our knowledge, this is the first study showing that MSCs significantly reduce oxidative stress in the cornea, although in non-ophthalmological tissues, organs and diseases as well as in in vitro studies, the suppression of oxidative stress by MSCs has been described (e.g., Valle-Prieto and Conget, 2010; Chen et al., 2011; Dey et al., 2012; Liu et al., 2012). Moreover, in this study nanofiber scaffolds seeded with MSCs were, for the first time, employed for MSC transplantation onto the alkali injured cornea.

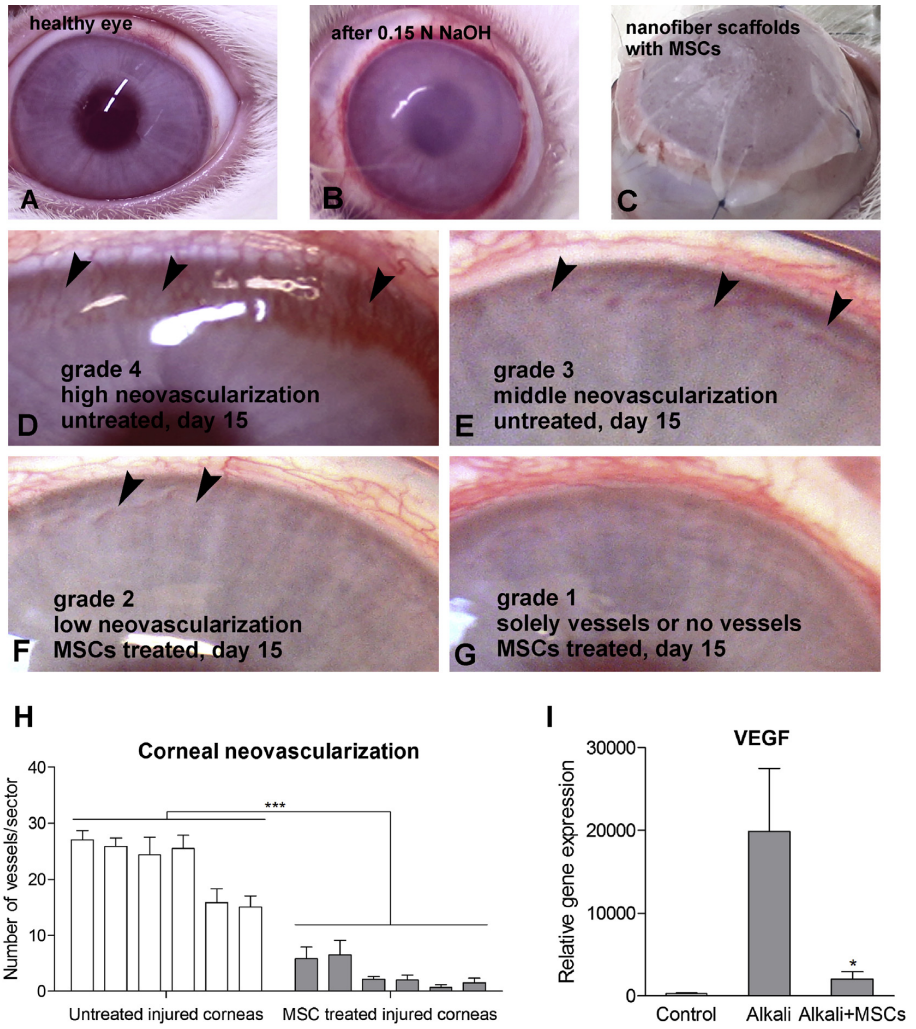

Fig. 10. Representative photographs of alkali-injured corneas (with 0.15 N NaOH) and corneal neovascularization on day 15 after the injury. A – A healthy rabbit eye. B – Immediately after the injury a cornea turns grayish. C – An injured cornea on which nanofiber scaffolds with MSCs were transferred and sutured with conjunctiva. (In some other corneas nanofiber scaffolds without MSCs were transferred and sutured). D – An alkali injured cornea untreated with MSCs with high neovascularization (grade 4). E – an alkali-injured untreated cornea with middle neovascularization (grade 3). F – A cornea injured with alkali and treated with MSCs with low neovascularization (grade 2). G – An alkali-injured cornea treated with MSCs with no or very low neovascularization (grade 1). H – Quantification of corneal neovascularization. The corneal surface was divided into six sixty degree angular sectors. Using the preparation microscope the vessels were manually counted in each sector. The mean value and standard deviation were estimated from six measurements for each cornea. Significant differences between groups (untreated injured corneas vs. injured corneas treated with MSCs) were found. Grades of neovascularization were introduced as follows: 20–30 vessels (per one sector) (grade 4), 10–19 vessels (grade 3), 3–9 vessels (grade 2) and no vessels or solely vessels (grade 1). I – Quantification of corneal neovascularization using real-time PCR (the expression of genes for VEGF). Real-time PCR was investigated in control healthy corneas (Ctrl), injured corneas (Alkali) or injured corneas treated with MSCs (Alkali + MSCs). Each column represents the mean ± SD from 4 determinations. The values with asterisks are significantly different ($P < 0.05$) from those found in injured, but untreated corneas.

Nanofiber scaffolds proved to be suitable for this purpose. Previous papers employed amniotic membrane for MSC transplantation onto the alkali-injured cornea (Ma et al., 2005; Jiang et al., 2010). Ye et al. (2006, 2008) hypothesized that corneal alkali injury resulted in the release of cytokines that recruit exogenously administered MSCs and, at the same time, increase bone marrow stem cell mobility, facilitating the mobilization of the MSCs into the circulation and to the sites of wound healing. These authors concluded that the results of their experiments show that MSCs systematically engraft to the alkali-injured cornea and promote healing by differentiation, proliferation and synergyzing with haematopoietic stem cells. Arnalich-Montiel et al. (2008) injected a suspension of human MSCs into a defect of the corneal stroma in rabbits; the corneas regenerated within three months. Yao et al. (2012) administered MSCs subconjunctivally in alkali-injured eyes and found that MSCs reduced corneal inflammation and neovascularization. These effects were related to a reduction in the number of infiltrated CD68(+) cells and the down-regulation of macrophage inflammatory protein-1 alpha, tumor necrosis factor-alpha and vascular endothelial growth factor.

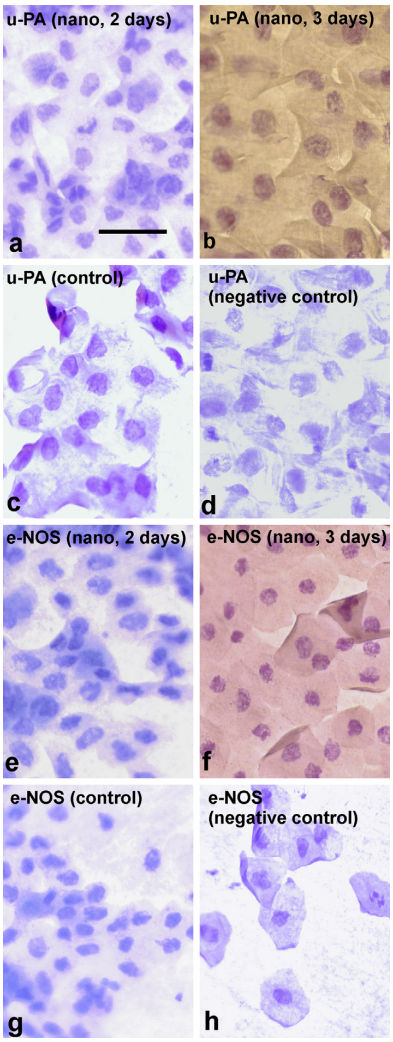

Fig. 11. Impression cytology samples of corneal epithelial cells. Scale bar: 10 μM a – The expression of u-PA is absent in a corneal cytology sample collected after two days of covering a healthy cornea with a nanofiber scaffold (and with the eyelids sutured). b – u-PA expression in a corneal cytology sample collected after three days of covering a healthy cornea with a nanofiber scaffold (and with the eyelids sutured). c – In a cytology sample of the epithelium of a control cornea, the expression of U-PA is absent. d – Corneal epithelial cells (cytology sample) are stained by counterstaining only (as a negative control for u-PA), when the primary antibody is omitted from the incubation medium. e – The expression of e-NOS is absent (or very low) in a corneal cytology sample collected after two days of the presence of a nanofiber scaffold on a healthy cornea (and with the eyelids sutured). f – The expression of e-NOS is increased in a corneal cytology sample collected following three days of the presence of a nanofiber scaffold on a healthy cornea. g – In a cytology sample of a control cornea e-NOS expression is low or completely absent. h – In a negative control for e-NOS (the primary antibody was omitted from the incubation medium), corneal epithelial cells are stained by counterstaining only. The cytology samples are counterstained with haematoxylin.

In this study, nanofiber scaffolds were used as carriers for MSCs and the healing results of alkali-injured corneas were compared with the healing of similarly injured corneas on which nanofiber scaffolds were transferred alone or on which MSCs were applied topically and eyelids sutured. We did not achieve positive healing results with last two approaches, even if Oh et al. (2008) described the anti-inflammatory and anti-angiogenic effect of topically applied MSCs in damaged rat corneas. Also in this case eyelids were sutured. It is suggested that different findings might be caused due to more severe injury in the rat corneas (100% ethanol and mechanically scraped corneal epithelium) which enabled the attachment of MSCs at the corneal surface. In our experiments mild alkali was employed which did not remove superficial layers of the corneal epithelium.

Because nanofiber scaffolds were used for the first time in our experiments with corneal alkali burns, we also examined how long the scaffold can remain on the corneal surface (with the eyelids sutured) without causing corneal damage. The nanofiber scaffolds were transferred onto the corneal surface of healthy rabbit eyes for one, two or three days and the eyelids sutured. Impression cytologies of the corneal epithelial cells were collected after the removal of the sutures and scaffolds. Impression cytology of corneal epithelial cells was recommended as a sensitive diagnostic method by Singh et al. (2005). We found previously that the expression of immunohistochemical markers in cryostat sections of the corneal epithelium tightly corresponds with the detection of similar markers in corneal impression cytology samples of the corneal epithelium (Cejkova et al., 2012). Using suitable immunohistochemical markers, impression cytology samples enable us to examine damage to corneal epithelial cells. In this study, impression cytologies were examined immunohistochemically for u-PA and e-NOS. The expression of these enzymes is negative or negligibly low in the corneal epithelium of healthy eyes and appears during various corneal injuries or diseases (e.g., Buddi et al., 2002; Watabe et al., 2003; Cejkova et al., 2010). Thus, these enzymes are very sensitive markers of corneal disorders. The results of this study show that after two days of a nanofiber scaffold covering the cornea, the corneal epithelial cells are undamaged (Fig. 6). Because this time interval is also sufficient for MSC attachment on the injured corneal surface, a two day interval was used in our experiments with MSCs and alkali-injured corneas.

Alkali evokes increased reactive oxygen species production (Kubota et al., 2011) leading - as shown in this study - to the decreased expression of ALDH3A1 in the epithelium of the injured cornea (Fig. 1). Mammalian corneal epithelial cells express high levels of ALDH3A1 (Piatigorsky, 2000), an enzyme that protects the cornea against oxidative damage (Downes et al., 1993; Manzer et al., 2003). Pappa et al. (2005) described that ALDH3A1 may protect corneal epithelial cells against oxidative stress not only through its metabolic function, but also by prolonging the cell cycle. In alkali-injured corneas treated with MSCs, both oxidative and nitrosative stress are suppressed, as shown in this study by the negative staining for NT and MDA, reduced apoptotic cell death and decreased MMP9 expression in corneal epithelial cells (Figs. 2–5). This is in contrast to untreated injured corneas, where NT and MDA expression as well as apoptotic cell death and MMP9 were high in the corneal epithelium. The demonstration of peroxynitrite formation (by the expression of NT), a toxic reaction product of nitric oxide and superoxide, serves as an important marker of free radical damage (Ceriello, 2002; Chirino et al., 2006) and the detection of MDA as a marker of lipid peroxidation (Buddi et al., 2002). In the normal cornea staining for NT as well as MDA is absent (or present at negligible levels). Their expression serves as a sensitive marker of oxidative damage. Due to reduced oxidative and nitrosative stress in the injured corneas treated with MSCs, the expression of the pro-inflammatory cytokine IL-8 and IL-1-β was greatly decreased in these corneas (Figs. 6 and 7). This is in contrast to the alkali-injured corneas without MSC treatment, where the expression of IL-8 and IL-1 β was high. (In the control corneas the staining for IL-8 as well as IL-1 β was negative or negligible low). Using real-time PCR we also

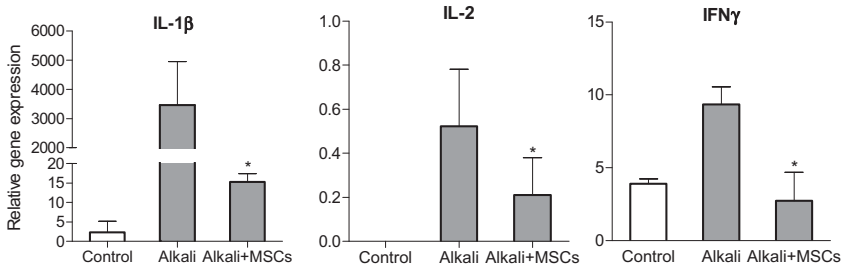

Fig. 12. The expression of IL-1 β, IL-2 and IFN-γ in cells from control, alkali injured or injured and MSC-treated corneas. The corneas were harvested on day 10 after an alkali-induced injury, and the expression of genes for IL-1 β, IL-2 and IFN-γ was determined by real-time PCR in control healthy corneas (Ctrl), injured corneas (Alkali) or injured corneas treated with MSCs (Alkali + MSCs). Each column represents the mean ± SD from 4 determinations. The values with asterisks are significantly different ($P < 0.05$) from those found in injured, but untreated corneas.

demonstrated the significantly reduced expression of genes for IL-1 β and some other proinflammatory cytokines (IL-2, IFN-γ) in the inflamed corneas after the treatment with nanofibers seeded with MSCs (Fig. 12). The reduced overexpression of pro-inflammatory cytokines is very important because pro-inflammatory cytokines are associated with corneal neovascularization (e.g., Sotozono et al., 1997, 1999). Results with real-time PCR (expression of genes for VEGF) show that corneal neovascularization is highly suppressed in injured corneas treated with MSCs on nanofiber scaffolds. Haematoxylin-eosin staining and immunohistochemical stainings with anti-macrophage and anti-VEGF antibodies showed in situ that corneal neovascularization as well as the number of inflammatory cells significantly decreased in injured corneas treated with MSCs compared to untreated injured ones (Fig. 9). Our findings are in accordance with the observations of other authors (e.g., Cursiefen et al., 2000; Philipp et al., 2000; Choi et al., 2011) that the immunohistochemical detection of VEGF as well as of macrophages serves as a very good marker of corneal inflammation and neovascularization. Also, the examination of the central corneal thickness, taken as an index of corneal hydration, showed that the increased central corneal thickness following alkali injury decreased to normal levels during ten days in corneas treated with MSCs, whereas in untreated injured corneas the central corneal thickness remained significantly increased (Fig. 8).

The central corneal thickness was measured by an ultrasonic pachymeter. This method was previously found to be very suitable for this purpose (Doughty and Cullen, 1989; O'Donnel and Efron, 2006; Cejka et al., 2007, 2010). To measure changes in corneal hydration is important because physiological (normal) corneal hydration is required for corneal transparency. The transparency of the cornea is a consequence of the detailed ultrastructure of the tissue and has been attributed to the narrow, uniform diameter collagen fibrils and to the regularity of their lateral packing (Maurice, 1957; Twersky, 1974). If the cornea swells, light scattering appears and the cornea becomes opaque, leading to a decrease in visual acuity. Thus, measuring the central corneal thickness after corneal injury and during corneal healing is a suitable approach for examining the restoration of corneal hydration and transparency accompanying positive healing (Fig. 8).

In conclusion, MSCs growing on nanofiber scaffolds and transferred onto the alkali-injured corneal surface effectively reduced oxidative stress in the cornea. MSCs protected against the formation of peroxynitrite, a toxic reaction product between nitric oxide and superoxide, reduced apoptotic cell death and decreased matrix metalloproteinase levels as well as the induction of pro-inflammatory cytokines. This resulted in suppressed corneal inflammation as well as neovascularization and significantly accelerated corneal healing.

Acknowledgments

Supported by the grant AVOZ50390512 from the Academy of Sciences of the Czech Republic, grants no. P304/11/0653 and P301/11/1568 from the Grant Agency of the Czech Republic, project no. 668012 from the Grant Agency of the Charles University, and the projects MSM0021620858 and SVV265211 from the Ministry of Education of the Czech Republic.

References

Arnalich-Montiel, F., Pastor, S., Blazquez-Martinez, A., Fernandez-Delgado, J., Nistal, M., Alio, J.L., De Miguel, M.P., 2008. Adipose-derived stem cells are a source for cell therapy of the corneal stroma. Stem Cells 26, 570–579.

Buddi, R., Lin, B., Atilano, S.R., Zorapapel, N.C., Kenney, M.C., Brown, D.J., 2002. Evidence of oxidative stress in human corneal diseases. Histochem. Cytochem. 50, 341–351.

Cejka, C., Platenik, J., Guryca, V., Sirc, J., Michalek, J., Brunova, B., Cejkova, J., 2007. Light absorption properties of the rabbit cornea repeatedly irradiated with UVB rays. Photochem. Photobiol. 83, 652–657.

Cejka, C., Platenik, J., Sirc, J., Ardan, J., Michalek, J., Brunova, B., Cejkova, J., 2010. Changes of corneal optical properties after UVB irradiation investigated spectrophotometrically. Physiol. Res. 59, 591–597.

Cejkova, J., Ardan, T., Simonova, Z., Cejka, C., Malec, J., Dotrelova, D., Brunova, B., 2008. Decreased expression of antioxidant enzymes in the conjunctival epithelium of dry eye (Sjögren's syndrome) and its possible contribution to the development of ocular oxidative injuries. Histol. Histopathol. 23, 1477–1483.

Cejkova, J., Cejka, C., Ardan, T., Sirc, J., Michalek, J., Luyckx, J., 2010. Reduced UVB-induced corneal damage caused by reactive oxygen species and decreased changes in corneal optics after trehalose treatment. Histol. Histopathol. 25, 1403–1416.

Cejkova, J., Cejka, C., Luyckx, J., 2012. Trehalose treatment accelerates the healing of UVB-irradiated corneas. Comparative immunohistochemical studies on corneal cryostat sections and corneal impression cytology. Histol. Histopathol. 27, 1029–1040.

Ceriello, A., 2002. Nitrotyrosine: new findings as a marker of postprandial oxidative stress. Int. J. Clin. Pract. Suppl. 129, 51–58.

Chen, Y.T., Sun, C.K., Lin, Y.C., Chang, L.T., Chen, Y.L., Tsai, T.H., Chung, S.Y., Chua, S., Kao, Y.H., Yen, C.H., Shao, P.L., Chang, K.C., Leu, S., Yip, H.K., 2011. Adipose-derived mesenchymal stem cell protects kidneys against ischemia-reperfusion injury through suppression oxidative stress and inflammatory reaction. J. Transl. Med. 9, 51–68.

Chirino, Y.I., Orozco-Ibarra, M., Pedraza-Chaverri, J., 2006. Role of peroxynitrite anion in different diseases (Article in Spain). Rev. Invest. Clin. 58, 350–358.

Choi, J.A., Choi, J.S., Joo, C.K., 2011. Effects of amniotic membrane suspension in the rat alkali burn model. Mol. Vis. 17, 404–412.

Cursiefen, C., Rummelt, C., Kuchle, N., 2000. Immunohistochemical localization of vascular endothelial growth factor, transforming growth factor alpha, and transforming growth factor beta in human corneas with neovascularization. Cornea 19, 526–533.

Dey, R., Kemp, K., Gray, E., Rice, C., Scolding, N., Wilkins, A., 2012. Human mesenchymal stem cells increase anti-oxidant defences in cells derived from patients with Friedreichs Ataxia. Cerebellum 11, 861–871.

Doughty, M.J., Cullen, A.P., 1989. Long-term effects of a single dose of ultraviolet-B on albino rabbit cornea. In vivo analyses. Photochem. Photobiol. 49, 185–1969.

Downes, J.E., Swann, P.G., Holmes, R.S., 1993. Ultraviolet light-induced pathology in the eye: associated changes in ocular aldehyde dehydrogenase and alcohol dehydrogenase activities. Cornea 12, 241–248.

Holan, V., Chudicková, M., Trosan, P., Svobodova, E., Krulova, M., Kubinova, S., Sykova, E., Sirc, J., Michalek, J., Juklickova, M., Munzarova, M., Zajicova, A., 2011. Cyclosporine A-loaded and stem cell-seeded electrospun nanofibers for cell-based therapy and local immunosuppression. J. Control Release 156, 406–412.

Jiang, T.S., Cai, L., Ji, W.Y., Hui, Y.N., Wang, Y.S., Hu, D., Zhu, J., 2010. Reconstruction of the corneal epithelium with induced marrow mesenchymal stem cells in rats. Mol. Vis. 16, 1304–1316.

Joyce, N.C., Harris, D.L., Markov, V., Zhang, Z., Saitta, B., 2012. Potential of human umbilical cord blood mesenchymal stem cells to heal damaged corneal endothelium. Mol. Vis. 18, 547–564.

Kooy, N.W., Lewis, S.J., Royall, J.A., Ye, Y.Z., Kelly, D.R., Beckman, J.S., 1997. Extensive tyrosine nitration in human myocardial inflammation: evidence for the presence of peroxynitrite. Crit. Care Med. 25, 812–819.

Kubota, M., Shimmura, S., Kubota, S., Miyashita, H., Kato, N., Noda, K., Ozawa, Y., Usui, T., Ishida, S., Umezawa, K., Kurihara, T., Tsubota, K., 2011. Hydrogen and N-acetyl-L-Cysteine rescue oxidative stress-induced angiogenesis in a mouse corneal alkali-burn model. Invest. Ophthalmol. Vis. Sci. 52, 427–433.

Lan, Y., Kodati, S., Lee, H.S., Omoto, M., Jin, Y., Chauhan, S.K., 2012. Kinetics and function of mesenchymal stem cells in corneal injury. Invest. Ophthalmol. Vis. Sci. 53, 3638–3644.

Liu, H., McTaggart, S.J., Johnson, D.W., Gobe, G.C., 2012. Original article anti-oxidant pathways are stimulated by mesenchymal stromal cells in renal repair after ischemic injury. Cytotherapy 14, 162–172.

Ma, Y., Xu, Y., Xiao, Z., Yang, W., Zhang, C., Song, E., Du, Y., Li, L., 2005. Reconstruction of chemically burned rat corneal surface by bone marrow-derived human mesenchymal stem cells. Stem Cells 24, 315–321.

Manzer, R., Pappa, A., Estey, T., Sladek, N., Carpenter, F., Vasiliou, V., 2003. Ultraviolet radiation decreases expression and induces aggregation of corneal ALDH3A1. Chemico-Biol. Interact. 143-144, 45–53.

Maurice, D.M., 1957. The structure and transparency of the corneal stroma. J. Physiol. 136, 263–286.

O'Donnel, C., Efron, N., 2006. Corneal hydration control in contact lens wearers with diabetes mellitus. Optom. Vis. Sci. 83, 22–26.

Oh, J.Y., Kim, M.K., Shin, M.S., Lee, H.J., Ko, J.H., Wee, W.R., Lee, J.H., 2008. The anti-inflammatory and anti-angiogenic role of mesenchymal stem cells in corneal wound healing following chemical injury. Stem Cells 26, 1047–1055.

Oh, J.Y., Roddy, G.W., Choi, H., Lee, R.H., Ylöstalo, J.H., Rosa Jr., R.H., Prockop, D.J., 2010. Anti-inflammatory protein TSG-6 reduces inflammatory damage to the cornea following chemical and mechanical injury. Proc. Natl. Acad. Sci. U. S. A. 107, 16875–16880.

Pappa, A., Brown, D., Koutalos, Y., DeGregori, J., White, C., Vasiliou, V., 2005. Human aldehyde dehydrogenase 3A1 inhibits proliferation and promotes survival of human corneal epithelial cells. J. Biol. Chem. 280, 7998–8006.

Philipp, W., Speicher, L., Humpel, C., 2000. Expression of vascular endothelial growth factor and its receptors in inflamed and vascularized corneas. Invest. Ophthalmol. Vis. Sci. 41, 2514–2522.

Piatigorsky, J., 2000. Review: a case for corneal crystallins. J. Ocul. Pharmacol. Ther. 16, 173–180.

Pinnamaneni, N., Funderburgh, J.L., 2012. Concise review: stem cells in the corneal stroma. Stem Cells 30, 1059–1063.

Singh, R., Joseph, A., Umapathy, T., Tint, N.L., Dua, H.S., 2005. Impression cytology of the ocular surface. Br. J. Ophthalmol. 89, 1655–1659.

Sotozono, C., He, J., Matsumoto, Y., Kita, M., Imanishi, J., Kinishita, S., 1997. Cytokine expression in the alkali-burned cornea. Curr. Eye Res. 16, 670–676.

Sotozono, C., He, J., Honma, Y., Kinoshita, S., 1999. Effect of metalloproteinase inhibitor on corneal cytokine expression after alkali injury. Invest. Ophthalmol. Vis. Sci. 40, 2430–2434.

Svobodova, E., Krulova, M., Zajicova, A., Prochazkova, J., Trosan, P., Holan, V., 2012. The role of mouse mesenchymal stem cells in differentiation of naive T cells into anti-inflammatory regulatory T cell and proinflammatory helper T-cell 17 population. Stem Cells Dev. 21, 901–910.

Trosan, P., Svobodova, E., Chudickova, M., Krulova, M., Zajicova, A., Holan, V., 2012. The key role of insulin-like growth factor I in limbal stem cell differentiation and the corneal wound-healing process. Stem Cells Dev. 21, 3341–3350.

Twersky, V., 1974. Transparency of pair-correlated, random distributions of small scatterers, with applications to the cornea. J. Opt. Soc. Am. 65, 524–530.

Valle-Prieto, A., Conget, P.A., 2010. Human mesenchymal stem cells efficiently manage oxidative stress. Stem Cells Dev. 19, 1885–1893.

Watabe, M., Yano, W., Kondo, S., Hattori, Y., Yamada, N., Yanai, R., Nishida, T., 2003. Up-regulation of urokinase-type plasminogen activator in corneal epithelial cells induced by wounding. Invest. Ophthalmol. Vis. Sci. 44, 3332–3338.

Yao, L., Li, Z.R., Su, W.R., Li, Y.P., Lin, M.L., Zhang, W.X., Liu, Y., Wan, Q., Liang, D., 2012. Role of mesenchymal stem cells on cornea wound healing induced by acute alkali burn. PLoS One 7 (2), e30842. http://dx.doi.org/10.1371/journal.pone.0030842. Epub 2012 Feb 17.

Ye, J., Yao, K., Kim, J.C., 2006. Mesenchymal stem cell transplantation in a rabbit corneal alkali burn model: engraftment and involvement in wound healing. Eye 20, 482–490.

Ye, J., Lee, S.Y., Kook, K.H., Yao, K., 2008. Bone marrow-derived progenitor cells promote corneal wound healing following alkali injury. Graefes Arch. Clin. Exp. Ophthalmol. 246, 217–222.

Zajicova, A., Pokorna, K., Lencova, A., Krulova, M., Svobodova, E., Kubinova, S., Sykova, E., Pradny, M., Michalek, J., Svobodova, J., Munzarova, M., Holan, V., 2010. Treatment of ocular surface injuries by limbal and mesenchymal stem cells growing on nanofiber scaffolds. Cell Transpl. 19, 1281–1290.